



**HAL**  
open science

# Role of Wnt5a in lysosomal function: intracellular cholesterol accumulation and atherosclerosis

Sara Awan

► **To cite this version:**

Sara Awan. Role of Wnt5a in lysosomal function: intracellular cholesterol accumulation and atherosclerosis. Subcellular Processes [q-bio.SC]. Université de Strasbourg, 2019. English. NNT: 2019STRAJ022 . tel-03270924

**HAL Id: tel-03270924**

**<https://theses.hal.science/tel-03270924>**

Submitted on 25 Jun 2021

**HAL** is a multi-disciplinary open access archive for the deposit and dissemination of scientific research documents, whether they are published or not. The documents may come from teaching and research institutions in France or abroad, or from public or private research centers.

L'archive ouverte pluridisciplinaire **HAL**, est destinée au dépôt et à la diffusion de documents scientifiques de niveau recherche, publiés ou non, émanant des établissements d'enseignement et de recherche français ou étrangers, des laboratoires publics ou privés.

**ÉCOLE DOCTORALE DES SCIENCES DE LA VIE ET DE LA SANTE**

*LABORATOIRE DE BIOIMAGERIE ET PATHOLOGIES*

*UMR CNRS 7021 Faculté de Pharmacie*

*Thèse présentée par*

**Sara AWAN**

*soutenue le 31 Mai 2019*

*pour obtenir le grade de*

**Docteur de l'université de Strasbourg**

*Discipline: Sciences du Vivant – Pharmacologie-Pharmaceutique-Pharmacie*

**Rôle de Wnt5a dans la fonction lysosomale,  
l'accumulation intracellulaire du cholestérol, et  
l'athérosclérose**

*THÈSE dirigée par:*

**M. Boucher Philippe**      *Professeur, Université de Strasbourg, France*

**RAPPORTEURS :**

**Jean Gruenberg**      *Professeur, Université of Geneva*

**Soraya Taleb**      *Charge de recherches, Université Paris Descartes, France*

**AUTRES MEMBRES DU JURY :**

**Joachim Herz**      *Professeur, UT South Western Médical Center, Dallas, Texas*

**Ali Hamiche**      *Préciser l'EPST, IGBMC, Illkirch-Graffenstaden, France*

**Catherine Tomassetto**      *Préciser l'EPST, IGBMC, Illkirch-Graffenstaden, France*



*M.Bilal*



## Acknowledgment

---

Many people helped me in completion of this project and i would like to thank them all.

First and foremost, i would like to express my gratitude to my mentor prof. Philippe BOUCHER and Jerome TERRAND for their valuable and continuous support during the last 3 years. Their kind suggestions, encouragement and constructive criticism helped me immensely during the project and enabled me through this journey.

I am also very thankful to Prof. Jean GRUENBERG, Madam Soraya TALEB and Professor Joachim HERZ for accepting our request to evaluate this thesis. I am also very grateful to our collaborators Fabien ALPY, Catherine –laure Tomasetto, Xavier COLLET, Christine Schaeffer REISS, Diane Julien DAVID and Motohide MURATE for their useful insights and helping us in the completion of this project. I am thankful to my lab colleagues Madam Rachel L. Matz, Helene Justiniano, Ali Imtiaz and Megalie Lambert for supporting and helping me during this project. I would also like to thank all my friends with whom i spent great time in France. Finally, i would like to express my deepest gratitude to my family members, my husband, parents and sisters for their unconditional love, care, support and encouragement throughout my life.



## Resume

---

La voie de signalisation Wnt joue un rôle critique au cours du développement embryonnaire et dans l'homéostasie cellulaire chez l'adulte. Ici, nous avons identifié, un ligand de Wnt, Wnt5a, comme faisant partie intégrante du complexe mTORC1, qui régule la fonction lysosomal et favorise le trafic intracellulaire du cholestérol. En diminuant l'activité de mTORC1 et en activant l'axe autophagie-lysosome, Wnt5a adapte les concentrations du cholestérol intracellulaire aux besoins de la cellule. Wnt5a favorise l'export du cholestérol depuis les endosomal/lysosomal (LELs) vers le réticulum endoplasmique (RE), limite l'accumulation intracellulaire du cholestérol, et protège contre l'athérosclérose. D'un point de vue mécanistique, Wnt5a se lie aux membranes riches en cholestérol et interagit spécifiquement avec la protéine membranaire Niemann-Pick C1 (NPC1), la protéine soluble Niemann-Pick C2 (NPC2), deux protéines lysosomales qui régulent l'export du cholestérol à partir des LELs. En conséquence, l'absence de Wnt5a inhibe la fonction lysosomale et l'autophagie, ainsi que la sortie du cholestérol hors des LELs. Ceci résulte en l'accumulation de larges corps d'inclusion intracellulaires, de larges LELs riches en cholestérol, d'une diminution du cholestérol au niveau du RE, et d'une activation de SREBP-2 (sterol regulatory element-binding protein-2) le principal régulateur de la biosynthèse du cholestérol endogène. Ces résultats révèlent une propriété inattendue de la voie de signalisation de Wnt5a, et fournissent de nouvelles bases conceptuelles pour le développement futur de médicaments visant à prévenir l'accumulation de cholestérol, l'athérosclérose et les maladies lysosomales.



## Abstract

---

Wnt signaling plays a critical role in development and adult tissue homeostasis. Here, we identified the Wnt ligand, Wnt5a, as a member of the nutrient/energy/stress sensor, mTORC1 scaffolding complex, which drives lysosomal function and promotes cholesterol trafficking. By decreasing mTORC1 activity and by activating the autophagy-lysosomal axis, Wnt5a senses changes in dietary cholesterol supply, promotes endosomal/lysosomal (LELs) cholesterol egress to the endoplasmic reticulum (ER), and protects against atherosclerosis. Moreover, Wnt5a binds cholesterol-rich membranes and specifically interacts with the polytopic membrane-bound Niemann–Pick C1 (NPC1) and soluble Niemann–Pick C2 (NPC2), two lysosomal proteins that regulate cholesterol export from LELs. Consequently, absence of Wnt5a decoupled mTORC1 from variations in LELs sterol levels, and this resulted in accumulation of large intracellular inclusion bodies, large LELs, decreased cholesterol content in the ER, activation of the sterol regulatory element-binding protein-2 (SREBP-2) a master regulator of cholesterol biosynthesis, and inhibition of autophagy. These results reveal an unexpected function of the Wnt5a pathway, and provide a conceptually new basis for future drug development to prevent cholesterol accumulation, atherosclerosis, and lysosomal storage diseases.

## *List of communications*

---

### **Oral and Poster presentations**

« Role of Wnt5a signaling in cholesterol homeostasis and prevention of atherosclerosis.

Archives of Cardiovascular Diseases Supplements. Volume 9, Issue 2, April 2017, Page 154. **SFC Nantes 6-7th April, 2017.**

« Wnt5a Decreases mTORC1/SREBP2 Activity and Promotes Endosomal Cholesterol Trafficking to the ER in Mice and in Human Vascular Smooth Muscle Cells.

Atherosclerosis supplements June 2018 Volume 32, Page 4. **ISA conference in Toronto June 9-12th, 2018.**

« Wnt5a Decreases mTORC1/SREBP2 Activity and Promotes Endosomal Cholesterol Trafficking to the ER in Mice and in Human Vascular Smooth Muscle Cells.

**Journees campus Illkirch (JCI) 2018.**

Part of the work is presented in the following article:

*«Loss of the adaptor protein ShcA in endothelial cells protects against monocyte macrophage adhesion, LDL-oxydation, and atherosclerotic lesion formation » (Abou-Jaoude et al., 2018).*

Antoine Abou-Jaoude, Lise Badiqué, Mohamed Mlih, Sara Awan, Sunning Guo, Alexandre Lemle, Clauda Abboud, Sophie Foppolo, Lionel Host, Jérôme Terrand, Hélène Justiniano, Joachim Herz, Rachel L. Matz & Philippe Boucher.  
*Scientific Reports, 2018.*



## List of abbreviations

---

**A**CAT1: acyl-CoA cholesterolacyltransferase 1

ASM: acid sphingomyelinase

AMPK: AMP-activated protein kinase

**C**AMKII: calmodulin dependent protein kinase II

CV: cardiovascular

CVD: cardiovascular disease

Chol: cholesterol

CETP: cholesteryl ester transfer protein

**D**SH: dishevelled

DHA: docosahexaenoic acid

**E**PA: eicosapentaenoic acid

ER: endoplasmic reticulum

**H**MGCoA: 3-hydroxy-3-methyl–glutaryl-coenzyme A

HEK: Human embryonic kidney

**I**NSIG1: Insulin-induced gene 1 protein

**J**NK: Jun N-terminal kinase

**L**ELs: late endosome/lysosomes

LDL: Low density lipoprotein

LAL: Lysosomal acid lipase

LIPA: lysosomal acid lipase type A

LAMP-2A: lysosomal associated membrane protein-2A

**M**EFs: mouse embryonic fibroblasts

mTORC1: mechanistic target of rapamycin

MEFs: mouse embryonic fibroblasts

MSTFA: (N-Methyl-N-(trimethylsilyl) trifluoroacetamide

**N**FAT: nuclear factor of activated T cell

NPD: Niemann-Pick disease

NPC: Niemen-Pick type C disease

NTD : N-terminal domain

**P**C: phosphatidylcholine

P: Pellets

PPAR- $\alpha$ : Peroxisome proliferator-activated receptor- $\alpha$

PI3K: phosphoinositide-3 kinase

PI3K: phosphoinositide 3-kinase

PKC: protein kinase C

PLC: phospholipase C

PRAS40: proline rich AKT substrate 40

PCSK9: Proprotein convertase subtilisin/kexin type-9 inhibitors

**R**CT: Reverse cholesterol hypothesis

**S**REBPs: Sterol regulatory element binding proteins

SREBP-2: sterol regulatory element-binding protein-2

SCAP: SREBP cleavage activating protein

SIM: selected ion-monitoring

SMCs: smooth muscle cells

S: Supernatant

**T**<sub>FEb</sub>: transcription factor EB

TSC: Tuberous sclerosis complex

**U**<sub>PR</sub>: unfolded protein response

**V**<sub>SMCs</sub>: vascular smooth muscle cells



## Table of figures

---

Figure 1: Foam cell formation.....	33
Figure 2: Structure of Cholesterol.....	34
Figure 3: Cholesterol synthesis pathway.....	36
Figure 4: Cholesterol biosynthesis via transcriptional regulation of HMGCoA reductase.....	38
Figure 5: Schematic representation of types of autophagy.....	41
Figure 6: Lysosomal cholesterol transport.....	43
Figure 7: mTOR signaling network in cells.....	51
Figure 8: Crystal structure of Wnt8.....	53
Figure 9: LDL receptor gene family members.....	54
Figure 10: Canonical Wnt signaling sequesters GSK3 into the endosomes.....	56
Figure 11: Canonical Wnt Pathway.....	57
Figure 12: Non-Canonical Wnt-Ca <sup>2+</sup> signaling pathway:.....	59
Figure 13: Non-Canonical planer cell polarity pathway:.....	61
Figure 14: Robinow syndrome patient with Wnt5a gene mutation.....	66
Figure 15: Transcription regulation of wnt5a.....	69
Figure 16: Generation of Wnt5a knockout mice.....	87
Figure 17: Accelerated formation of atherosclerotic lesions in smWnt5a- mice.....	89
Figure 18: Increased lipid accumulation in absence of wnt5a.....	90
Figure 19: Lipid accumulation in mice in absence of Wnt5a.....	91
Figure 20: Wnt5a deletion in VSMCs.....	
Figure 21: SMCs transdifferentiation to macrophage like cells.....	95
Figure 22: Cholesterol accumulation in VSMCs Wnt5a-/-.....	96
Figure 23: Increased cholesterol synthesis in VSMCs Wnt5a-/-.....	98
Figure 24: Lipofuscin accumulation in absence of Wnt5a.....	100

Figure 25: Decreased ACAT1 expression in VSMCa Wnt5a-/-.....	101
Figure 26: Decreased ACAT1 expression in MEF LRP-/- cells.....	102
Figure 27: Cholesterol quantification in lysosomal and ER fractions. ....	104
Figure 28: Cholesterol accumulates in lysosomal vesicles in VSMCs Wnt5a-s. .....	107
Figure 29: Regulation of lysosomal function in absence of Wnt5a. A).....	109
Figure 30: Increased mTORC1 and its target genes in absence of Wnt5a. A).	111
Figure 31: Increased mTORC1 and its target genes in absence of Wnt5a. ....	111
Figure 32: Wnt5a downregulates PI3Kinase/mTORC1 pathway.....	113
Figure 33: Cholesterol trafficking rescue by mTORC1 inhibition. ....	116
Figure 34: Wnt5a triggers autophagy.....	117
Figure 35: Wnt5a binds to cholesterol. ....	119
Figure 36: Wnt5a interacts with NPC proteins.. ....	121
Figure 37: Wnt5a counteracts U18666A mediated mTORC1 upregulation.....	122
Figure 38: Significant increase in SLC38A9 expression in absence of Wnt5a.	124

## Table of Contents

---

<b>Acknowledgement</b> .....	<b>5</b>
<b>Resume</b> .....	<b>7</b>
<b>Abstract</b> .....	<b>9</b>
<b>List of communications</b> .....	<b>10</b>
<b>List of abbreviations</b> .....	<b>13</b>
<b>Table of figures</b> .....	<b>17</b>
<b>Table of contents</b> .....	<b>19</b>
<b>Introduction/bibliography</b> .....	<b>24</b>
<b>1. Atherosclerosis</b> .....	<b>25</b>
1.1 General introduction.....	25
1.2 Atherosclerosis develops due to cholesterol accumulation .....	25
<b>2. Actual prevention of atherosclerosis</b> .....	<b>27</b>
2.1 HMG-CoA reductase inhibitors .....	27
2.2 cholesterol absorption inhibitors .....	27
2.3 Bile acid sequestrants .....	28
2.4 Proprotein convertase subtilisin/kinase type-9 inhibitors.....	28
2.5 n-3 fatty acids .....	29
2.6 HDL-C increasing therapy .....	29
<b>3. foam cell formation</b> .....	<b>30</b>
3.1 Macrophages .....	30
3.1 Vascular smooth muscle cells .....	31
<b>4. Cholesterol structure, function and sources in cells</b> .....	<b>34</b>
4.1 Structure and function of cholesterol .....	34
4.2 Endogenous cholesterol synthesis.....	35
4.3 Endocytosis of exogenous cholesterol .....	39
4.4 Autophagy .....	39

<b>5. Cholesterol trafficking in cells .....</b>	<b>42</b>
<b>6. Cholesterol trafficking is altered in atherosclerosis and other cholesterol accumulation diseases .....</b>	<b>44</b>
6.1 Niemann-pick disease .....	44
6.2 Wolman disease.....	45
6.3 Cholesteryl ester storage disease.....	45
<b>7. How cholesterol is sensed at cellular levels .....</b>	<b>46</b>
7.1 The mTORC1 complex .....	46
7.2 Regulation of mTORC1 complex .....	48
7.2.1 Upstream inhibitors of mTORC1.....	48
7.2.2 Upstream activators of mTORC1 .....	49
<b>8. Wnt proteins and signaling pathways .....</b>	<b>51</b>
8.1 canonical Wnt signaling.....	55
8.2 Non-canonical Wnt signaling.....	58
8.3 Wnt signaling in lipid homeostasis .....	62
8.4 Wnt signaling implications in atherosclerosis .....	63
<b>9. Wnt5a .....</b>	<b>64</b>
9.1 Wnt5a mutation disorder.....	64
9.2 Role of wnt5a in cells .....	67
9.1 Role of Wnt5a in atherosclerosis.....	67
<b>Material &amp; Methods .....</b>	<b>71</b>
<b>1. Standard procedures.....</b>	<b>72</b>
1.1 Western blot analysis .....	72
1.2 RNA extraxtion and RT-PCR .....	74
1.3 Transfection of plasmids .....	74
<b>2. Experiments in Vivo (mice model).....</b>	<b>75</b>
2.1 SM22 Wnt5a- mice generation .....	75
2.2 Paigen diet regimen.....	76

2.3 Dissection and coloration of mice aorta.....	76
2.3.1 H&E staining .....	76
2.3.2 Orcein staining .....	76
2.3.3 Sudan IV staining.....	77
2.3.4 Oil Red O staining .....	77
2.4 Dissection of embryos.....	77
2.5 Electronic microscopy of mice tissues.....	77
2.6 Immunohistochemistry in mice tissues .....	77
<b>3. Invitro experiments (cell model) .....</b>	<b>78</b>
3.1 Cell culture and media preperation .....	78
3.2 Immunoprecipitation .....	78
3.3 Adipogenic differentiation .....	79
3.4 Oil red O coloration .....	79
3.5 Treatment of CMLVs with conditioned media from LMTK.....	79
3.6 Wnt5a purification.....	79
3.7 Immunoflorescence .....	80
3.8 Lipofuscin measurement .....	80
3.9 Lysotracker red staining.....	80
3.10 Autophagy measurement.....	81
3.11 Neutral lipids and sterol analysis .....	81
3.12 Liposome preparation and conditioned media treatment.....	83
3.13 Statistical analysis .....	84
<b>Results//Part-I.....</b>	<b>85</b>
<b>1. Accelerated atherosclerosis in mice deleted for wnt5a in VSMCs. ....</b>	<b>86</b>
1.1 smWnt5a- mice generation .....	86
1.2 Sudan IV staining in aortas of mice on pagen diet .....	88
1.3 Immunofluorescence and Oil red O labelling for wnt5a in mice aortas ...	89
1.4 Electronic microscopic data in mice aortas.....	90
<b>2. Lipid accumulation in Wnt5a-/- human VSMCs. ....</b>	<b>91</b>

2.1 Generation of Wnt5a <sup>-/-</sup> cells using CRISPR/Cas9 guided nuclease .....	91
2.2 VSMCs transdifferentiate to macrophage like cells in absence of wnt5a	93
2.3 Lipid quantification in Wnt5a <sup>-/-</sup> VSMCs and the controls.....	95
2.4 Wnt5a inhibits the expression of HMGCoA reductase, synthase and SREBP2.....	97
<b>3. Cholesterol accumulates in lysosomes.....</b>	<b>98</b>
3.1 Cholesterol accumulates in lysosomes in absence of Wnt5a.....	98
3.2 Decreased ACAT1 expression in absence of Wnt5a .....	100
3.3 Cholesterol quantification in lysosomal and ER fractions .....	102
<b>4. Altered lysosomal function .....</b>	<b>104</b>
4.1 Quantification of co-localization of cholesterol in subcellular lysosomal vesicles .....	105
4.2 Regulation of lysosomal function in absence of Wnt5a .....	107
<b>5. Wnt5a downregulates mTORC1 pathway and triggers autophagy.....</b>	<b>110</b>
5.1 Increased mTORC1 phosphorylation in absence of Wnt5a.....	110
5.2 Increased phosphorylation of tyrosine kinase in Wnt5a absence .....	112
5.3 Effects of LiCl and everolimus on cholesterol trafficking .....	113
5.4 Wnt5a promotes autophagy.....	116
<b>6. Wnt5a physically interacts with cholesterol and NPC proteins. ....</b>	<b>117</b>
6.1 Wnt5a binding to cholesterol .....	117
6.2 Wnt5a interacts with NPCs .....	120
6.3 Wnt5a counteracts activation of mTORC1 mediated by U18666A .....	121
6.4 Increased expression of SLC38A9 in absence of Wnt5a.....	123
<b>Results//Part-II .....</b>	<b>125</b>
1. Loss of adaptor protein SchA in endothelial cells protects against atherosclerosis lesion formation.....	126
<b>Article.....</b>	<b>128</b>
<b>Discussion .....</b>	<b>140</b>

Conclusion.....	143
Future perspectives.....	144
<b>References .....</b>	<b>146</b>
Résumé de thèse.....	158

# **Introduction bibliography**

# 1. ATHEROSCLEROSIS

## *1.1 General Introduction*

Atherosclerosis is a growing cause of mortality in western countries. Its clinical manifestations include coronary artery disease and stroke. This disease reached epidemic proportions during the last decades (Taleb, 2016). Lifestyle changes reduce the exposure of risk factors that predispose to atherosclerosis and drug therapy such as Statins were expected to lower the occurrence of the atherosclerotic disease epidemic (Michael S. Brown & Goldstein, 1996). However, despite the use of most recent technologies and secondary therapies for prevention, the recurrence of cardiovascular events after the first acute coronary event is still of about 10% within the first year (Jernberg *et al.*, 2015; Mega *et al.*, 2012; Wallentin *et al.*, 2009). Recently new drug therapy Proprotein convertase subtilisin/kexin type-9 inhibitors (PCSK9) has appeared and is now being used to lower cholesterol levels. But long term effects and efficacy of this therapy is still not known. Thus, in order to increase a healthy life expectancy and treat atherosclerosis, there is a serious need for developing new drug therapies.

## *1.2 Atherosclerosis develops due to cholesterol accumulation*

Atherosclerosis is well recognized as a chronic inflammatory disease that develops due to the accumulation of cholesterol in the intima of the artery (Camejo *et al.*, 1975; Skålén *et al.*, 2002; Ira Tabas *et al.*, 2007). Under normal physiological conditions cholesterol containing lipoproteins can freely enter

and exit the intima of artery (Ira Tabas *et al.*, 2007). However, with increasing concentrations of LDL-C and accompanying endothelial dysfunction, there is a retention of these lipoproteins in arteries and initiation of atherosclerotic lesion development (Ference *et al.*, 2017). Cholesterol retention is then followed by low grade inflammation at susceptible arterial sites with a disturbed blood flow resulting in fatty streak formation. Further damage to the vascular wall is caused with circulating cytokines and growth factors secreted by endothelial cells and smooth muscle cells leading to the development of atherosclerotic plaque (Aziz and Yadav, 2016). The plaque development is however reversible as proposed by the Reverse cholesterol hypothesis (RCT) (Fisher *et al.*, 2012). RCT is a process by which excess cholesterol is removed from tissues and transported to liver. Liver converts this excess cholesterol to bile acid and salts. Lipoproteins involved in this process are HDL-C. The main lipoprotein of HDL-C is Apo A-1. It is synthesized in the intestine and liver. It then moves to the peripheral tissues such as heart and arteries, where it can interact with cholesterol, this results in formation of HDL nascent particles. Binding of these HDL-C particles to ATP-binding cassette, sub-family G, member 1 (ABCG1) and ATP-binding cassette, sub-family A, member 1 (ABCA1) which are a cholesterol export proteins, results in formation of mature HDL-C particles that deliver excess cholesterol to the liver (Marques *et al.*, 2018).

Thus, developing new strategies to reduce cholesterol accumulation and to promote cholesterol reverse may help to prevent atherosclerosis development.

## **2. Actual prevention of atherosclerosis**

Several strategies are used to lower cholesterol accumulation. These include the following:

### ***2.1 HMG-CoA reductase inhibitors (statins)***

HMGCoA reductase inhibitors (3-hydroxy-3-methyl–glutaryl-coenzyme A) commonly known as statins are competitive inhibitors of HMG-CoA reductase, an enzyme required for the cholesterol biosynthesis through mevalonate pathway. Inhibition of the enzyme reduces cholesterol synthesis in the liver. Statins also cause an increase in expression of LDL receptors on the hepatocyte surface which then leads to the increased uptake of LDL-C from blood, lowering the circulating LDL-C levels. Statins can reduce all-cause or mortality by 16% (Wilt *et al.*, 2004). Moreover, they also lower blood triglyceride levels (Catapano *et al.*, 2011). The main causes of statin therapy failure are statin intolerance and the fact that they are not achieving physiological LDL-C levels in high risk cardiovascular patients (Vonbank *et al.*, 2013).

### ***2.2 Cholesterol absorption inhibitors***

Ezetimibe reduces the LDL-C levels by lowering the intestinal absorption of cholesterol coming from dietary sources, but it does not effects the absorption of fat soluble nutrients. When administered as monotherapy, ezetimibe lowers LDL-C levels by 15-22%. However, in combination to statins there is an

increased lowering of LDL-C levels (Bergheanu *et al.*, 2017). There are no known major adverse effects for this class of drugs (Catapano *et al.*, 2011).

### ***2.3 Bile acid sequestrants***

Under normal physiological conditions, bile acids synthesized from cholesterol are secreted in the lumen of intestine but most of them are re-absorbed from the ileum. Bile acid sequestrants bind to the bile acids and prevent their re-absorption thereby depleting liver of its cholesterol contents. When administered at highest doses, bile acid sequestrants cause a reduction of 18–25% in blood LDL-C levels. This group includes cholestipol, cholestyramine and cholesevelam. Gastrointestinal tract intolerance is a common side effect of cholestyramine and cholestipol. However, cholesevelam is better tolerated (Catapano *et al.*, 2011).

### ***2.4 Proprotein convertase subtilisin/kexin type-9 inhibitors***

Proprotein convertase subtilisin/kexin type-9 inhibitors (PCSK9) binds to the LDL receptors, promoting its absorption and degradation in the liver. Thus, inhibition of PCSK9 blocks this LDL-R binding and degradation, thereby promoting LDL-C absorption from plasma. Alirocumab and evolocumab are two FDA approved monoclonal antibodies that inhibit PCSK9 (Robinson *et al.*, 2015; Sabatine *et al.*, 2015). In clinical trial when PCSK9 inhibitor alirocumab and atorvastatin (statin) were administered as monotherapy to patients with non-familial hypercholesterolemia to compare the efficacy of the two drugs, PCSK9 inhibitor lowered LDL-C levels by 50-60% more in comparison with statins (Chaudhary *et al.*, 2017). High cost of therapy and development of immune reaction is a limiting factor in the use of these drugs.

Manufacturing of another PCSK9 inhibitor compound bococizumab was stopped due to development of auto-antibodies that hindered the LDL-C lowering function of this drug in body (Bergheanu *et al.*, 2017). Therefore, this class of drugs so far is a promising candidate for the treatment of atherosclerosis but there is still a need for developing new low cost effective therapies.

### ***2.5 n-3 fatty acids***

Lipid lowering mechanisms of n-3 fatty acids are poorly understood. However, n-3 fatty acids can lower triglycerides levels up to 45% by interacting with PPARs. A study in hypercholesteremic patients conducted in Japan, reported a reduction of cardiovascular disease (CVD) by 19% upon administration of n-3 fatty acids in fish oil to the patients (Aung *et al.*, 2018). The group includes eicosapentaenoic acid (EPA) and docosahexaenoic acid (DHA) (Kotwal *et al.*, 2012).

### ***2.6 HDL-C increasing therapy***

#### ***Cholesteryl ester transfer protein (CETP) inhibitors***

Small molecule inhibitors cause a direct inhibition of CETP thus increasing the HDL-C levels by  $\geq 100\%$ . However, this increase in HDL-C has shown no effects on Cardiovascular (CV) endpoints (Barter *et al.*, 2007; Nicholls *et al.*, 2015; Schwartz *et al.*, 2012). The drugs included in this group are Evacetrapib and Torcetrapib.

### **3. Foam cell formation**

Foam cells are the macrophage or smooth muscle cells in arterial intima that take up oxidized LDL and become lipid laden. This gives them a foamy appearance (Yan *et al.*, 2011). Until recently, it was considered that macrophages are the sole source of foam cells (Libby *et al.*, 2014; I. Tabas *et al.*, 2015). However, about 40-50% of foam cells that accumulate in atherosclerotic plaques originate from VSMCs (Allahverdian *et al.*, 2014; Rong *et al.*, 2003; Shankman *et al.*, 2015).

#### ***3.1 Macrophages***

The prime drivers of atherogenesis are the monocyte-derived macrophage cells. Upon cholesterol accumulation or decreased cholesterol efflux by ATP-binding cassette A1 (ABCA1), which is member of A subfamily of ABC proteins and causes cholesterol efflux to apolipoprotein A-1, there is enhanced production of monocyte derived macrophage cells and atherogenesis is initiated (Murphy *et al.*, 2014). Macrophages at site of lesion in the intima of artery have an ability to uptake the cholesterol carrying lipoproteins either by endocytosis, scavenger receptor mediated engulfing of cholesterol, or pinocytosis (Haka *et al.*, 2009). The accumulated cholesterol promotes cholesteryl ester accumulation in these cells and modulate their function as well. Tabas and colleagues exemplified that cholesterol may affect the macrophage function (Feng *et al.*, 2003; I. Tabas, 2004). As most of the cholesterol taken up by the macrophages is ultimately converted to cholesteryl esters by the ACAT1 enzyme in the ER and stored as foam cells, some of the

un-esterified cholesterol can stay and get accumulated in the ER. This results in the activation of unfolded protein response (UPR) that may lead to cell apoptosis. UPR is a cellular response to ER stress conditions such as accumulation of un-esterified cholesterol or unfolded proteins in the ER. This stress state is sensed by several ER sensors having luminal, transmembrane and cytoplasmic domains and cellular response is initiated to alleviate ER stress. If alleviation is not possible UPR leads to cell death. The clinical significance of UPR and its role in atherogenesis and plaque rupture are in studies (Bravo *et al.*, 2013). It represents one way how the cholesterol can modulate the macrophage function.

### **3.2 *Vascular smooth muscle cells***

Other cell types that accumulate cholesterol in vascular wall are VSMCs. VSMCs account for 40-50% of foam cells formation (Allahverdian *et al.*, 2014; Rong *et al.*, 2003; Shankman *et al.*, 2015). The plasticity of VSMCs is of particular importance, because VSMC-derived macrophage-like cells have impaired phagocytic functions and efferocytosis, critical for phagocytic removal of apoptotic cells, and vesicular and cholesterol trafficking events (Kasikara *et al.*, 2018). Cholesterol loading of smooth muscle cells (SMCs) *in vitro* results in loss of SMC specific marker such as smooth muscle alpha actin (Acta2) and myosin heavy chain (Myh11) on these cells and induces the expression of macrophage markers such as Mac2 and CD68 (**Fig.1**) (Rong *et al.*, 2003). There is a decreased expression of cholesterol efflux transporter protein ABCA1 in SMCs in early and advanced atherosclerotic disease stages. Kruppel-like factor 4 (KLF4) is a zinc finger transcription factor and plays

role in cellular proliferation and differentiation. KLF4 acts as a transcription repressor in the phenotype switching of SMCs to macrophages (I. Tabas *et al.*, 2015). Expression of ABCA1 was greatly reduced in foam cells coming from smooth muscle cells that expressed SMC specific marker actin+ as compared to smooth muscle cells that expressed macrophage specific marker CD68+. Thus these foam cells have an impaired cholesterol reverse transport and they contribute to plaque cholesterol accumulation (Allahverdian *et al.*, 2014).

Cholesterol is a major structural component of plasma membrane in mammalian cells. However, it can be toxic in high concentrations and leads to development of foam cell and cellular stiffening, which may compromise vascular integrity and signaling at cellular levels. Therefore, cholesterol synthesis, uptake and export in cells needs to be tightly regulated.

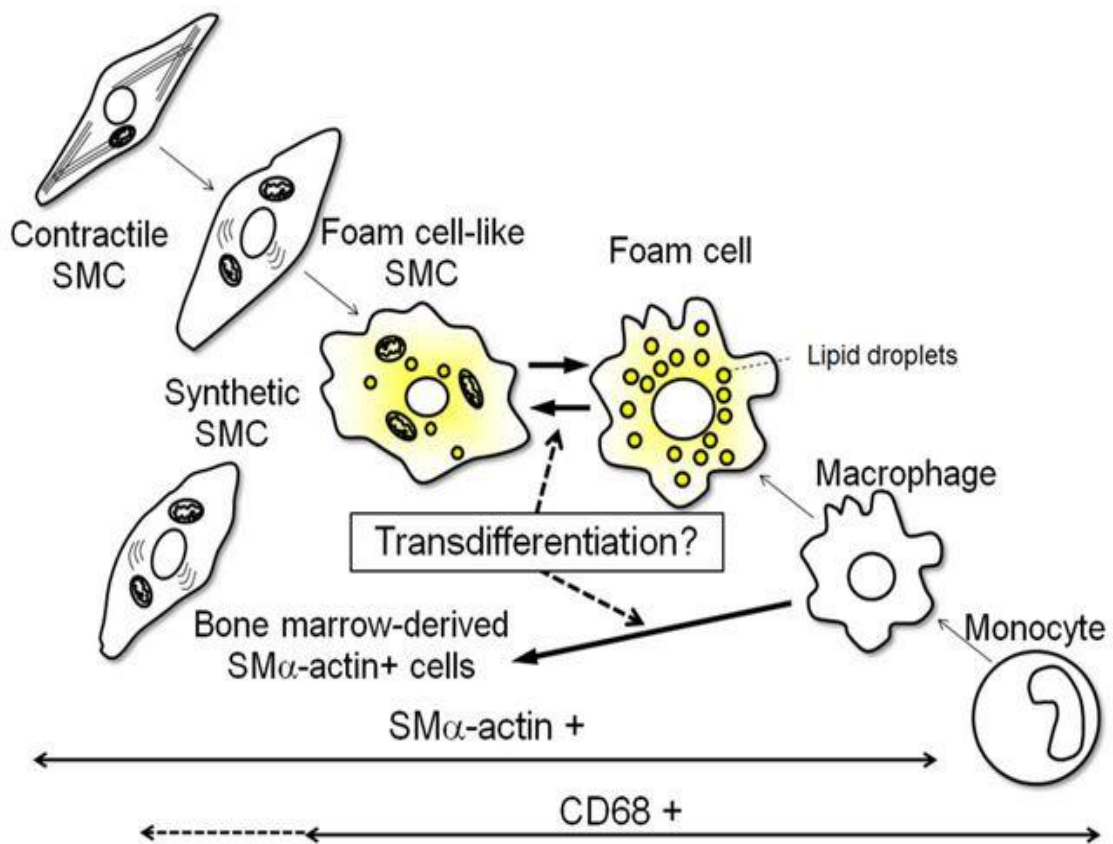


**Figure 1: Foam cell formation.** Foam cell formation in smooth muscle cells and macrophages. Transdifferentiation of SMCs to macrophage like cells in the atherosclerotic plaque (Hiroshi and Masanori, 2015).

## 4. Cholesterol structure, function and sources in cells

### *4.1 Structure and function of cholesterol*

Cholesterol is a sterol (US library of medicine) and an organic molecule. Its structure contains a tetracyclic ring. On one side there is a methyl group and in the other side there is an iso-octyl group and a hydroxyl group attached to the two carbons C17 and C3 respectively (**Fig.2**). It is synthesized in most of the animal cells and is an integral structural components of cell membranes. Cholesterol is important for the synthesis of bile acids, steroidal hormones and vitamin D (Hanukoglu, 1992).

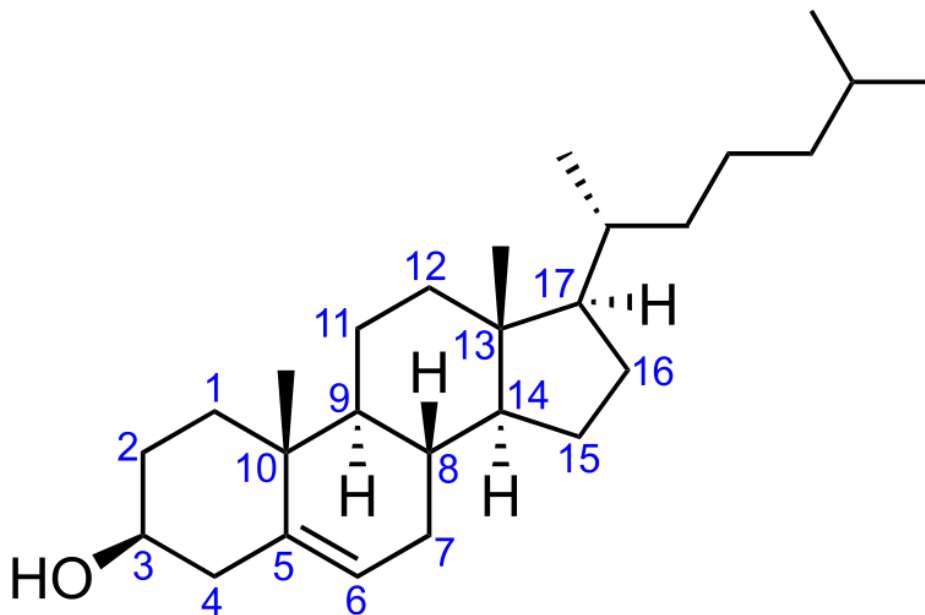


**Figure 2: Structure of Cholesterol.** Cholesterol is a rigid molecule with a hydrophilic group attached at C3 and a hydrophobic side chain at C17 (Wkimedia commons).

Cholesterol facilitates free movement of other lipids in plasma membrane and provides support to it as it is more rigid than most of the membrane lipids (Maxfield & van Meer, 2010). It modulates plasma membrane fluidity and thickness and is distributed non-randomly in the membrane (Song *et al.*, 2014). The Variations in cholesterol levels can lead to disturbance in signal transduction (Linton *et al.*, 2019). It affects many membrane receptors (Paila & Chattopadhyay, 2010), peptides (Tripathi & Jeremic, 2011), ion channels (Levitan *et al.*, 2014), transporters (Hong & Amara, 2010; Yeagle *et al.*, 1988). Cholesterol is an integral component of lipid rafts in the plasma membrane. Lipid rafts are cholesterol and sphingolipids-rich microdomains in the cell membrane. They are the site for colocalization of proteins responsible for signal transduction. Lipid rafts are of two types: Caveolae: they also have flask like invaginations which contains caveolin-1 as their main protein. The caveolin 1 is involved in signal transduction and vesicular trafficking. The other type of rafts are planer lipid rafts. They are found in neurons and have flotillin as their main protein. Flotillin functions to recruit signaling proteins into the rafts (Lemaire-Ewing *et al.*, 2012).

#### ***4.2 Endogenous cholesterol synthesis***

Cholesterol is synthesized endogenously in all animal cells. 80% of this synthesis occurs in liver and intestines. Cells synthesize cholesterol endogenously by the mevalonate pathway (**Fig.3**) (Harvard health, 2017).

### *Cholesterol synthesis mevalonate pathway*

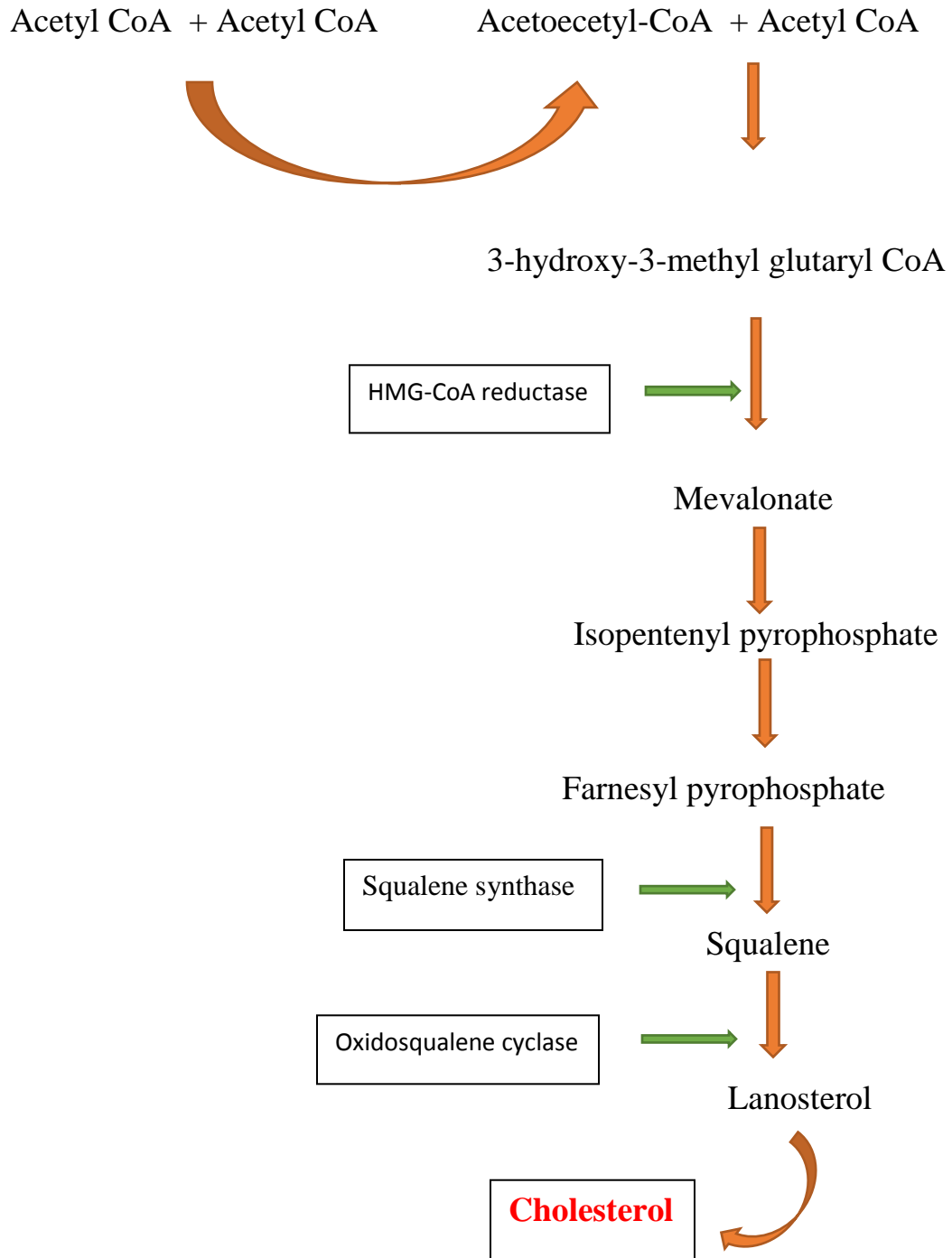


**Figure 3: Cholesterol synthesis pathway.** Successive enzymatic reactions leading to the synthesis of cholesterol (Griffin *et al.*, 2017).

This cholesterol synthesis in cells depends on the cholesterol sensing function of Endoplasmic reticulum (ER). In ER, Sterol regulatory element binding proteins (SREBPs) are transcription factor family and are involved in regulating cholesterol synthesis (Brown and Goldstein, 1997) in association with two other proteins, INSIG1 (Insulin-induced gene 1 protein) and SCAP (SREBP cleavage activating protein) in the ER. INSIG is an ER membrane protein that binds to SCAP and blocks the export of SCAP/SREBP2 from ER. Under normal circumstances the SREBP2 is bound to INSIG and SCAP. In conditions of low cellular cholesterol, there is a conformational change in the SCAP that leads to dissociation of INSIG1 from the complex (Radhakrishnan *et al.*, 2008) and the SREBP2-SCAP together leave the ER and enter Golgi where SREBP2 leaves SCAP under the action of S1P and S2P proteases. The activated SREBP2 enters the nucleus and activates transcription of its target genes, thus initiating cholesterol synthesis (**Fig.4**) (Horton *et al.*, 2002). SREBPs initiate the expression of HMG-CoA reductase and synthase enzymes and also mevalonate kinase, enzymes responsible for cholesterol synthesis by mevalonate pathway hence increasing cellular cholesterol synthesis.

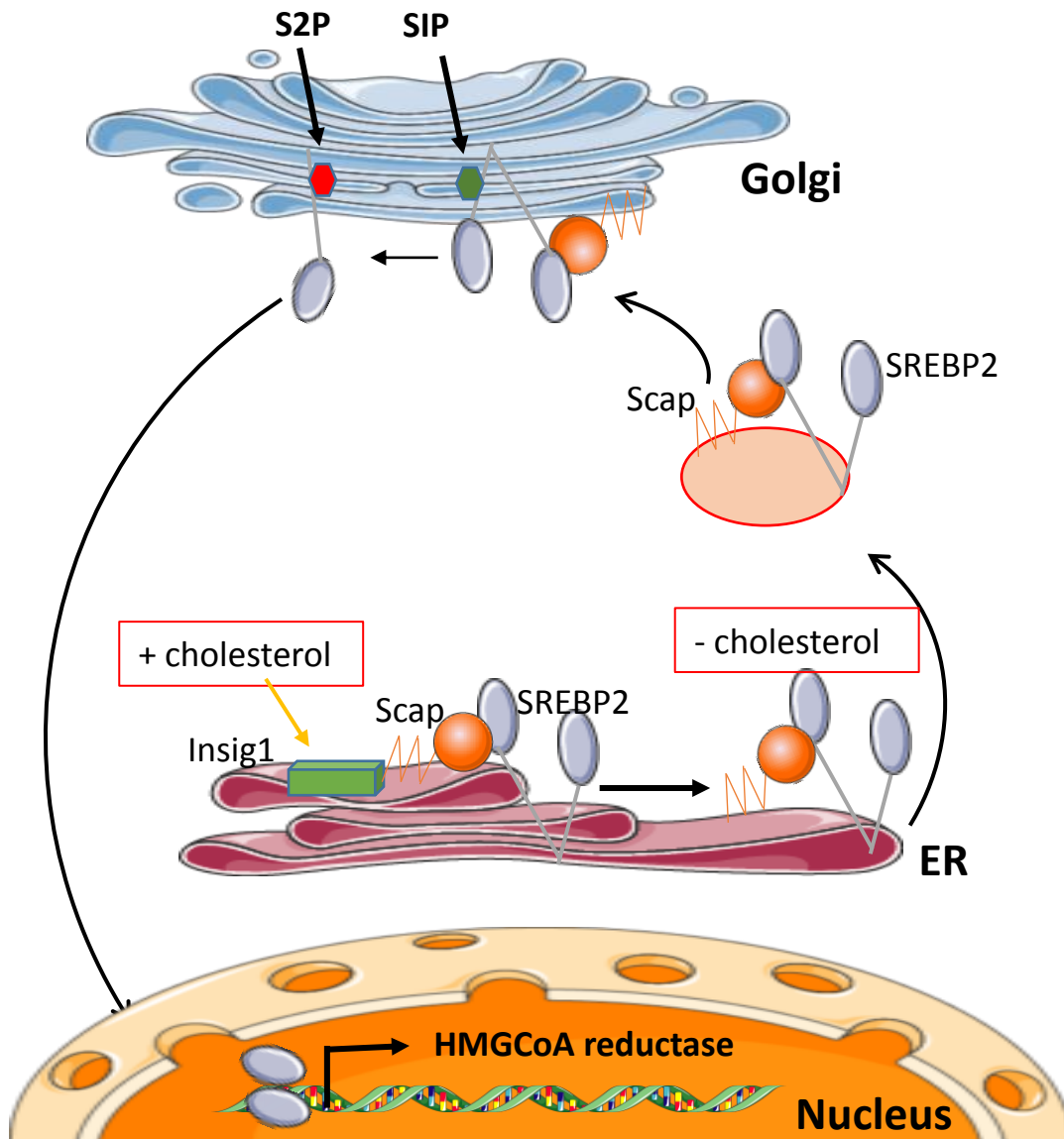


**Figure 4: Cholesterol biosynthesis via transcriptional regulation of HMGCoA reductase.** Scap-Insig-SREBP2 complex is present in the ER membrane. In conditions of low cholesterol, insig disintegrates from Scap and scap-SREBP2 moves to the Golgi. Action of two proteases releases active SREBP2 which enters the nucleus and activates the transcription of target genes including HMGCoA-reductase. In condition of high cholesterol, Insig-scap-SREBP2 stay together as a complex in ER, there is no nuclear translocation of SREBP2 thereby inhibiting cholesterol biosynthesis (Goldstein and Brown).

### ***4.3 Endocytosis of exogenous cholesterol***

30% of body cholesterol comes from the dietary sources. Therefore, an appropriate balance of dietary cholesterol is important for maintaining a healthy wellbeing and steady state blood cholesterol concentrations (Lichtenstein *et al.*, 2006). The cholesterol is hydrophobic in nature and cannot enter the cell. The cell takes up exogenous cholesterol by two processes phagocytosis or receptor mediated endocytosis.

Phagocytosis by cells is responsible for uptake of large particles. After a phagosome is formed there is acidification and fusion of phagosome to the endosome/lysosome that results in breakdown of large particles into simple components (Casem, 2016).

Cells uptake LDL particles by receptor mediated endocytosis (Casem, 2016). LDL particles bind to LDL receptor (LDLR) on the target cells plasma membrane and are endocytosed by a clathrin-mediated process. Clathrin coated vesicles are parts of cell membrane coated with a bristle shape structure called clathrin, specialized to perform receptor-mediated endocytosis. As the clathrin coated vesicles uncoat, the LDL-receptor complex gains entry in the endosomal pathway through endocytosis, where by the LDLR is recycled to plasma membrane and the LDL cholesterol is converted to free cholesterol (Goldstein & Brown, 2015).

### ***4.4 Autophagy***

Autophagy is a cellular recycling and degradation process for the removal of misfolded proteins, pathogens and organelles such as mitochondria & ER. It is characterized into three types. First is the Microautophagy, in this the

lysosomal membrane protrudes directly to endocytose the cargo proteins to be recycled. Second is the Macroautophagy, in this the double membrane autophagosomes fuse to the membrane of lysosomes to deliver the cytosolic contents to the lumen of lysosomes. Third is the chaperon mediated autophagy (CMA), here the substrate proteins having a KFERQ motif (a pentapeptide sequence on substrate proteins necessary for their recognition by cytosolic chaperon proteins) translocate across the lysosomal membrane in association with the chaperone proteins which are detected by the lysosomal receptor lysosomal associated membrane protein-2A (LAMP-2A) (**Fig.5**) (Glick *et al.*, 2010; Orenstein & Cuervo, 2010). LAMP2A is a lysosomal membrane glycoprotein responsible for translocation of cytosolic proteins across the lysosomal membrane (Issa *et al.*, 2018).

LC3 is a marker of autophagy measurement. LC3 I is localized in the cytosol of autophagosomes while LC3 II is bound on the outer and inner autophagosome membrane. Upon fusion to lysosomes, the outer LC3 detaches whereas the cytosolic LC3 is degraded in the lysosome (Mizushima *et al.*, 2010).

Another marker for autophagy measurement is SQSTM1/p62, P62 is a receptor for ubiquitinated cargo proteins and upon binding to them it sequesters them into the autophagosome lumen to bind the LC3. P62 turnover represents the autophagy activity of cells (Orhon & Reggiori, 2017).

Autophagy is involved in metabolism of proteins, glucose and recently it has been demonstrated to have a role in cholesterol metabolism (Kovsan *et al.*, 2010). In autophagy, double membrane autophagosomes are formed that collect the cell debris from the cell cytoplasm such as cholesterol and amino acids for degradation. These autophagosomes then fuse to the lysosomes to deliver cholesterol and other components into the lysosomal lumen, where

these cholesterol and proteins are reused (Ouimet *et al.*, 2011) other cell debris like dead organelles are degraded. Thus, autophagy is responsible for delivering these membrane rich autophagosomes to the lysosomes.

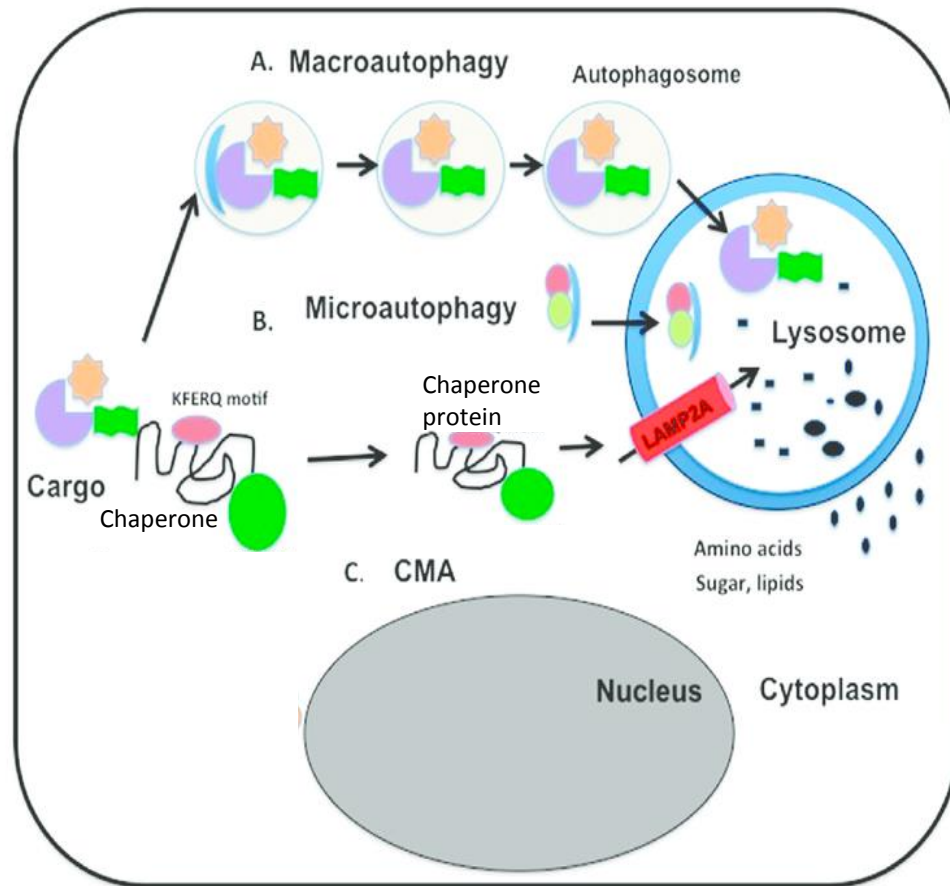


**Figure 5: Schematic representation of types of autophagy.** Three types of autophagy are Macroautophagy, microautophagy and chaperon mediated autophagy. Autophagy delivers cargo proteins to the lysosome for degradation (Dash *et al.*, 2016).

## **5 Cholesterol trafficking in cells**

Cholesterol trafficking is not a well-known process. What is known is that in the lumen of lysosomes, LDLR separates from LDL particles and is recycled to the plasma membrane, whereas, lysosomal acid lipase type A (LIPA) enzyme acts on the LDL particles and causes their de-esterification into cholesterol and triglycerides (Chang *et al.*, 2006). As free cholesterol is not soluble in the hydrophilic environment of lysosomes it requires the action of two proteins for its transport out of lysosomes, these proteins are called NPC1 (Niemann-Pick type C 1) and NPC2 (Niemann-Pick type C 2) (Infante *et al.*, 2008; Mesmin *et al.*, 2013). NPC2 is a luminal protein and functions to transport cholesterol out of the lysosomal lumen. Structural analysis of NPC2 shows that the protein has a cholesterol binding domain in a hydrophobic pocket (Xu *et al.*, 2007). Cholesterol entering the lysosome is taken up by NPC2.

NPC1 is a transmembrane protein located at the lysosomal membrane, structural analysis of NPC1 reveals that the protein has a hydrophobic pocket and an N-terminal domain (NTD) that also enables cholesterol binding (Kwon *et al.*, 2009). It is suggested that Cholesterol is transferred from NPC2 to NTD of NPC1 (**Fig.6**) (Gong *et al.*, 2016) but only part of mechanism is described so far.

Cholesterol transport between NPC1 and NPC2 was studied by Michael S. Brown and colleagues using purified proteins. They found that cholesterol transfer reaction kinetics from NPC2 to NPC1 (NTD) was rapid at 4°C and 37°C. While the inverse transfer of cholesterol from NPC1 (NTD) to NPC2 was very slightly possible only at 37 °C (Infante *et al.*, 2008). The transfer kinetics from NPC1 to NPC2 could be slower because of the absence of

another protein. In physiological situation cholesterol transfer might require some other protein that works together with NPC1 and NPC2 proteins.

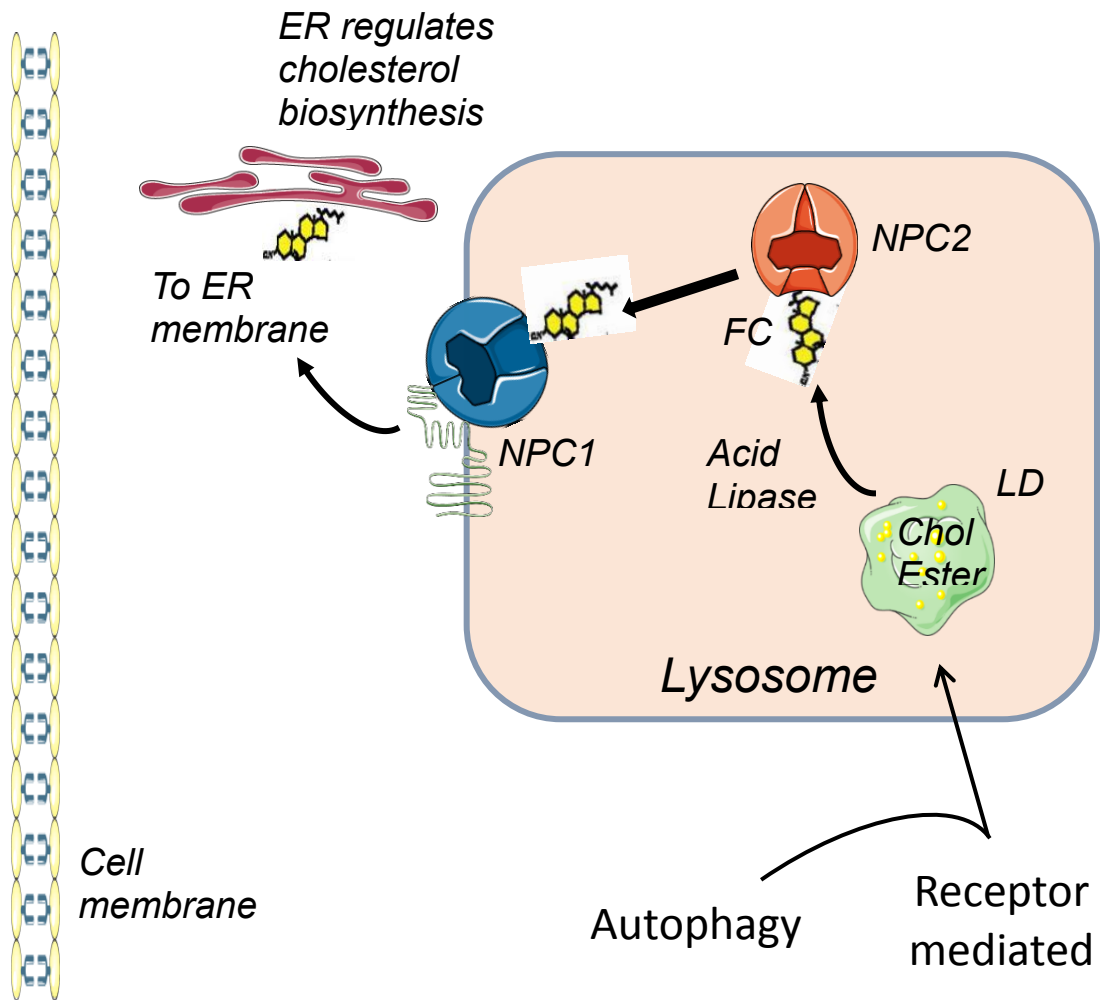


**Figure 6: Lysosomal cholesterol transport.** Model of cholesterol transport from LDL particles to lysosomal membrane mediated by NPC1 & 2 proteins. Endocytosed free cholesterol in lysosome is taken up by NPC2 protein, which then delivers it to NPC1. Cholesterol is then exported out of lysosome to the ER (Infante *et al.*, 2008).

## **6 Cholesterol Trafficking is altered in atherosclerosis and also in other cholesterol accumulation diseases**

Macromolecules as lipids and oligosaccharides are routinely catabolized in lysosomes and broken down into simpler subunits which are exported and reused in cell metabolism. However, in conditions of dysfunctional lysosomal catabolic processing, these complex undegraded molecules accumulate in the cells and tissues in large amounts. Lysosomal storage diseases (LSDs) are a group of 70 different diseases involving lysosomal dysfunction. These are autosomal inherited disorders affecting 1 out of 5000 births. It mostly occur at childhood and infancy however, it can also develop in adulthood (Platt *et al.*, 2018). There is no cure for these pathologies. Most common LSDs are Niemen-Pick type C disease (NPC), and Wolman disease. Other severe form of the cholesterol accumulation disease is cholesteryl ester storage disease.

### ***6.1 Niemann-Pick disease***

Niemann-Pick disease (NPD) is a rare genetic disorder due to impaired fat metabolism. It is characterized into 05 types as NPD types A, B, C, D, and E. NPD type A and B develop due to a deficiency of enzyme acid sphingomyelinase (ASM), the enzyme is responsible for breaking down sphingomyelin, a fatty substance mostly found in the nervous tissues. In this disease there is frequent accumulation of sphingomyelin, in the spleen, brain and liver tissue. Niemann-Pick disease type C (NPC) is an autosomal rare genetic disorder that effects 1:120,000 in a population (Rosenbaum et al.,

2011). NPC develops due to functional mutation in two genes *NPC1* and *NPC2* (Bi & Liao, 2010). In 95% of cases the mutations are in *NPC1* gene and 5% in *NPC2* gene (Zech *et al.*, 2014). These genes encode for two lysosomal proteins NPC1 (Niemann-Pick type C 1) and NPC2 (Niemann-Pick type C 2) that are involved in cholesterol transport in the lysosomes. Genetic mutations in these genes result in cholesterol accumulation in lysosomes and its impaired transport. NPC disease can present fatal neonatal disease to neurological disorders in adults. Clinical diagnosis of NPC disease is difficult as disease presentation is mainly uncharacteristic with only motor delay, mild clumsiness and hepatomegaly (Tängemo *et al.*, 2011).

## ***6.2 Wolman disease***

Wolman disease is also a genetic rare autosomal recessive disorder that develops due to a genetic mutation that leads to complete absence of lysosomal acid lipase enzyme (Lohse *et al.*, 1999). The disease can be fatal in the early stages of life. In absence of the enzyme, lipids and cholesterol accumulate in many tissues and organs of the body that result in a variety of symptoms like bloating, adrenal calcifications, liver and spleen enlargement and vomiting (Pagani *et al.*, 1998).

## ***6.3 Cholesteryl ester storage disease (CESD)***

Cholesteryl ester storage disease is a rare genetic disorder that develops due to partial deficiency of Lysosomal acid lipase (LAL) enzyme. There is a different LIPA gene mutation than from the one responsible for Wolman disease. Patients have low levels of enzymatic activity sufficient to survive into adulthood (Lohse *et al.*, 1999). LAL is responsible for hydrolysis of cholesteryl ester and triglycerides, in absence of the enzyme complex

carbohydrates (mucopolysaccharides) and lipids (mucolipids) accumulate in the lumen of lysosomes thus increasing their size. The consequences of this lipid accumulation are fatty steatosis resulting in hepatomegaly and fibrosis leading to micro nodular cirrhosis (Pagani *et al.*, 1998).

## **7 How cholesterol is sensed at cellular levels**

### ***7.1 The mTORC1 complex***

Mechanistic target of rapamycin (mTORC1), is an atypical serine/threonine kinase belonging to phosphoinositide 3-kinase (PI3K) and acts as cholesterol, nutrient, energy, amino acid and stress sensor in cells (Laplante & Sabatini, 2012). It controls many cell functions as differentiation, proliferation, transcription, translation, cell growth and metabolism. Downstream effectors of mTORC1 are p70 ribosomal protein S6 kinase 1(S6K1) and eIF4E binding protein 1(4EBP1) (Menon *et al.*, 2014). Under normal circumstances, they are bound to eIF3 and are inactive (Goldstein *et al.*, 2006). Binding of activated mTORC1 to eIF3 phosphorylates S6K1 and 4EBP1 (Jelinek *et al.*, 2011; Millard *et al.*, 2005). The phosphorylation of 4EBP1 by mTORC1, releases it from translation initiator eIF4E and initiates translation of proteins and cell growth (Jelinek *et al.*, 2011).

mTORC1 is also associated with amino acid metabolism. Lysosomes are the site of activation of mTORC1 where it is activated by the nutrient signals carried by amino acids and glucose. This activation of mTORC1 is mediated by the Rag GTPases. Rag GTPases are a group 4 enzymes that include Rag A,B, C and D. They are present in dimers. GTP loading of Rag A and B causes

the hydrolysis of Rag C and D leading to the binding of Rag heterodimer to mTORC1 and anchoring mTORC1 to the lysosomal surface (E. Kim *et al.*, 2008; Sancak *et al.*, 2010; Sancak *et al.*, 2008). Another GTPase Rheb at the lysosomal membrane activates the kinase activity of mTORC1 and substrate phosphorylation is activated (Menon *et al.*, 2014; Perera & Zoncu, 2016; Sancak *et al.*, 2008). SLC38A9 is a lysosomal membrane protein homologous to amino acid transporters. It serves as an arginine sensor protein in the mTORC1 complex (Wyant *et al.*, 2017) and regulates the transport of many amino acids out of lysosomes. Arginine activates SLC38A9, this activates mTORC1 phosphorylation and amino acid efflux out of lysosomes (Wyant *et al.*, 2017).

Autophagy is activated resulting in a higher cholesterol delivery to the lysosomes and hence more cholesterol is transported from lysosomes to ER, increasing the ER cholesterol levels (Eid *et al.*, 2017). mTORC1 limits autophagy by regulating nuclear translocation of Transcription factor EB (TFEB). Transcription factor EB (TFEB) belongs to MiT/TFE family of transcription factors (Fang *et al.*, 2017). It controls the transcription of lysosomal genes thereby regulating lysosomal biogenesis and autophagy (Fang *et al.*, 2017). In conditions of aberrant lysosomal functioning, mTORC1 promotes dephosphorylation and nuclear translocation of TFEB where it activates transcription of its target genes. This results in enhanced autophagosome-lysosomal complexes and lysosomal biogenesis (Sardiello *et al.*, 2009).

Cholesterol entering the cell is endocytosed into the lysosomal compartments and it is also synthesized endogenously in cells. Cells therefore, need to adapt the cholesterol levels to their metabolism. Hence, there are some cholesterol

sensing mechanisms in cells that regulate cellular cholesterol levels. Recently it was discovered that mTORC1 is involved in lysosomal cholesterol regulation (Castellano *et al.*, 2017). Lysosomal cholesterol controls mTORC1 activation via SLC38A9-NPC1 complex (FERENCE *et al.*, 2017). Cholesterol entering the lysosomes activates the phosphorylation of mTORC1 through SLC38A9 and its conserved cholesterol responsive motifs. Phosphorylated mTORC1 inhibits cholesterol trafficking and drives cholesterol synthesis in cells. This results in increased cholesterol accumulation inside the cells. To export this accumulated cholesterol out of the cells another lysosomal membrane protein NPC1 is activated. NPC1 binds to SLC38A9 and inhibits mTORC1 phosphorylation, thus promoting cholesterol export (Castellano *et al.*, 2017).

## ***7.2 Regulation of mTORC1 complex***

### ***7.2.1 Upstream inhibitors of mTORC1***

Tuberous sclerosis complex (TSC) is an autosomal disease where benign tumors develop in multiple organs of the body such as skin, kidney, brain and heart. It is a rare disorder due to the mutation of genes encoding for TSC 1 & 2 protein (Yang & Guan, 2007). TSC1 & 2 proteins exist in a complex where the role of TSC1 is to stabilize the complex and TSC 2 exerts GTPase activity on downstream effectors. In cells TSC complex is the main inhibitor of mTORC1. TSC complex directly inhibits Rheb protein which is a positive regulator of mTORC1, resulting in the inhibition of mTORC1 activity to slow down the cell growth and proliferation (Yang & Guan, 2007).

TSC1/2 are downstream effectors in PI3kinase-AKT pathway. Activation of AKT causes phosphorylation of TSC2 and direct inhibition of TSC1/2 complex, thereby promoting mTORC1 activity and cell growth (Manning & Cantley, 2003). AKT can also inhibit PRAS40 (proline rich AKT substrate40). PRAS40 is a protein present in the mTORC1 complex and can bind to the kinase domain of mTORC1 thereby inhibiting its function. Thus, the phosphorylation and subsequent inhibition of PRAS 40 by AKT results in activation of mTORC1 protein (Yang & Guan, 2007). To summarize, TSC1/2 and PRAS40 are inhibitors of mTORC1, while AKT inhibits TSC1/2 and PRAS40 (**Fig.7**).

### ***7.2.2 Upstream activators of mTORC1***

AMP-activated protein kinase (AMPK) acts as an energy sensor for mTORC1 in cell by monitoring the ATP to AMP ratio. In conditions of stress cellular AMP levels increase. This activates AMPK as a result it switches on catabolic processes in cells to generate more ATP and inhibits anabolic processes (Gowans & Hardie, 2014). In low energy states, AMPK phosphorylates TSC2. Phosphorylated TSC inhibits Rheb resulting in down regulation of mTORC1 and dephosphorylation of S6K and 4EBP1 (Yang and Guan, 2007). AMPK also bridges Wnt signaling to the TSC-mTORC1 regulation. Wnt are a family of secreted glycoproteins that bind to frizzled receptors and activate a variety of signaling pathways. Wnt binding to its receptor inhibits through the canonical pathway Glycogen synthase kinase 3 (GSK3) a serine/threonine kinase involved in many cellular functions such as gene expression, apoptosis and mobility (Richard S. Jope *et al.*, 2007). GSK3 has also been reported to phosphorylate more than 40 different proteins (R. S. Jope, 2003). The inhibition of GSK3 $\beta$  results in stabilization and nuclear translocation of  $\beta$ -

catenin (Taelman *et al.*, 2010). This activates transcription of genes for cell growth.

Activation of TSC2 phosphorylation by AMPK acts as a priming phosphorylation for subsequent TSC2 phosphorylation by GSK3 $\beta$ . This hyperphosphorylated TSC2 then inhibits mTORC1 (Inoki *et al.*, 2006). One of the Wnt ligands Wnt3a acts through canonical Wnt signaling and inhibits GSK3 $\beta$ , thereby releasing the inhibitory effects of TSC2 phosphorylation on mTORC1 (Inoki *et al.*, 2006). Thus Wnt3a signaling activates the phosphorylation of mTORC1. However, Other Wnt ligands might behave differently. For instance Wnt3a and Wnt5a, the prototype canonical and non-canonical Wnt ligands activate LRP6 and ROR2 co-receptors respectively by competing for the same Frizzled receptor (Grumolato *et al.*, 2010). Therefore, Wnt ligands are not equivalent regarding the regulation of mTORC1 activation.

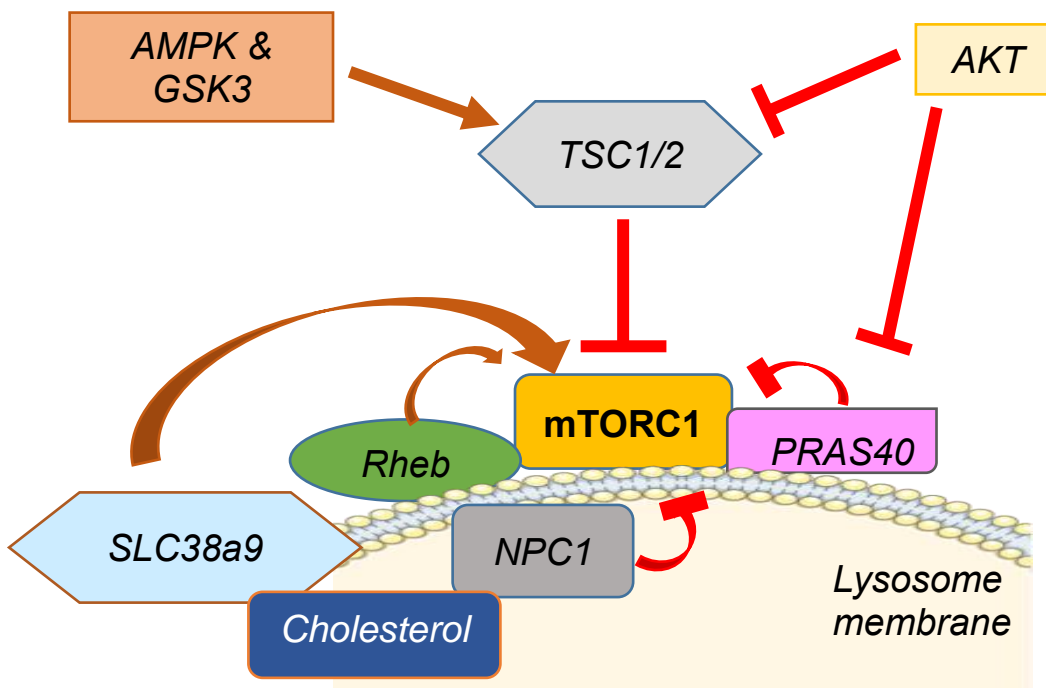


**Figure 7: mTOR signaling network in cells.** mTORC1 is a stress and energy sensor. TSC1/2 via Rheb inactivates mTORC1 signaling. PRAS40 causes direct inhibition of mTORC1. Lysosomal cholesterol controls mTORC1 activation via SLC38A9-NPC1 complex.

## **8 Wnt proteins and signaling pathways**

Wnt (Wingless) genes code for a family of lipid modified secreted proteins. They can bind to various cell types and extracellular matrix and are critical for cell proliferation and differentiation (Clevers, 2006; Logan & Nusse, 2004). Wnt signaling is involved in important biological processes such as embryonic development, angiogenesis and cardiac development (Marinou *et al.*, 2012). Wnts act through various extracellular cysteine domain of frizzled receptors (Fzd). Frizzled are transmembrane receptors having homologous to the G-protein coupled receptors (Angers & Moon, 2009; Logan & Nusse, 2004). Structural analysis of Wnt bound to its Fzd receptor shows that lipids hanging out of Wnt binds Wnt to the receptor. This structural analysis was performed using purified Wnt8-Fzd complexes (Janda *et al.*, 2012). Wnt8 structure has a thumb like N-terminal domain and finger like C-terminal domain to interact with the globular frizzled cysteine-rich domain (CRD). Lipid hangs out from the thumb like NTD of Wnt8 as shown in (**Fig.8**) (Janda *et al.*, 2012). Some of the Wnt proteins need co-receptors for their functioning such as tyrosine kinase receptor RYK, orphan receptor 2 (ROR2), and Low density Lipoprotein receptor related protein 5/6 (Angers & Moon, 2009; Li *et al.*, 2008). LDL receptor gene family is a family of seven type-1 membrane

receptors having an extracellular domain with variable ligand binding sites for extracellular ligand binding and a cytoplasmic domain with internalization motifs and protein binding sites (Howell & Herz, 2001) (**Fig.9**). Canonical Wnt signaling acts through LRP5/6 co-receptors. Wnt binding to ROR2 receptor activates non-canonical Wnt signaling. ROR2 receptor belongs to Tyrosine kinase receptor superfamily. They control many cellular processes such as cell migration, proliferation and differentiation (A. Mikels *et al.*, 2009). So, depending on the receptor type present, various Wnt ligands may act through canonical or/and non-canonical signaling pathways. These signaling pathways are described as below.

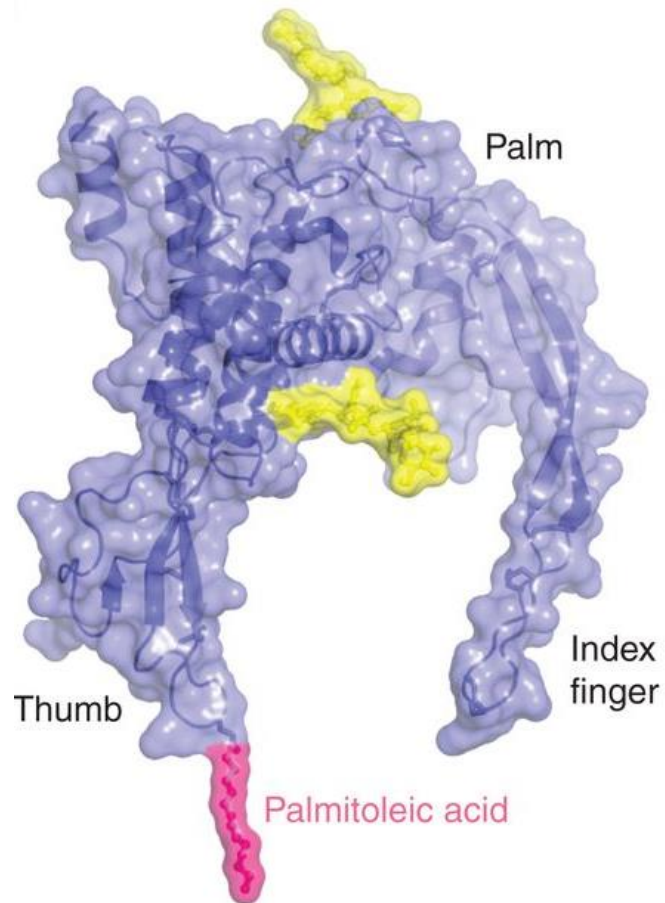


**Figure 8: Crystal structure of Wnt8.** Wnt8 has a Thumb like NTD and a Finger like CTD and a palm. A lipid palmitoleic acid hangs out from the NTD of the structure (Willert and Nusse, 2012).

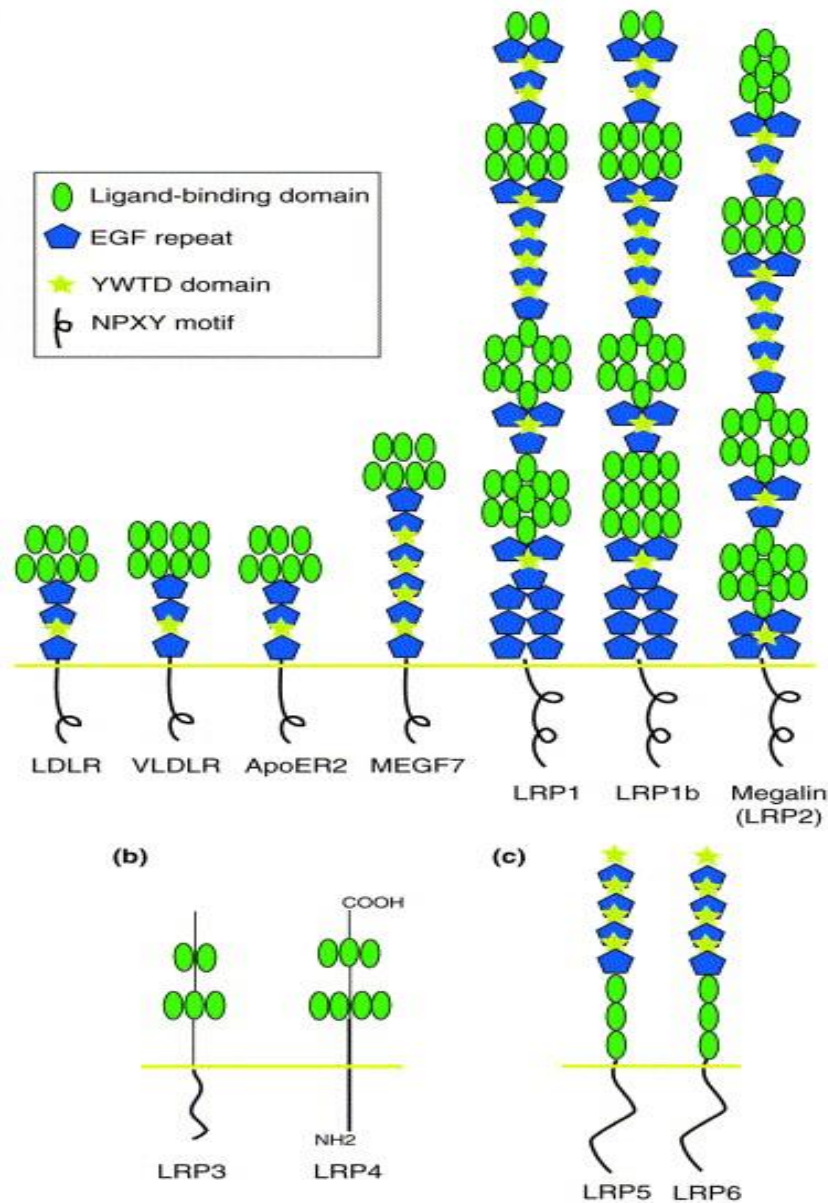


**Figure 9: LDL receptor gene family members.** These receptors have an extracellular domain with ligand binding sites. And an intracellular NPXY with internalization motifs and protein binding sites (Howell & Herz, 2001).

## ***8.1 Canonical Wnt signaling***

Canonical Wnt signaling is involved in cell proliferation and cell fate. It performs many functions at various stages of embryogenesis (Clevers, 2006). Canonical Wnt proteins include Wnts-1, -2b, -3a,-4, -5a, -5b, -6, -7b -8a, -8b, -10a, and -10b, -11, -18 (Siar *et al.*, 2012).

In the absence of Wnt, cytosolic  $\beta$ -catenin is phosphorylated and ubiquitinated for degradation by a destruction complex that includes GSK3 (glycogen synthase kinase 3) (phosphorylates  $\beta$ -catenin at Ser33 and Ser37 sites to generate binding site for  $\beta$ -TrCP), AXIN, CK1 $\alpha$  (casein kinase 1 $\alpha$ ) and APC (adenomatous polyposis coli) (P. M. Bhatt & Malgor, 2014). The destruction complex generates  $\beta$ -TrCP (an adapter protein that assists ubiquitination of  $\beta$ -catenin) recognition site on  $\beta$ -catenin resulting in its ubiquitination and degradation by the proteasome. Canonical Wnt pathway is activated when Wnt binds to frizzled (Fzd) and LRP5/6 receptor at cell surface, activating disheveled (DSH). DSH acts as a relay protein in Wnt signaling connecting receptors to downstream effectors. Its activation recruits AXIN (a large scaffolding protein having binding sites for CK1, GSK3 $\beta$  and  $\beta$ -catenin) to bind to the membrane to bind LRP5/6 and thus, the destruction complex is deactivated. This leads to decreased degradation of low density lipoprotein receptor related protein 5/6 (LRP5/6), GSK3 $\beta$  also leaves the destruction complex and moves to the cell membrane, from where it is sequestered into the endosomal compartments (**Fig.10**). This stabilizes cytosolic  $\beta$ -catenin levels resulting in its increased nuclear migration (**Fig.11**) (Clevers H, 2006) (Logan and Nusse, 2004).

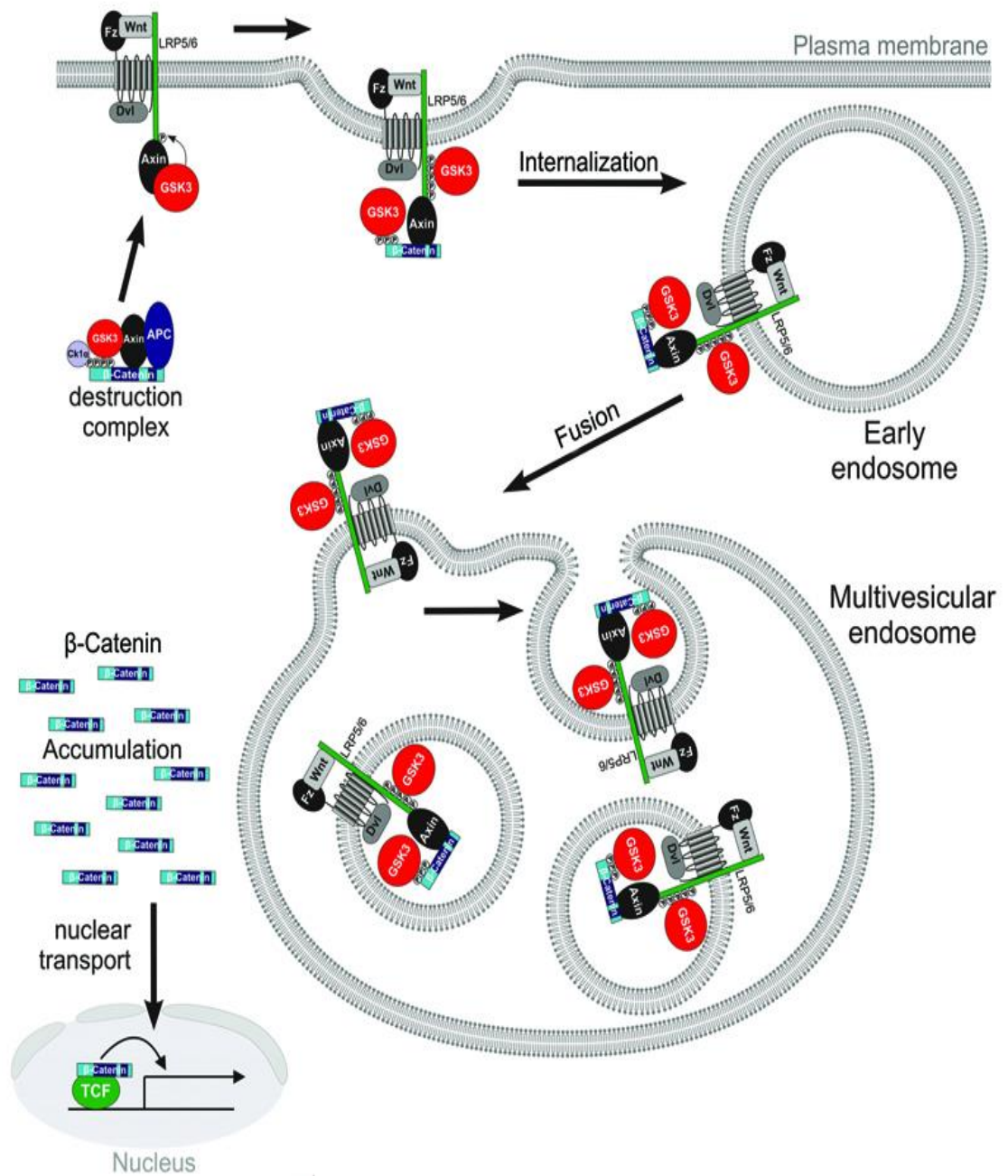


**Figure 10: Canonical Wnt signaling sequesters GSK3 into the endosomes.** Binding of Wnt to its frizzled receptor causes GSK3 to leave the cytosolic destruction complex and bind to Fzd receptor on cell membrane. This sequesters the GSK3 into the endosomal compartments resulting in a stabilization of  $\beta$ -catenin levels (Figure modified from Taelman et al., 2010).

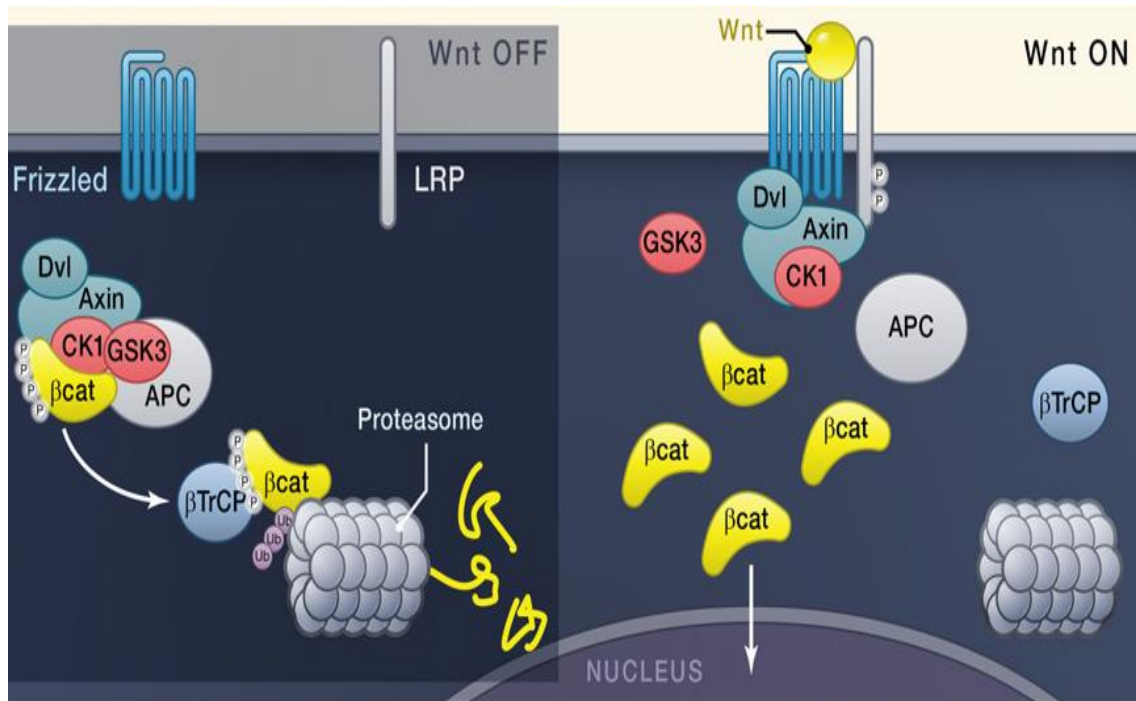


**Figure 11: Canonical Wnt Pathway.** In absence of Wnt, the proteasomal degradation complex is present in cytoplasm, where it binds the  $\beta$ -catenin and it is ubiquitinated and degraded. Wnt induces binding of Axin -LRP(5/6 receptor) thereby the destruction complex falls apart and  $\beta$ -catenin is stabilized.

## ***8.2 Non-canonical Wnt signaling***

Non-canonical Wnt signaling is a  $\beta$ -catenin independent signaling and involves Wnt- $\text{Ca}^{2+}$  and planer cell polarity pathway.

### ***Wnt- $\text{Ca}^{2+}$ signaling Pathway:***

Wnt- $\text{Ca}^{2+}$  signaling pathways controls cells migration, movement and proliferative activities along with controlling cell behavior. It also controls cell fate during embryogenesis (Angers & Moon, 2009; Kuhl *et al.*, 2001; A. J. Mikels & Nusse, 2006). Wnt proteins acting through non-canonical Wnt pathway include Wnts-4, -5a, -5b, -6, 7a, -7b, and -11 (Siar *et al.*, 2012). Wnt5a can act through both canonical and non-canonical Wnt signaling pathways. Wnt binding to Fzd receptor activates DSH. Activated DSH promotes PLC (phospholipase C) mediated release of intracellular  $\text{Ca}^{2+}$  from the ER. Depending on the receptor involved, the increased  $\text{Ca}^{2+}$  levels can either activate serine/threonine kinases PKC (protein kinase C) or CAMKII (calmodulin dependent protein kinase II) (Kuhl *et al.*, 2001). Both PKC and CAMKII activate regulatory proteins NF $\kappa$ B (Nuclear factor kappa B) and NFAT (nuclear factor of activated T cell) that are nuclear transcription factors and control the activation of other genes (**Fig.12**) (Angers & Moon, 2009; De, 2011; Kohn & Moon, 2005).

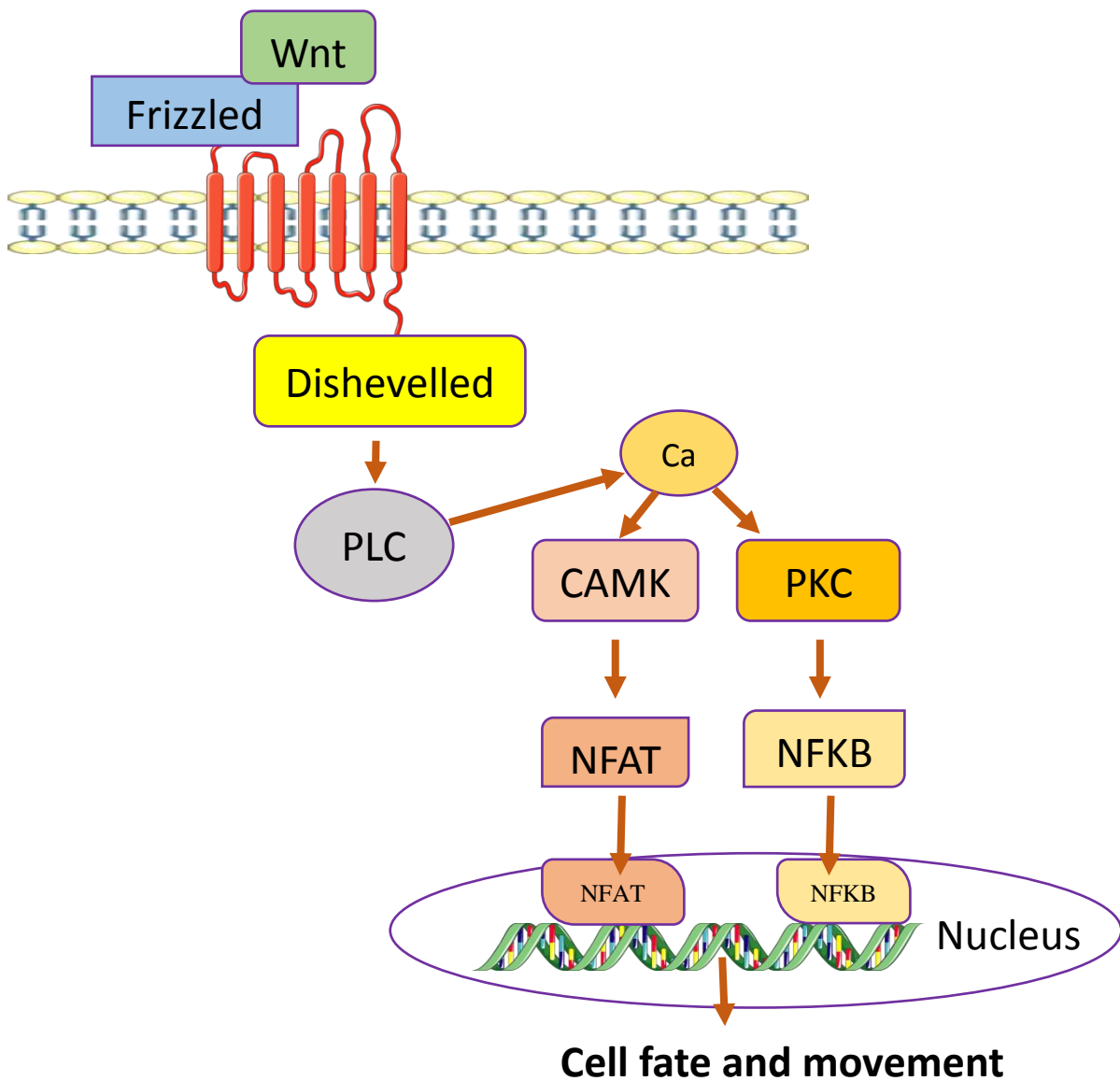


**Figure 12: Non-Canonical Wnt-Ca<sup>2+</sup> signaling pathway:** In Wnt-Ca<sup>2+</sup> signaling, Wnt binding to receptor leads intracellular Ca<sup>2+</sup> release. This leads to activation of cAMP, NF-kB and nuclear factor associated with T-cell translocates to nucleus and activate transcription of genes (Waqas et al., 2018).

***Planer cell polarity pathway (PCP):***

Planer cell polarity pathway gets its name from its function to align clustures of cells along a specific axis. It is involved in cytoskeleton rearrangement and actin polymerization. In this pathway, Wnt binding to Fzd receptors activates DSH. Active DSH then binds to Dishevelled associated activator of morphogenesis 1 (Daam1) protein that connects DSH to small GTPase RhoA. RhoA activates Rho-associated kinase (ROCK) that controls the cytoskeleton movements (Gordon & Nusse, 2006; Komiya & Habas, 2008).

DSH can also bind to another small GTPase Rac1 (encoded by Rac-1 gene). Rac1 activates c-Jun N-terminal kinase (JNK) that controls actin polymerization in cells (Angers and Moon, 2009) (Komiya and Habas, 2008) **(Fig.13)**.

Canonical and non-canonical Wnt pathways may interact at some points. For instance, activation of non-canonical Wnt-Ca<sup>2+</sup> signaling inhibits  $\beta$ -catenin mediated canonical Wnt signaling pathway. Likewise, Wnt-JNK is involved in non-canonical signaling pathway, it may lead to  $\beta$ -catenin phosphorylation promoting its nuclear translocation in canonical Wnt signaling (Williams & Insogna, 2009).

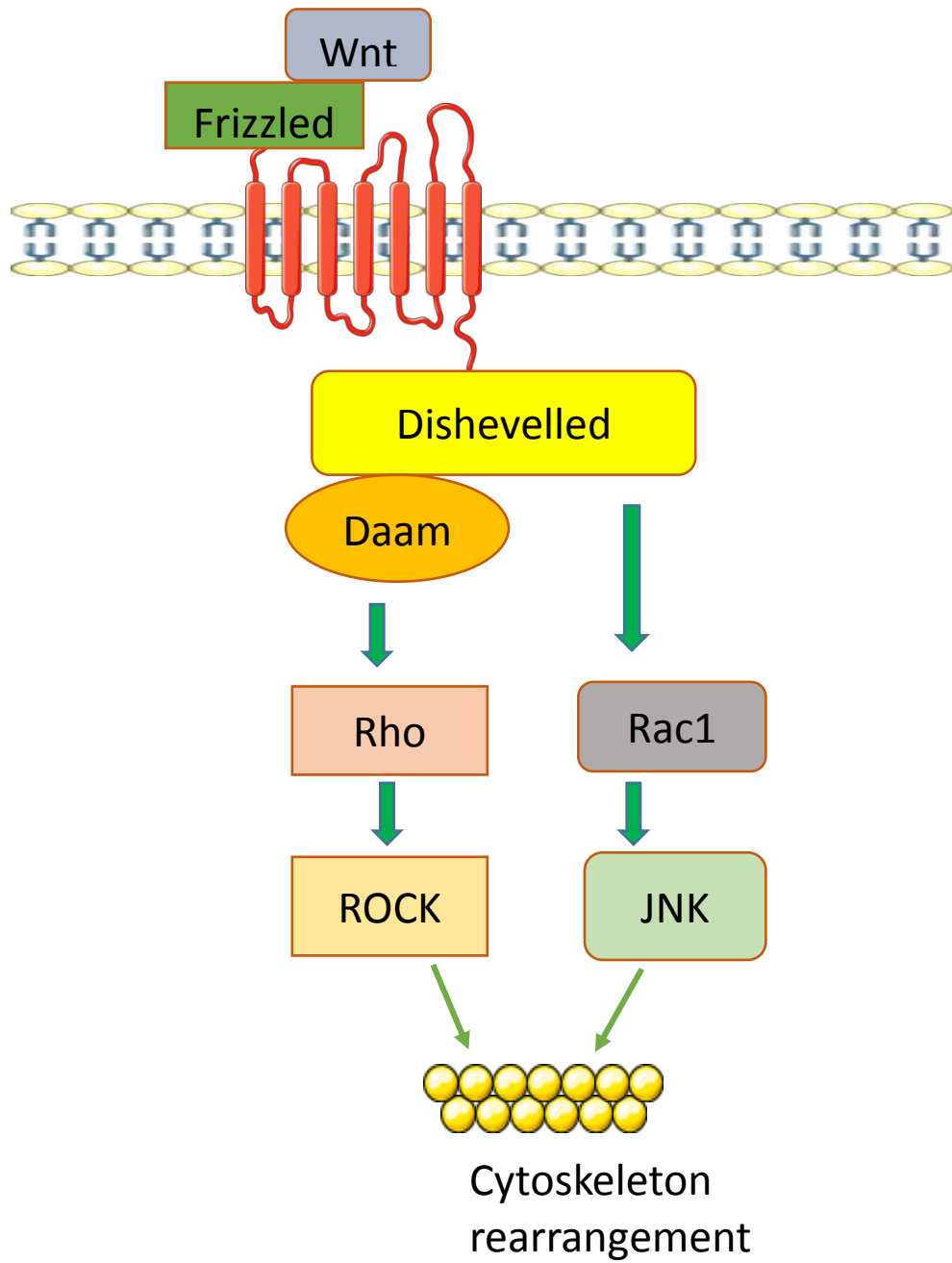


**Figure 13: Non-Canonical planer cell polarity pathway:** In planner cell polarity pathway a particular Frizzled receptor is activated by Rho and Rac GTPases leading to cytoskeleton rearrangement (Lee *et al.*, 2011).

### ***8.3 Wnt signaling in lipid homeostasis***

There is increasing evidence that Wnt signaling is implicated in lipid homeostasis. For instance, Wnt10b regulates adipocyte differentiation in cells (Bennett *et al.*, 2002). It reduces the differentiation of pre-adipocytes and decreases the accumulation of fats and adipose mass (Longo *et al.*, 2004). In mice overexpressing Wnt10b, there is a partial inhibition of white adipose tissue development whereas the formation of brown adipose tissue is completely blocked. Microscopic analysis shown a disruption in development or function of brown adipose tissue in these mice (Bachman *et al.*, 2002; Enerbäck *et al.*, 1997; Moitra *et al.*, 1998). As a result these mice have a lower oxygen consumption and cold sensitivity (Longo *et al.*, 2004).

Secreted frizzled-related proteins (sFRPs) are a family of secreted glycoproteins that act as a negative regulator of Wnt signaling pathway. sFRPs inhibit Wnt signaling either by limiting its binding to fzd receptors or by binding itself to fzd receptors and making non-functional complexes (Kawakami *et al.*, 2011). sFRPs can antagonize Wnt5a and Wnt11. Mice knockout for sFRP5 when fed with high fat diet for 12 weeks had increased body mass as compared to wild type mice. Histological analysis of these mice reveals larger adipocyte formation. sFRP5 deletion induces metabolic dysfunction in mice fed with a cholesterol rich diet and not in the ones on regular diet (Ouchi *et al.*, 2010).

It has been demonstrated that Wnt pathway has protective roles in liver under stress conditions. In mice, a liver specific knockout of  $\beta$ -catenin, the signaling factor of the Wnt pathway, results in both steatosis and a marked increase of

cholesterol levels in the liver (Behari *et al.*, 2010). A high fat diet in these mice resulted in increased bile acids production and enhanced cholesterol biosynthesis, hence its accumulation in the hepatocytes. Bile acids accumulation in liver results in enhanced oxidative stress and reduced bile acids export (Behari *et al.*, 2010).

Role of Wnt3a in lipid homeostasis has also been studied (Scott *et al.*, 2015). Wnt3a regulates the endocytosis of LDL-C and its flux to the endosomal compartment. Lysosomal acid lipase enzyme in the endosomes converts this the LDL-C derived cholesteryl ester to free cholesterol hence, it is stored as lipid droplets. Thus, Wnt3a promotes lipid droplet formation and regulates cholesterol homeostasis. This increase in LDs correlates with cancer disease progression. However, cells have various mechanisms to fight against this increased lipid storage such as decreasing cholesterol synthesis by preventing nuclear translocation of SREBP2 (J. Terrand *et al.*, 2009) or increasing its efflux (Cameron *et al.*, 2015).

In addition, there is increasing evidence that the Wnt5a pathway limits cholesterol accumulation (El Asmar *et al.*, 2016; J. Terrand *et al.*, 2009; Zhou *et al.*, 2009) and foam cell formation (Scott *et al.*, 2015), promotes plaque regression (Ramsey *et al.*, 2014), and may be a target in atherosclerosis. This will be described in paragraph 9.

#### **8.4 *Wnt signaling implications in atherosclerosis***

Wnt1, Wnt2 and Wnt3a regulate the smooth muscle cell proliferation that leads to intimal wall thickening in atherosclerosis (Takahashi *et al.*, 2016; Wang *et al.*, 2002).

Atherosclerosis is also a consequence of toll like receptors (TLRs) activation. Toll like receptors are a group of pattern recognition receptors that are expressed in antigen presenting cells such as dendritic cells and macrophages. Upon recognition of a pathogen they activate innate and adaptive immune responses development (Kaisho & Akira, 2006). In LDL receptor knockout mice fed with a high fat diet, deletion of toll like receptor 2 (TLR2) result in regression of atherosclerosis disease and minimal lesion development (Curtiss & Tobias, 2009). Suggesting an important role of these receptors in atherosclerosis disease development.

Loss of function of the Wnt co-receptors LRP5 and LRP6 have been associated with coronary artery disease in humans and in mice (Mani *et al.*, 2007). In last decade studies have shown role of Wnt5a in atherosclerosis, sepsis and other inflammatory diseases (Pooja M. Bhatt *et al.*, 2012; Blumenthal *et al.*, 2006; Christman *et al.*, 2008; Logan & Nusse, 2004; Sen *et al.*, 2000).

Wnt signaling is also involved in vascular calcification and atherosclerosis. It increases the binding of monocytes to endothelial cells (EC) and promotes the expression of pro-inflammatory markers in endothelial cells via activating non-canonical Wnt5a-Ca<sup>2+</sup> pathway. These events are a hallmark of atherosclerosis (Ueland *et al.*, 2009).

## **9. Wnt5a**

### ***9.1 Wnt5a mutation disorder***

Genetic mutations in gene encoding for Wnt5a result in Robinow syndrome. Mutations in disheveled 1(Dsh1) a mediator of canonical and non-canical Wnt signaling also result in osteosclerotic robinow syndrome (Bunn *et al.*, 2015).

Robinow syndrome is a rare genetic autosomal dominant disorder characterized by skeletal abnormalities resulting in retarded development of limbs (**Fig.14**). It develops due to mutations in genes encoding for tyrosine kinase receptor ROR2 that is a putative receptor in Wnt signaling pathways. Wnt5a is a ligand of ROR2 receptor acting via non-canonical Wnt signaling. Two missense mutations in gene encoding Wnt5a leads to amino acid substitution of highly conserved cysteine residues, resulting in development of Robinow syndrome. Thus Wnt5a/ROR2 signaling is important in skeletal and craniofacial development (Person *et al.*, 2010). The phenotype of the disease includes midface hypoplasia, hypertelorism, a short nose, a broad mouth, bigger eyes and low ear positioning, shortening of limbs (Roifman *et al.*, 2015).



**Figure 14: Robinow syndrome patient with *Wnt5a* gene mutation.** Phenotype presents bigger eyes, shortening of arms, depressed nose bone and low ear positioning (Roifman *et al.*, 2015).

## **9.2 Role of Wnt5a in cells**

Wnt5a is expressed ubiquitously (El Asmar *et al.*, 2016). In endothelial cells Wnt5a regulates proliferation and initiates inflammation by inducing cytokines via its non-canonical  $\beta$ -catenin independent pathway. It also plays role in determining endothelial cell fate and vascular remodeling (Cheng *et al.*, 2008). Wnt5a is also endogenously expressed in vascular smooth muscle cells. Expression of Wnt5a was first identified in pulmonary artery smooth muscle cells (Wright *et al.*, 1999). It is involved in SMCs differentiation and proliferation by acting through both canonical and non-canonical pathways (J. Kim *et al.*, 2010; Mill & George, 2012).

Wnt5a is also expressed in adipocytes. Mice overexpressing Wnt5a in adipose tissue (aTgWnt5a) show a reduced levels of cholesterol synthesis enzyme HMGCoA reductase and increased cholesterol export protein ABCG1 and ABCA1 (El Asmar *et al.*, 2016). There was also a twofold reduction in cholesterol accumulation in these cells suggesting that Wnt5a decreases cholesterol synthesis and promotes its export.

## **9.3 Role of Wnt5a in atherosclerosis**

Studies show that there is an increased expression of Wnt5a in mice and human atherosclerotic plaque regions. In one study, mice lacking ApoE<sup>-/-</sup> fed with high fat diet had an increased Wnt5a expression in macrophage rich regions of the plaque (Christman *et al.*, 2008). Our lab and others have reported that Wnt5a expression correlates with fatty streaks and in early atherosclerotic lesions in human, and its expression increased robustly in advanced atherosclerotic lesions (Christman *et al.*, 2008; Mill *et al.*, 2014;

Tsaousi *et al.*, 2011; Estelle Woldt *et al.*, 2012). However, this increase in Wnt5a could be a compensatory mechanism adopted by cells to limit cholesterol accumulation.

For instance, low density lipoprotein receptor-related protein 1 (LRP1) is a membrane receptor belonging to LDL receptor gene family. In a study where LRP1 was knocked down in vascular smooth muscle cells of mice, mice developed foam cell formation and atherosclerotic plaque formation. LRP1 controls the transcriptional activation of Wnt5a (Fig.15) and integrates TGF- $\beta$  at the cell membrane (El Asmar *et al.*, 2016). Endogenous expression of Wnt5a in cells is very low. However, Extracellular chain of LRP1 mediates TGF- $\beta$  (a cytokine that controls cell proliferation and differentiation) induced enhancement in Wnt5a expression in cells (El Asmar *et al.*, 2016). This expression of Wnt5a decreased foam cell formation and cholesterol accumulation whereas deletion of Wnt5a in MEF and adipocytes of mice resulted in accumulation of larger amounts of cholesterol within cytosolic vesicles in the perinuclear region compared to controls (El Asmar *et al.*, 2016).

Taken together these data indicates that Wnt5a is present in advanced atherosclerotic lesions. However, there is still no evidence whether there is a causative relationship between Wnt5a presence and atherosclerosis disease progression as Wnt5a expression could be a rescue mechanism by the cells to develop protection against atherosclerosis. In order to study the role of wnt5a in atherosclerosis, we generated mice specifically knockout for Wnt5a in vascular smooth muscle cells (VSMCs) and in human VSMCs knockout for Wnt5a using CRISPR Cas9 guided nuclease technology. We analyzed the phenotype in mice and cells and observed increased cholesterol accumulation

in lysosomes, foam cells formation and atherosclerosis. These data indicate that Wnt5a is essential for cholesterol trafficking and lysosomal function.

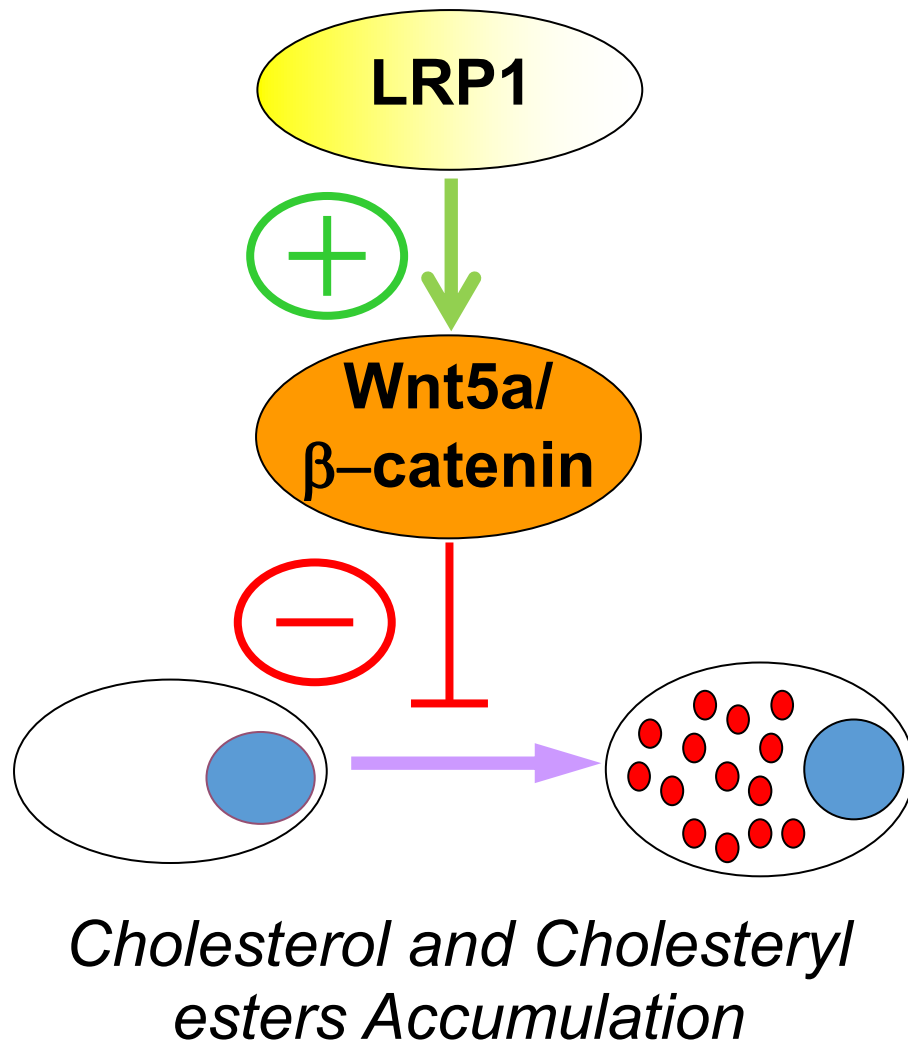


**Figure 15: Transcription regulation of wnt5a.** LRP1 controls transcription regulation of Wnt5a. Wnt5a protein expression prevents the development of foam cells in fibroblasts (El Asmar Z. *et al.* 2016).



# **Material & Methods**

# 1. Standard procedures

## *1.1 Western blot analysis*

### *Protein extraction in cells:*

The cells were washed with PBS and lysed with cold RIPA buffer (Tris HCl 50mM, NP40 1%, deoxycholate sodium 0.25%, NaCl 150mM, EDTA 1mM, PMSF 1mM, aprotinin 1µg/ml, leupeptin 1µg/ml, pepstatin 1µg/ml, Na<sub>3</sub>VO<sub>4</sub> 1mM, NaF 1mM). Extract was passed through a 22G syringe 20 times and incubated on ice for 10 min. Then centrifuged 30 min, 4°C at 12000G. The proteins in the supernatant were dosed by the Bradford assay.

### *Protein extraction in mice tissues:*

The aorta and heart tissue sections of mice were broken down into RIPA buffer and the lysate was passed through a 22G syringe 20 times. Then centrifuged at 30 min, 4°C at 12000G. The proteins in the supernatant were dosed by the Bradford assay.

### *Sample preparation and western blot:*

50µg of proteins were mixed with denaturing Laemli 4X (with β-mercaptophenol) and heated for 10 mins at 95°C for denaturing the proteins. 50µg proteins were loaded in a polyacrylamide gel and separated by electrophoresis using a migration buffer (Tris-glycine, SDS20%) at 110V. Proteins were then transferred to a nitrocellulose or PVDF membrane using a transfer buffer (Tris-glycine, ethanol 100%) at 70V for 02 hrs. The non-specific binding sites were saturated using a TBS-Tween 10%, 5% milk or BSA for 1hr on the membrane. The membrane was incubated with the primary

antibody overnight at 4°C. The membrane was then washed 05 times 5 min each with TBS-Tween 10% and incubated with antibody secondary for 1hr. Then washed again 05 times and revealed by Clarity Western ECL substrate kit (Bradford).

<b>Antibody</b>	<b>Dilution</b>	<b>Manufacturer/Supplier</b>
Wnt5a	1/200	R&D systems
p-mTOR	1/1000	Cell signaling
mTOR total	1/1000	Cell signaling
p-4EBP1	1/1000	Cell signaling
4EBP1 total	1/1000	Cell signaling
p-AKT	1/1000	Cell signaling
AKT total	1/1000	Cell signaling
p-S670 Kinase	1/1000	Cell signaling
SM22 alpha	1/1000	Abcam
PI3kinase p85 alpha	1/1000	Abcam
p-Tyrosine clone 4G10	1/500	Merck millipore
Lamp1	1/200	DSHB
anti-Flag M2	1/1000	Sigma
anti- eGFP	1/5000	Merck millipore

LC3-B	1/1000	Abcam
p62	1/1000	Abcam
Galectin-3	1/500	Abcam
Anti-GAPDH	1/5000	Sigma
Tom-20	1/1000	Santa Cruz
GM-130	1/1000	Proteintech
anti-EEA1	1/1000	Transduction laboratories
anti-Caveolin	1/1000	BD Transduction laboratories

## ***1.2 RNA extraction and RT-PCR***

RNA was isolated using TRIzol reagent (Sigma, St Louis) according to the manufacturer's instructions. A total of 50 ng of RNA was converted to cDNA using the high-capacity cDNA Archive kit (Applied Biosystems, Foster City, CA). PCR amplification was performed using SYBRGreen PCR master mix (Applied Biosystems) according to the manufacturer's instructions.

## ***1.3 Transfection of plasmids***

Transfection was performed to transiently over-express a protein or generate a stable cell line. Monolayers of cells were seeded in plates until they reach 60% confluence. Cells were transfected with cDNA plasmid (1 $\mu$ g in 06-well

plates, 5µg in petri plate 10cm) using Fugene 6 Reagent and DMEM media without serum and antibiotics. After 06 hours the media of cells is changed with FBS10% medium (DMEM, FBS 10%, penicillin/streptomycin and ultraglutamine). The cells overexpress the protein until 72 hrs. For generating stable cell lines cells were treated with 1mg/ml of antibiotic for a month.

## **2. Experiments in Vivo (mice models)**

### ***2.1 SM22 Wnt5a- mice generation***

Wnt5aflox mice were generated using the plasmid EUCOMM-Wnt5a Vectors (target-final) as described (Estelle Woldt *et al.*, 2012). We achieved smooth muscle-specific Wnt5a inactivation by crossing SM22Cre transgenic mice (Holtwick *et al.*, 2002) with Wnt5aflox animals. To increase susceptibility to spontaneous atherosclerotic lesion development, these animals were crossed to LDL receptor knockout (LDLR<sup>-/-</sup>) mice to generate SM22Cre, Wnt5aflox/flox, LDLr<sup>-/-</sup> mice. The LDLR<sup>-/-</sup> mouse is an excellent model for studying human atherosclerosis, because atherosclerotic lesion formation can be accelerated and experimentally controlled over a wide range by cholesterol feeding (Ishibashi *et al.*, 1993). Mutant mice were then referred to as SM22Cre<sup>+</sup> (SM22Cre<sup>+</sup>, Wnt5aflox/flox, LDLr<sup>-/-</sup>) & their littermate controls are referred as SM22Cre<sup>-</sup> (SM22Cre<sup>-</sup>, Wnt5aflox/flox, LDLr<sup>-/-</sup>). Animals were fed paigen diet for 5 months and kept on a 12h light/dark cycle as described (Boucher *et al.*, 2003). All animals used in the experiments were age-sex matched and littermates. Experiments were conducted according to standard procedures approved by the Institutional Animal Care and Use Committee at University of Strasbourg, France.

## ***2.2 Paigen diet regimen***

Paigen is a cholesterol rich diet. It was prepared by melting 250g of butter, mixed with 12.5g cholesterol and 5g of cholic acid. The mixture is added in 775g of flour A03 and mixed thoroughly for 05 minutes. 250ml of distilled water was added to the dough and balls of food were prepared and wrapped in parafilm to be stored at -20°C.

## ***2.3 Dissection and coloration of mice aortas***

For histological studies, mice were transcardially perfused with a 4% paraformaldehyde solution in phosphate-buffered saline, aorta of mice were embedded in paraffin, and cut in 5 µm slices.

### ***2.3.1 H& E staining***

The paraffin fixed tissue sections were deparaffinized with 2 washes of histosol, ethanol 100%, ethanol 95% and water milliq. Colored with hematoxylin solution for 2min. Rinse with water milliq 3min. Then de-differentiated in a 0.1% HCl in Ethanol 70% solution. The sections were then passed through Scott's tap water solution for 30sec and rinse with ethanol 95%. Coloured with Eosine solution for 60sec and dehydrated again using ethanol 100% and histosol. The slides are mounted using Eukitt.

### ***2.3.2 Orcein staining***

The sections were deparaffinized and rehydrated. Stained for 30min in 1% orcein solution. The slides were then rinse with deionized water, 95% and 100% ethanol to remove excessive stain. Sections turned pale brown and were further decolorized in acid alcohol solution for 10min. Rinsed with water and counterstained in aniline blue/orange G solution during 3 min. Rinsed with water again and dehydrated, cleared and mounted using Eukitt.

### ***2.3.3 Sudan IV staining***

Mice were dissected and aorta tissue was cut opened and pinned on a paraffin tray. Rinsed with ethanol 100% and stained with Sudan IV staining solution for 15mins, rocking periodically. The staining solution was decanted and the tissue was decolorized using an 80% ethanol solution. Tissue is then kept in water.

### ***2.3.4 Oil red O staining***

Mice aortic arch tissue was fixed in OCT compound (Tissue Tek) and stored at -80°C. 7-10µm tissue sections were cut and slides were hydrated in PBS for 2mins. Stained in Oil Red O solution for 03 minutes under constant gentle agitation. Rinsed in deionized water for 30sec and mounted using DAPI.

## ***2.4 Dissection of embryos***

The female mouse was dissected at day 17 of conception and embryos were collected and dissected for genotyping, mice tissue collection for proteins and histology.

## ***2.5 Electronic microscopy of mice tissues***

Electronic microscopy was performed on mice aorta and heart tissues fixed in paraformaldehyde and glutaraldehyde solution, as described in (Garratt *et al.*, 2000).

## ***2.6 Immunohistochemistry in mice tissues***

Paraffin fixed mice tissue sections cut in 5µm slices were deparaffized using histosol and decreasing dilutions of ethanol. Rinsed with water and trypsinized at 37°C for 17mins. Rinsed with PBS twice and incubated with 3% H<sub>2</sub>O<sub>2</sub> in ethanol for 30 mins. Rinsed with TBST and incubated with normal

serum 5% for 1hr. After blocking, the sections are incubated with primary antibody overnight at 4°C. Washed 3 times with TBST and incubated with secondary antibody at 1/200 dilution. The sections are then rinsed with TBST and incubated with VECTASTAIN AB reagent for 30min, rinsed with PBS, and DAB solution is added on the sections to develop the brown coloration for antibody labelling. The sections are rinsed in acetic acid solution and dehydrated. Mounted using Eukitt.

### **3. In Vitro experiments (In cell model)**

#### ***3.1 Cell culture and media preparation***

Human Vascular Smooth Muscle cells (CMLVs) Wnt5a<sup>-/-</sup> was generated with the Dharmacon™ Edit-RTM CRISPR-Cas9 Genome Engineering system. crRNA was directed against exon 3 of the Wnt5a gene. Human Vascular Smooth Muscle cells (CMLVs) and Human Embryonic Kidney cells (HEK) cells were seeded in 100 mm dishes and grown to 80% confluence in Dulbecco's modified Eagle's medium (DMEM) (Invitrogen, CA) supplemented with 10% (v/v) new-born calf serum, penicillin/streptomycin & ultra-glutamine. Wnt5a Knockout human CMLVs were treated with varying doses of reagents as described in results section.

#### ***3.2 Immunoprecipitation***

Monolayers of human embryonic kidney (HEK) 293 cells were transfected with plasmids using Fugene 6 Reagent (Promega) according the manufacturer's protocol. Immunoprecipitation experiments were performed as described previously (Boucher *et al.*, 2003). Briefly, cells were washed with cold PBS and lysed in phosphate lysis buffer supplemented with protease inhibitor cocktail on ice for 20min. Lysates were precleared, incubated with

indicated antibodies and protein A/G-plus agarose beads at 4 °C overnight. Immunoprecipitates were washed twice with lysis buffer. Proteins were eluted from beads with SDS sample buffer, separated by SDS–polyacrylamide gel electrophoresis, transferred to nitrocellulose membrane and blotted with the indicated antibody.

### ***3.3 Adipogenic differentiation***

Cholesterol accumulation was induced using an adipogenic cocktail as described (J rome Terrand *et al.*, 2009). Cells were fixed in 4% paraformaldehyde and neutrals lipids were stained with Oil-Red-O (Sigma-Aldrich).

### ***3.4 Oil Red O coloration***

Cells were washed with cold PBS and fixed with 4% paraformaldehyde for 15-30min. Rinsed 3 times with cold PBS. Stained with Oil Red O solution for 30minutes at room temperature. Cells were then washed 3 times with cold PBS to remove the unincorporated Oil Red O. Stored at room temperature in PBS.

### ***3.5 Treatment of CMLVs with conditioned media from LMTK***

The media FBS 10% from LMTK+ and LMTK- cells was taken and centrifuged at 3000rpm for 10 mins. The media is further filtered using a 0.22 m filter and the adipogenic markers are added in this media and the media is further loaded on CMLVs.

### ***3.6 Wnt5a purification***

The HEK cell overexpressing pcDNA3.1-Wnt5aHis were lysed using buffer and PIC. Cells were homogenized and sonicated, 500 units of benzonase were added. Incubated 1hr at 4 C and passed through a 23G syringe. The

homogenate was centrifuged at 27000G for 1hr at 4°C. Supernatant was collected and filtered using a 0.45µm filter. The clear supernatant is then loaded on Nickel column, the His-tag Wnt5a protein is eluted in fractions.

### ***3.7 Immunofluorescence***

Immunofluorescence was performed using CMLVs knockout for Wnt5a and the controls as per the protocol described (Wilhelm *et al.*, 2017). Cells were labelled with GFP-D4. Antibody used was mouse anti-Lamp1 H4A3 (1:50; DSHB) and Alexa Fluor 546 secondary antibody. Slides were mounted in fluorescence mounting medium (Dako). Immunofluorescence-labelled cells were analyzed using a Leica TSC SPE confocal microscope with the 63x oil immersion objective. GFPD4 positive lamp1 vesicles in cells were counted with Image-J using a Macro program. Macro quantified the number of lamp1 vesicles that co-localize with cholesterol.

### ***3.8 Lipofuscin measurement***

VSMCs WT & KO for wnt5a were seeded on coverslips in 24-well glass bottom plates. Cells were labelled with mouse anti-Lamp1 H4A3 (1:50; DSHB) antibody and Alexa Fluor 546 secondary antibody. Slides were mounted in fluorescence mounting medium (Dako). Immunofluorescence-labelled cells were analyzed using a Leica TSC SPE confocal microscope with the 63x oil immersion objective. Lipofuscin was detected by its autofluorescence.

### ***3.9 LysoTracker red staining***

VSMCs WT & KO for wnt5a were seeded on coverslips in 24-well glass bottom plates. Cells were incubated with 100nM lysotracker red (Thermo fisher scientific) for few minutes at 37°C. After the cells were fixed with

paraformaldehyde 4% for 10 minutes. Washed three times with cold PBS and stained with DAPI for 10 minutes to obtain nuclear staining. Slides were mounted in fluorescence mounting medium (Dako). Lysotracker-labelled cells were analyzed using a Leica TSC SPE confocal microscope with the 63x oil immersion objective.

### ***3.10 Autophagy measurement***

For autophagy analyses, cells were starved by incubation in Earle's balanced salt solution (EBSS) for 2 hr. as described (Lin *et al.*, 2012; Nascimbeni *et al.*, 2017; Tuloup-Minguez *et al.*, 2011). The accumulation of LC3-II and the level of p62 were analyzed by western blotting.

### ***3.11 Neutral lipids and sterol analysis***

Lipids corresponding to 1 million of cells were extracted according to Bligh and Dyer (Bligh & Dyer, 1959) in dichloromethane/methanol/water (2.5 :2.5 :2.1, v/v/v), in the presence of the internal standards : 4µg of stigmaterol, 4µg of cholesteryl heptadecanoate, 8µg of glyceryl trinonadecanoate. Dichloromethane phase were evaporated to dryness and dissolved in 30µl of ethyl acetate. 1µl of the lipid extract was analyzed by gas-liquid chromatography on a FOCUS Thermo Electron system using an Zebron-1 Phenomenex fused silica capillary columns (5m X 0,32mm i.d, 0.50µm film thickness) (Barrans *et al.*, 1994). Oven temperature was programmed from 200°C to 350°C at a rate of 5°C per min and the carrier gas was hydrogen (0.5 bar). The injector and the detector were at 315°C and 345°C respectively. After evaporation, the extract was then submitted to derivatisation in N,O-Bis (trimethylsilyl) trifluoroacetamide/acetonitrile (50:50 ; v/v) for 1h at 80°C and solubilized in 20ml heptane for analysis by gas chromatography-mass spectrometry. It was performed on a ThermoScientific Trace GC coupled to a

Trace TSQ Mass selective detector (ThermoScientific). The silylated sterols were separated on an Agilent J&W HP-5MS capillary column (30 m, 0.25 mm, 0.25  $\mu$ m phase thickness). The oven temperature program was as follows: 180°C for 1 min, 20°C/min to 250°C, 5°C/min to 300°C where the temperature was kept for 8 min, and then 35°C/min to 325°C. High purity helium was used as carrier gas at a flow rate of 0.8 mL/min in constant flow mode. The samples were injected in a splitless mode with an injection volume of 1  $\mu$ L. The injector, transfer line and source temperature was 270°C, 280°C and 250°C respectively. The mass spectrometer was operated in the selected ion-monitoring (SIM) mode. Peak detection, integration and quantitative analysis were executed using Xcalibur Quantitative browser (ThermoScientific) based on calibration lines built with commercially available sterol standards (Sigma Aldrich or Interchim).

Analysis of free cholesterol in the ER and LELs fractions was performed as described previously (Zhang *et al.*, 2005). Briefly, prior to extraction 10  $\mu$ L of  $\beta$ -sitosterol (purified according to Zhang X *et al.*, 2005) solution (0.5 mg/mL in ethyl acetate (analytical grade, Acros, Geel, Belgium)) was added to the cellular fraction as an internal standard. Extraction of lipids was then extracted 3 times by ethyl acetate. The combined organic extracts were evaporated and dried under nitrogen flow. Then the sterol residue was converted to trimethylsilyl ethers with 15  $\mu$ L of pyridine and 15  $\mu$ L of MSTFA (N-Methyl-N-(trimethylsilyl) trifluoroacetamide, Sigma-Aldrich, Steinheim, Germany) at room temperature in the dark overnight and then, diluted with 20  $\mu$ L of isooctane (analytical grade, Merck, Darmstadt, Germany). One microliter of each sample was injected into the GC-MS system. GC-MS analyses were performed on a Varian STAR 3400 GC instrument equipped with an on-column SPI injector coupled to a Varian SATURN 2000 mass

sensitive detector (Varian, France) with an Electronic Impact as ionization source (EI, ionization energy of 70 eV) working with a range of mass from 40 to 600 m/z. Data acquisition and processing were done on Varian Saturn Work Station 5.11 software. Analytes were separated in a VF-5ms capillary column (phase stationary: 5 % phenyl–95 % dimethylpolysiloxane, thickness of 0.1  $\mu$ m, 60 m  $\times$  0.25 mm, Varian, France). The column temperature gradient was programmed from 55°C (hold for 1 min) to 320°C at 7°C/min and hold for 6 min. The injector operating conditions were as follows: injection volume 1  $\mu$ L; initial injector temperature of 55°C was increased to 300 °C at 100°C/min (hold for 37 min). Helium (purity 99.9995 %) was used as a carrier gas with a flow rate of 1 mL/min. Cholesterol was quantified compared to  $\beta$ -sitosterol as internal standard as described (Zhang *et al.*, 2005).

Quantification of total cholesterol (free + esterified) in the ER and LELs fractions was also performed as described (Zhang *et al.*, 2005). Briefly, a previous step of saponification (before extraction) was necessary. It consisted of adding to the cellular fraction, ethanol (Carlo Erba, France) and saturated potassium hydroxide (KOH, from Merck Darmstadt, Germany) aqueous solution. The sample was purged with nitrogen, and was put into a rotary shaker (Edmund Buhler, Johanna Otta GmbH, Hechingen, Germany) at ambient temperature in the dark overnight (15 h). Then the extraction was done as previously described (Zhang *et al.*, 2005).

### ***3.12 Liposomes preparation and conditioned treatment***

Stock solutions of DOPC and Cholesterol were prepared in Chloroform. Solutions of DOPC with or without cholesterol were dried under liquid nitrogen stream. Lipid film is further dried under vacuum for an hour. Hepes-

Potassium acetate buffer at pH 6.8-8 is used to dissolve the dried lipid film, vortexed to prepare the liposomes.

### ***3.13 Statistical analysis***

Values are reported as mean±S.E.M. of at least triplicate determinations. For in vivo analysis, 3–6 male and female mice were used for each genotype. Statistical significance ( $P < 0.05$ ) was determined by unpaired Student's t-test (Statview, Abacus Concepts, Berkeley, CA).

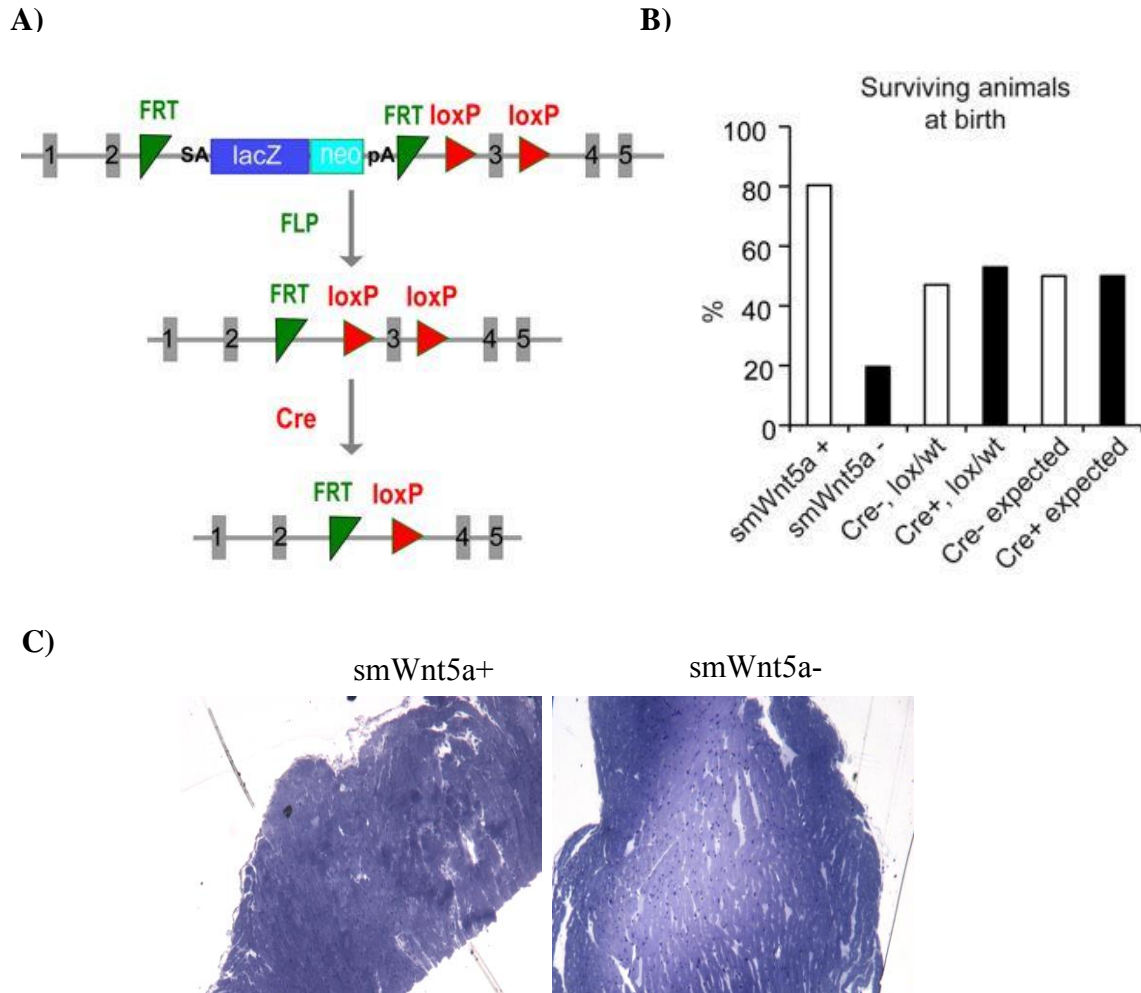
# Results // Part-I

# 1. Accelerated atherosclerosis in mice deleted for *wnt5a* in VSMCs.

Previously our lab had shown that the extracellular ( $\alpha$ ) chain of LRP1 mediates TGF $\beta$ -induced enhancement of Wnt5a which limits intracellular cholesterol accumulation by inhibiting cholesterol biosynthesis and by promoting cholesterol export (El Asmar *et al.*, 2016).

## 1.1 *smWnt5a*- mice generation

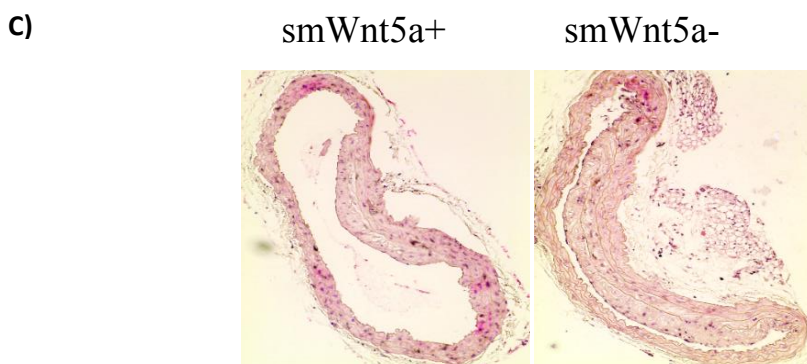
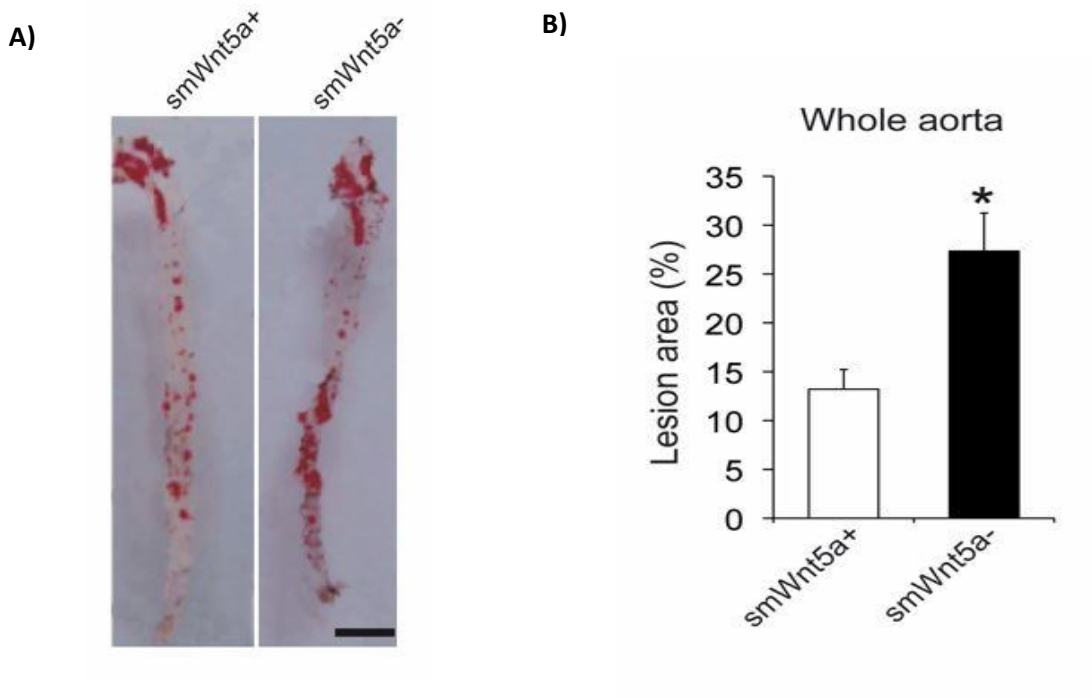
To test whether Wnt5a protects against atherosclerosis, we generated SM22Cre<sup>+</sup>/Wnt5a<sup>flox/flox</sup>/LDLR<sup>-/-</sup> mice (*smWnt5a*-) and littermate controls SM22Cre<sup>-</sup>/Wnt5a<sup>flox/flox</sup>/LDLR<sup>-/-</sup> mice (*smWnt5a*+) using the Cre/lox system which is a site specific deletion in the DNA to obtain gene deletion or insertion. To obtain smooth muscle cell specific gene deletion in mice, SM22 Cre transgenic mice were crossed with Wnt5a<sup>flox/flox</sup> animals. To accelerate lesion generation SM22Cre<sup>+</sup>/Wnt5a<sup>flox</sup> mice were crossed with LDL receptor<sup>-/-</sup> mice to generate SM22Cre<sup>+</sup>/Wnt5a<sup>flox/flox</sup>/LDLR<sup>-/-</sup> mice (*smWnt5a*-) (**Fig.16A**) as described (Boucher *et al.*, 2003), and studied their vascular phenotype. In **Fig.16A** LacZ and neomycin are in the construct to select the positive blastocyst cells. Flippase cuts between FRT to remove the selection cassette and Cre is to excise exon-3 of Wnt5a between two lox-P sites so that Wnt5a is not expressed in the smooth muscle cells of these mice. Only 20% of the SM22Cre<sup>+</sup>/Wnt5a<sup>flox/flox</sup>/LDLR<sup>-/-</sup> mice (*smWnt5a*-) were born alive (**Fig.16B**). Death might be due to some cardiac defects as suggested by necrosis in cardiac tissue (**Fig.16C**). Surviving animals looked healthy and lived normally.



**Figure 16: Generation of Wnt5a knockout mice.** A) Schematic representation of Wnt5a<sup>lacZ,fl,cre</sup> alleles. Exons are shown as grey boxes and marked by a number. SA is a splicing acceptor; IRES is an internal ribosome entry site; lacZ is the lac operon (lactose operon); pA is a poly(A) signal; Neo is neomycin-resistant gene driven by lacZ promoter; FLP is flp recombinase; CRE is cre recombinase. There are two LoxP sites for Cre recombinase on the 5' and 3' ends of third exon of Wnt5a. Rxfp1<sup>fl</sup> allele is produced by flp-induced recombination, and the deleted allele without exon 3 is produced by cre-induced recombination as shown. smWnt5a<sup>+</sup>, smWnt5a<sup>-</sup>, and heterozygote SM22Cre<sup>+</sup>/Wnt5a<sup>lox/wt</sup>/LDLR<sup>-/-</sup>, B) SM22Cre<sup>+</sup>/Wnt5a<sup>lox/wt</sup>/LDLR<sup>-/-</sup> mice alive at birth, compared to the expected percentage of surviving animals (Cre<sup>-</sup> expected, Cre<sup>+</sup> expected) (n=236). C) Toluidine blue staining in mice cardiac tissue showing necrosis in mutant mice vs controls.

## 1.2 Sudan IV staining in aortas of mice on paigen diet

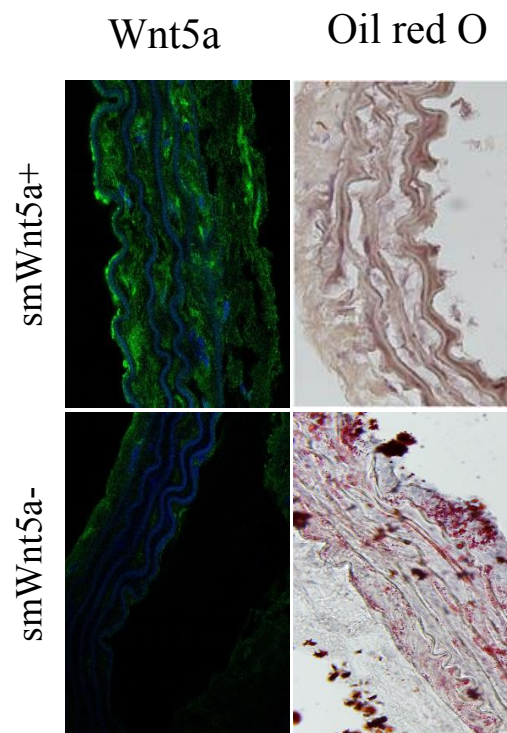
The surviving mice were fed a cholesterol-rich (Paigen) diet for 5 months. Mice were dissected and aorta tissue was cut opened and pinned on a paraffin tray. The aorta of mice were labelled with Sudan IV (it labels lipids, triglycerides and lipoproteins) (**Fig.17A**), quantification of lesion area (**Fig.17B**) shows that mutant mice develop twice as much atherosclerosis as controls ( $p < 0.05$ ). H & E staining of mice aorta also shows that mutant mice develop twice as much atherosclerosis as controls when fed a cholesterol-rich (Paigen) diet for 5 months (**Fig.17C**).



**Figure 17: Accelerated formation of atherosclerotic lesions in smWnt5a- mice.** **A)** Opened and Sudan IV-stained aortas from cholesterol-fed mice that express (smWnt5a+) or lack Wnt5a (smWnt5a-) in VSMCs. Red staining indicate lipid-laden (Sudan positive) atherosclerotic lesions. Scale bar is 0.5 cm. **B)** Quantitative analysis of atherosclerotic lesion size in aortas from cholesterol-fed mice (n=6 mice per group). **C)** H&E staining of mice aorta shows lesion size in mutant mice vs controls.

### ***1.3 Immunofluorescence and Oil red O labelling for wnt5a in mice aortas***

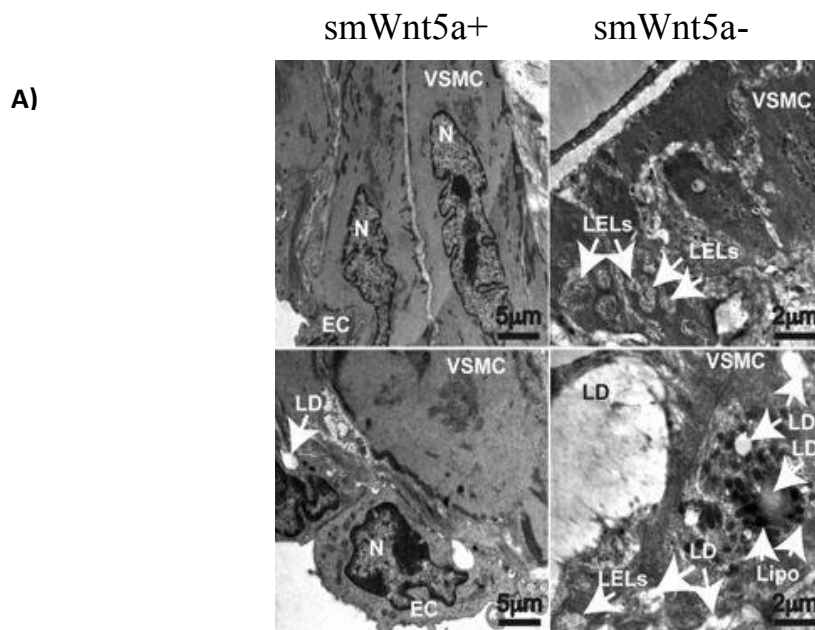
Immunofluorescence analysis of the aorta of mice on paigen diet (**Fig.18A**) shows an efficient deletion of Wnt5a in the media (VSMCs) of mutant mice compared to controls. Interestingly, Oil-Red-O staining (**Fig.18B**) shows accumulation of lipids in mutant animals even in the media and VSMCs from non-lesion areas, whereas in control mice, lipid accumulated within lesions only. These results suggest that in absence of Wnt5a VSMCs accumulated more cholesterol and foam cells and that cholesterol accumulation is not limited to the lesional areas.



**Figure 18: Increased lipid accumulation in absence of *wnt5a*.** Immunofluorescence labelling of mice aorta in left panel shows efficient absence of Wnt5a in the media (VSMCs) of mutant mice compared to controls. **B)** Oil Red O staining in right panel shows lipid accumulation in the media (VSMCs) of non-lesion areas. Scale bar is 30 $\mu$ m.

### ***1.4 Electron microscopy data in mice aortas***

Electron microscopy (EM) analysis revealed accumulation of large lipid droplets and numerous abnormally large late endosome/lysosomes (LELs) within VSMCs of mutant mice aortas compared to control animals (**Fig. 19A** white arrows). Interestingly aortas of smWnt5a<sup>-</sup> mice also accumulated large electron-dense cytoplasmic lipofuscin containing vesicles, indicating that lysosomal function is impaired in the absence of Wnt5a. EM of cardiac tissue also shows cardiac tissue disruption and lipofuscin accumulation in the cardiac tissue of smWnt5a<sup>-</sup> mice (**Fig.19B**). Thus, Wnt5a in VSMCs not only limits cholesterol accumulation, but also protects against atherosclerosis in mice, and in its absence lysosomal function is impaired.



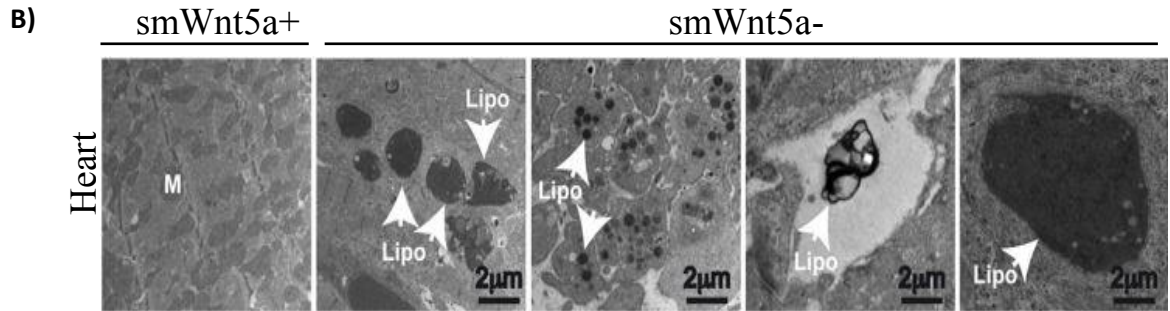


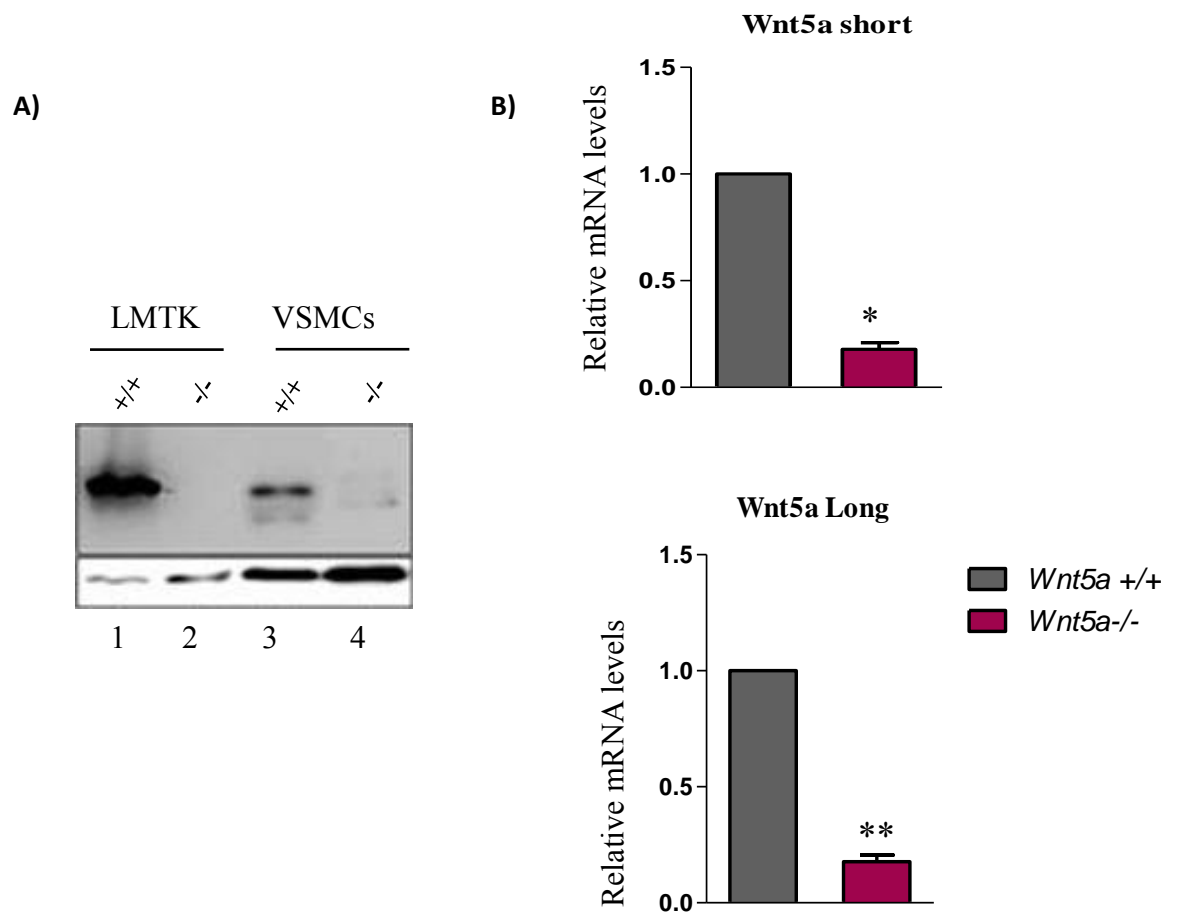
**Figure 19: Lipid accumulation in mice in absence of Wnt5a.** A) Representative electron micrographs show presence of electron-dense lipofuscin containing vesicles (Lipo), and accumulation of lipid droplets (LD) in VSMCs of mutants vs controls. Note large late endosomes/lysosomes (LELs) in VSMCs of smWnt5a- mice. Endothelial cells and nuclei are indicated (EC, N). \*,  $p < 0.05$ . Values are mean  $\pm$  SEM. B) Representative electron micrographs of heart tissue from smWnt5a+ and smWnt5a- mice fed a Paigen diet. White arrows show large lipofuscin pigment granules (Lipo) in mutants vs controls. Mitochondria are indicated (M).

## 2. Lipid accumulation in Wnt5a<sup>-/-</sup> human VSMCs

### 2.1 Generation of Wnt5a<sup>-/-</sup> cells using CRISPR/Cas9 guided nuclease

To determine how Wnt5a alters cholesterol homeostasis in human VSMCs, we used a CRISPR/Cas9 guided nuclease approach to generate human VSMCs knockout for Wnt5a (Wnt5a<sup>-/-</sup> VSMCs) and human VSMCs non-targeted controls (Wnt5a<sup>+/+</sup> VSMCs) (**Fig.20A**). The Wnt5a gene produces two very similar alternate scripts, by utilizing alternative transcription starting sites. The resulting Wnt5a protein isoforms are termed as Wnt5a short (Wnt5a-S) and Wnt5a long (Wnt5a-L) isoforms. Wnt5a-long carrying additional 18 N-terminal amino acids. The Wnt5a-L inhibits proliferation of cancer cells in breast, cervix and neuroblastoma cancer. Whereas Wnt5a-S

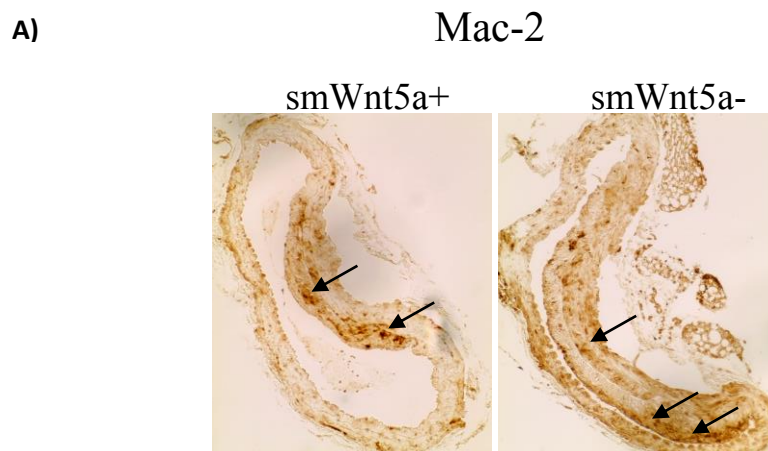
promotes the proliferation of these cells (Huang *et al.*, 2017). Both isoforms of Wnt5a were deleted in human VSMCs (**Fig.20B**).



**Figure 20: Wnt5a deletion in VSMCs.** **A)** Western blot analysis for Wnt5a in LMTK cells stably transfected with an expression vector coding for Wnt5a (Ctrl+/+) or mock (Ctrl-/-), and human VSMCs transfected with a CRISPR/Cas9 Wnt5a targeted vector (-/-) or a non-targeted vector (+/+). **B)** Relative transcript levels of Wnt5a long and short isoforms in human VSMCs.

## ***2.2 VSMCs transdifferentiate to macrophage-like cells in absence of wnt5a***

As described previously, that upon Cholesterol loading smooth muscle cells (SMCs) lose SMC specific marker such as smooth muscle alpha actin (Acta2) and myosin heavy chain (Myh11) and start to express the macrophage markers such as Mac2 and CD68 (Rong *et al.*, 2003). We studied this VSMC transdifferentiation in vitro and in vivo. Aorta of mice on pagen diet were labelled with Mac-2, (**Fig.21A**) shows that mutant mice have more labelling for macrophage marker Mac-2 vs controls. However, no difference in expression of Acta-2 (a SMC specific marker) was observed in mutant vs controls (**Fig.21B**). Further human SMCs were treated with a cholesterol accumulation protocol for 08 days. Western blot analysis of the macrophage marker Mac-2 shows that in absence of Wnt5a, SMCs switch for a macrophage like phenotype (**Fig.21C**). Expression of KLF4 (a zinc finger transcription factor and plays role in cellular proliferation and differentiation) is also enhanced in SMC cells in absence of Wnt5a (**Fig.21D**). This data correlates with already published research that in absence of Wnt5a SMCs accumulate more cholesterol and transdifferentiate into macrophage like cells (Rong *et al.*, 2003). However, there is still a need for more experimentation to confirm the transdifferentiation of these VSMCs to macrophage-like cells.



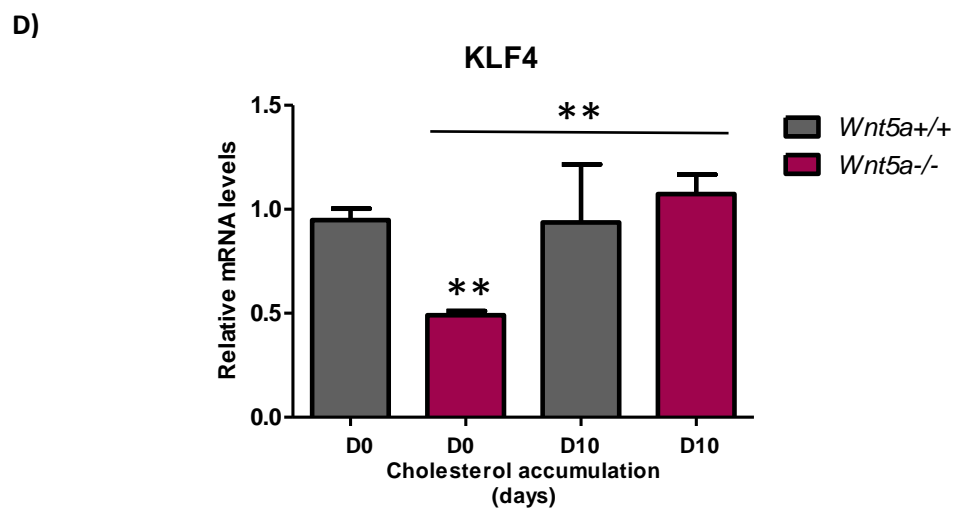
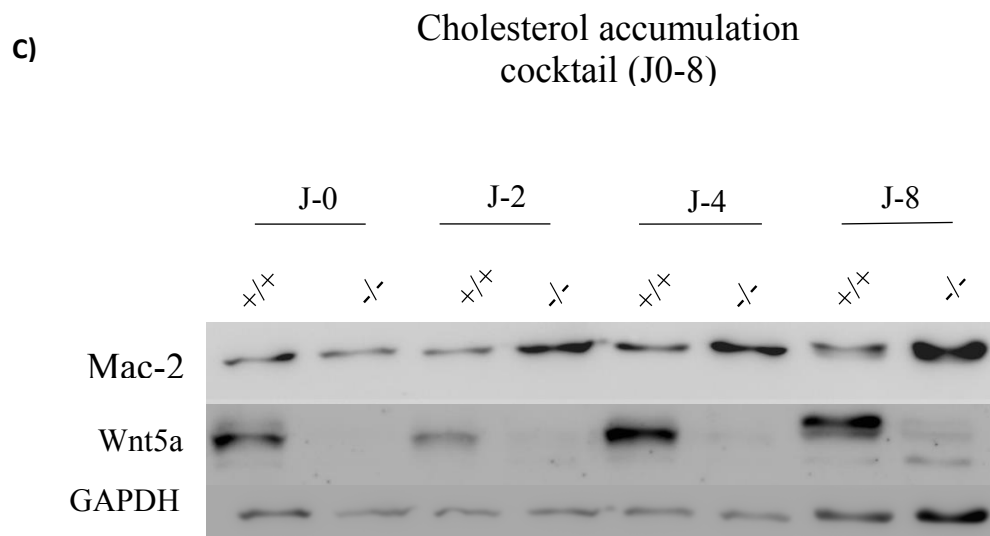
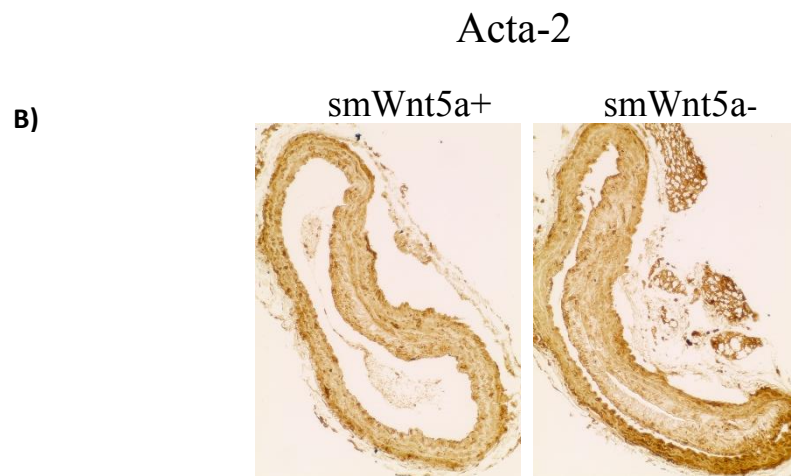


**Figure 21: SMCs transdifferentiation to macrophage like cells.** A) Immunohistochemistry labelling of mice aorta shows enhanced Mac-2 labeling in mutant mice vs controls. B) Immunohistochemistry labelling of mice aorta for Acta-2 shows no difference in labelling in mutant mice vs controls. C) Western blotting of Mac-2 upon treatment for cholesterol accumulation during 8 days. D) Relative transcript levels of KLF4 in human *Wnt5a*<sup>-/-</sup> VSMCs vs controls before (D0) and upon cholesterol accumulation protocol (D10) (n=3 independent experiments).

### ***2.3 Lipid quantification in Wnt5a<sup>-/-</sup> VSMCs and the controls***

Cells were cultured in normal conditions (DMEM plus 10% new born calf serum) or treated with adipogenic cocktail consisting of Insulin, IBMX, dexamethasone and Rosiglitazone for 10 days (Terrand *et al.*, 2009) and lipid quantification was performed in collaboration with Xavier Collet, Inserm U1048, Toulouse. Upon cholesterol feeding, *Wnt5a* protein levels increased over time in wild type human VSMCs (Fig. **22A**) and neutral lipids accumulated modestly as shown by Oil-Red-O staining (Figure **22B**). By contrast, neutral lipids strongly accumulated in *Wnt5a*<sup>-/-</sup> VSMCs compared to *Wnt5a*<sup>+/+</sup> VSMCs. When cultured in normal conditions, total cholesterol increased slightly in *Wnt5a*<sup>-/-</sup> VSMCs when compared to controls. However, cholesteryl-ester concentrations were significantly higher in *Wnt5a*<sup>-/-</sup> VSMCs (Fig. **22C**). At day 10, cholesteryl-esters levels were strongly increased in *Wnt5a*<sup>-/-</sup> VSMCs, and total cholesterol concentrations were elevated as well. In both treated and untreated cells, triglyceride levels (Fig. **22C**) were similar in *Wnt5a*<sup>-/-</sup> VSMCs and controls. Thus, *Wnt5a* prevents accumulation of cholesterol and cholesteryl esters in VSMCs. These data are in agreement with our lab's previously published results that *Wnt5a* prevents cholesterol

accumulation and limits foam cell formation in MEF cells and mouse adipocytes (El Asmar *et al.*, 2016).

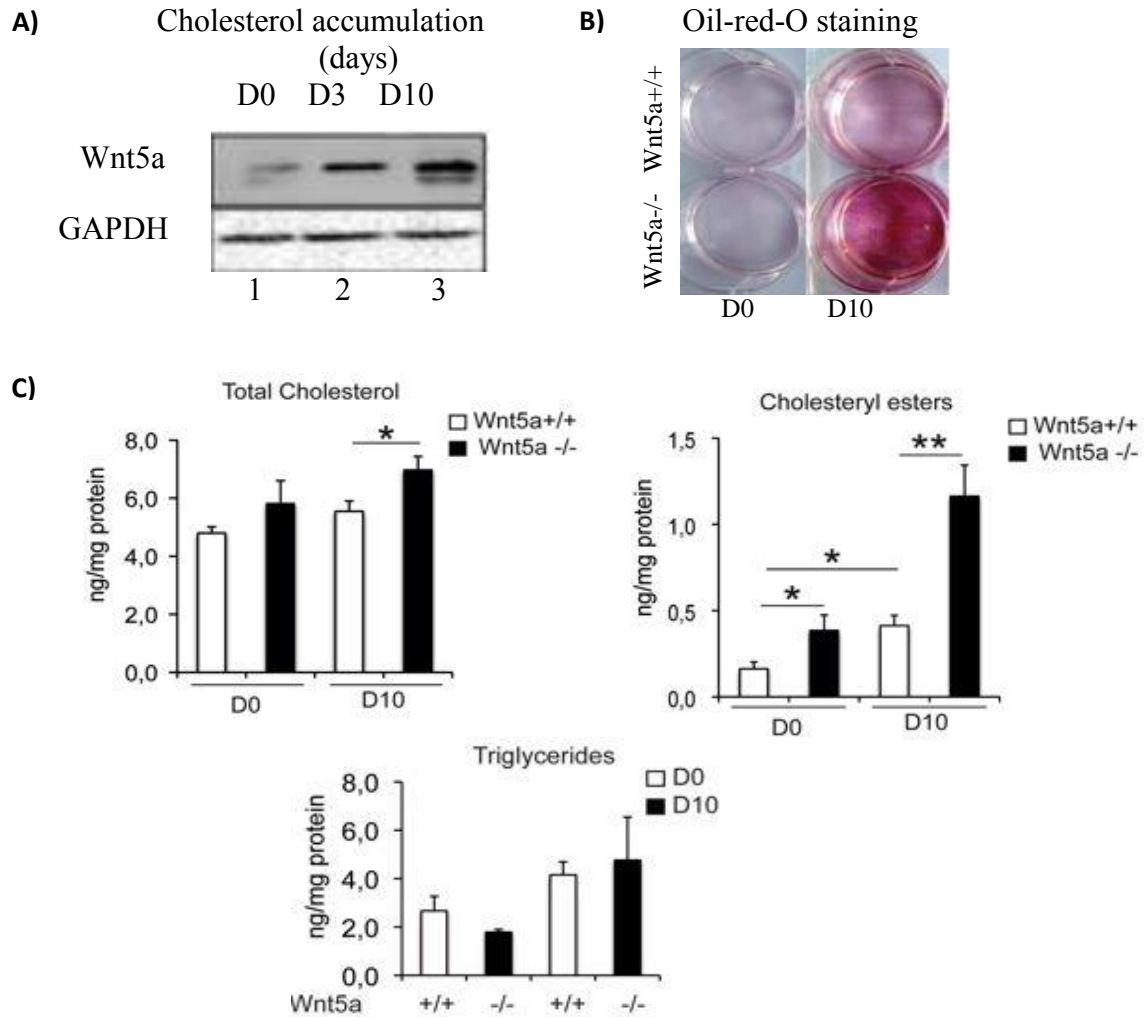


**Figure 22: Cholesterol accumulation in VSMCs Wnt5a<sup>-/-</sup>.** **A)** Western blot analysis of Wnt5a protein levels in human VSMCs over the course of a 10 days cholesterol accumulation protocol. **B)** Oil Red O staining. **C)** Quantification of total cholesterol and cholesteryl esters in untreated (n=7) and treated cells (n=10). Quantification of triglycerides in human Wnt5a<sup>-/-</sup> VSMCs and controls (Wnt5a<sup>+/+</sup>) untreated (D0) (n=7) or treated (D10) (n=10) for cholesterol accumulation during 10 days.

## 2.4 *Wnt5a* inhibits the expression of HMGCoA reductase, synthase and SREBP2

We next tested whether loss of *Wnt5a* activates cholesterol biosynthesis genes in VSMCs, as previously reported in MEFs, HEK 293 cells, and adipocytes (El Asmar et al., 2016). We found that mRNA levels of SREBP-2, and of its target genes HMG CoA synthase and HMG CoA reductase (**Fig. 23A**) were increased in VSMCs cultured under normal conditions (no added cholesterol) in the absence of *Wnt5a*. Similarly, upon cholesterol accumulation, SREBP-2 mRNA levels (**Fig. 23B**) and HMG CoA reductase protein levels (**Fig. 23C**) were higher in *Wnt5a*<sup>-/-</sup> VSMCs compared to controls. Thus, loss of *Wnt5a* in human VSMCs increased SREBP-2 mRNA levels and its target genes, and is accompanied by cholesterol and cholesteryl-ester accumulation.

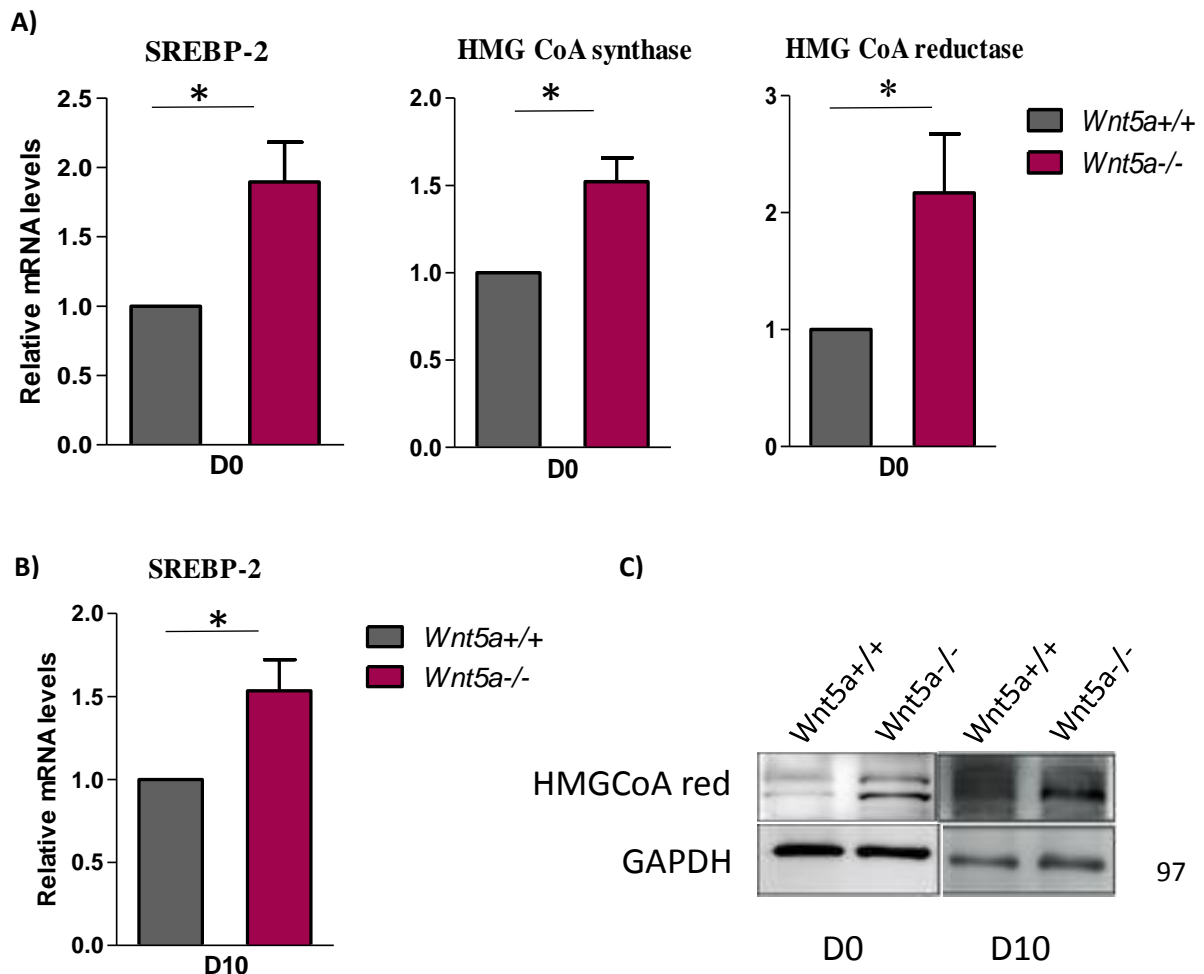


**Figure 23: Increased cholesterol synthesis in VSMCs Wnt5a<sup>-/-</sup>.** A) Relative transcript levels of SREBP-2, HMG CoA synthase, and HMG CoA reductase in untreated cells (n=5). B) Relative transcript levels of SREBP-2 in human Wnt5a<sup>-/-</sup> VSMCs and controls (Wnt5a<sup>+/+</sup>)(n=5). C) Western blotting of HMGCoA reductase upon no treatment and treatment for cholesterol accumulation during 10 days. Values are means  $\pm$  S.E.M. with  $p < 0.05$  (\*).

### 3. Cholesterol accumulates in lysosomes

#### 3.1 Cholesterol accumulates in lysosomes in absence of Wnt5a

Electron microscopic analysis of treated human Wnt5a<sup>-/-</sup> VSMCs (analyzed in collaboration with Motohide Murate from UMR 7021, University of Strasbourg) revealed accumulation of lipid droplets and of numerous very large endosome/lysosome (LELs) containing cholesterol crystals (**Fig. 24A**). In addition, human Wnt5a<sup>-/-</sup> VSMCs accumulated very large electron-dense cytoplasmic lipofuscin containing vesicles that were comparable in shape and size to those seen in the heart and in aortas of smWnt5a<sup>-</sup> mice. Lipofuscin are yellowish-brown granules made up of lipids from lysosomal degradation products. They also contains oxidized proteins, metals and sugar. Lipofuscin formation can be the result of decreased degradation of macromolecules and lipids in the lysosomes (Hohn & Grune, 2013). Thus, lipofuscin accumulation may lead to altered lysosomal function. To determinate in which compartment lipofuscin accumulated we used confocal imaging and the late endosomes marker (lysosome-associated membrane protein 1) Lamp1. We found that Lipofuscin-enriched large cytosolic vesicles that accumulate in Wnt5a<sup>-/-</sup> VSMCs are in fact Lamp1 positive LELs (**Fig. 24B**).

Taken together, these data indicate that Wnt5a boosts lysosomal function, protects against cholesterol accumulation, decreases constitutive SREBP-2

activity, and limit cholesterol biosynthesis, without affecting cellular triglycerides levels. This revealed Wnt5a as an unpredicted new component of the lysosomal cholesterol-sensing machinery in mammalian cells.

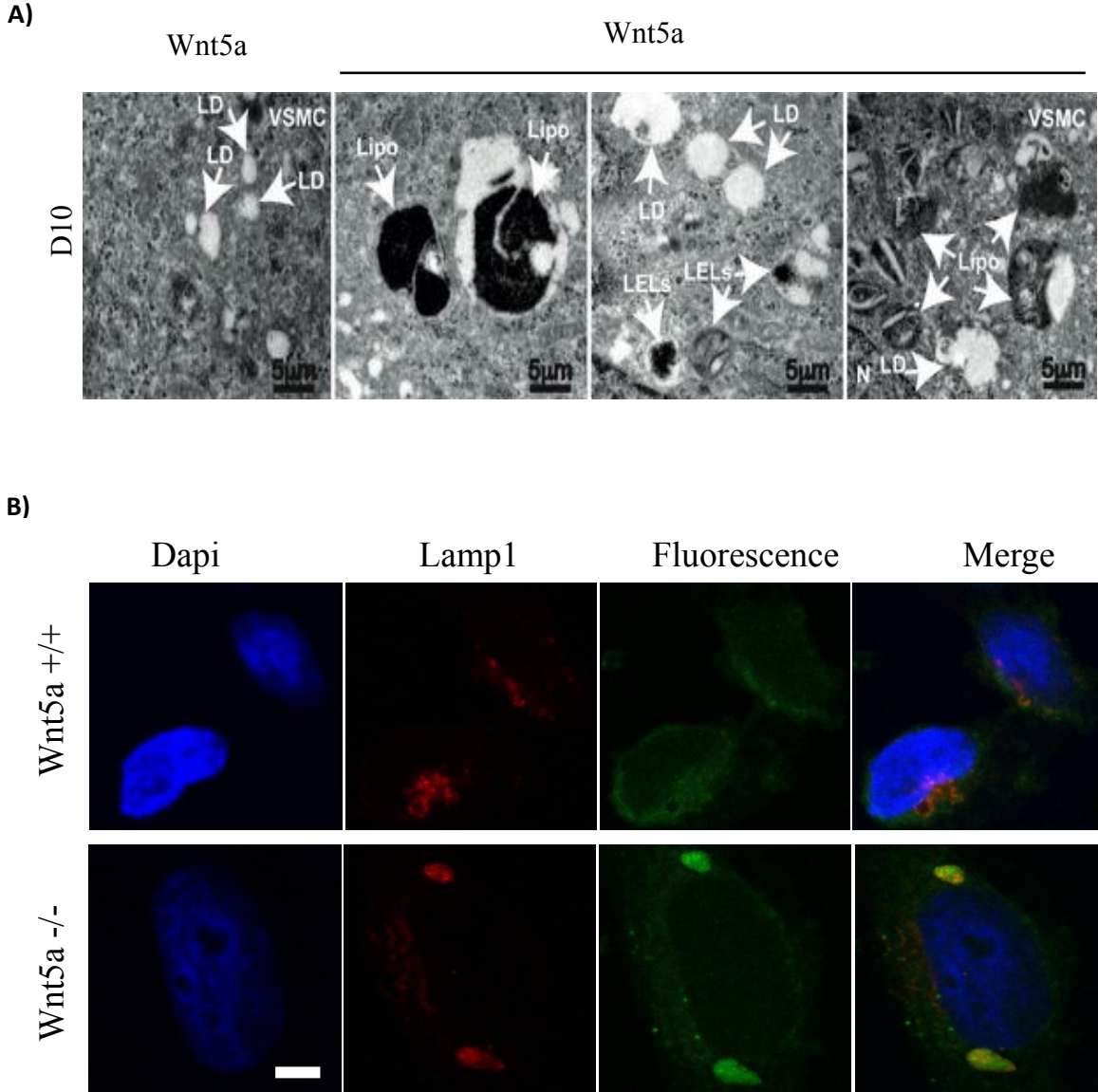


**Figure 24: Lipofuscin accumulation in absence of Wnt5a.** **A)** Representative electron micrographs of human *Wnt5a*<sup>-/-</sup> VSMCs and controls (*Wnt5a*<sup>+/+</sup>) show presence of large electron-dense cytoplasmic lipofuscin containing vesicles (Lipo), accumulation of lipid droplets (LD) and large LELs in VSMCs of mutants vs controls. **B)** To visualize lipofuscin granule formation upon cholesterol accumulation, human *Wnt5a*<sup>+/+</sup> VSMCs) and *Wnt5a*<sup>-/-</sup> were labeled with anti-Lamp1 antibodies (red) a LELs marker, and analyzed by confocal imaging using green fluorescence. Nuclei were stained in blue (Dapi). Merge images of lipofuscin green fluorescence and Lamp1 signals are shown. Arrows indicated lipofuscin pigment granules. Scale bar is 5 $\mu$ m. Values are mean  $\pm$  SEM.

### 3.2 Decreased ACAT1 expression in absence of Wnt5a.

Because lysosome-derived cholesterol correlates closely with ER cholesterol (M. S. Brown & Goldstein, 1986), we indirectly assessed ER cholesterol levels by measuring ACAT1 (acyl-CoA cholesterolacyltransferase 1) expression. ACAT1 is an ER resident enzyme that converts free cholesterol to cholesteryl ester. Its activity is controlled by cholesterol availability in the ER membrane (Suckling & Stange, 1985). ACAT1 protein (Fig. 25A) and mRNA (Fig. 25B) levels were markedly decreased in human *Wnt5a*<sup>-/-</sup> VSMCs compared to controls, indicative of low ER cholesterol.

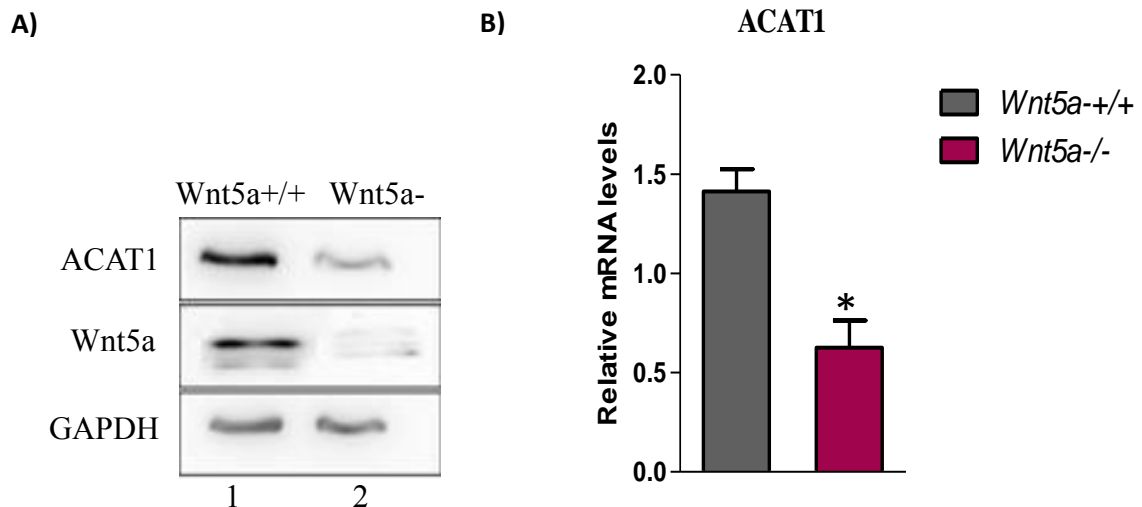


**Figure 25: Decreased ACAT1 expression in VSMCs Wnt5a<sup>-/-</sup>.** A) Western blot analysis of ACAT1 and B) its relative transcript levels in human Wnt5a<sup>-/-</sup> VSMCs vs controls upon cholesterol accumulation protocol.

ACAT1 transcript levels increased by 50% upon 10 days of cholesterol administration in LRP1<sup>+/+</sup> MEFs expressing endogenous Wnt5a, which is indicative of high levels of cholesterol in the ER (**Fig.26**). By contrast, LRP1<sup>-/-</sup> MEFs lacking endogenous Wnt5a (El Asmar *et al.*, 2016) expressed lower ACAT1 mRNA levels than controls, and ACAT1 expression did not increase upon cholesterol accumulation, indicative of an ER deprived of cholesterol. Thus, in the absence of Wnt5a, lysosomal function is impaired, resulting in the accumulation of cholesterol and cholesteryl-ester in Lamp1 positive compartments, and this gives rise to large LELs and electron-dense cytoplasmic lipofuscin containing vesicles.

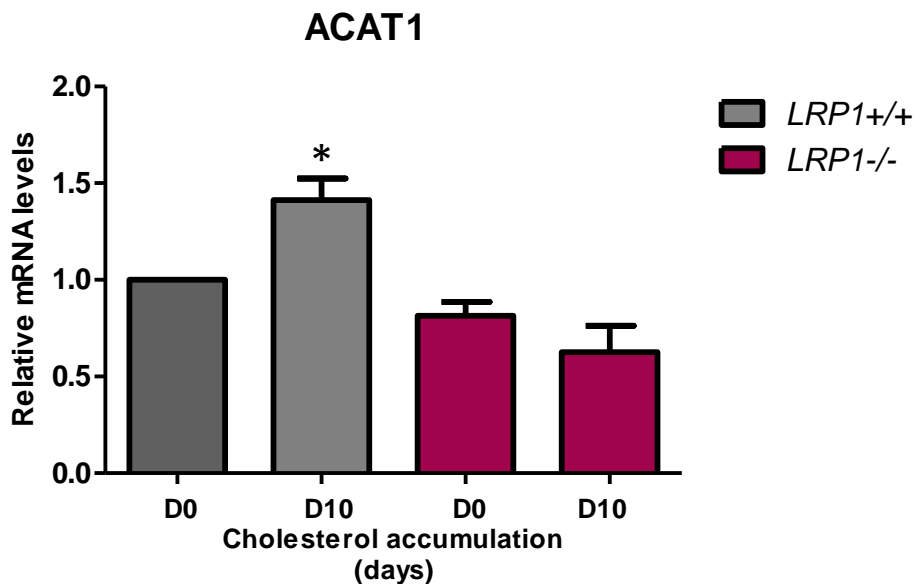
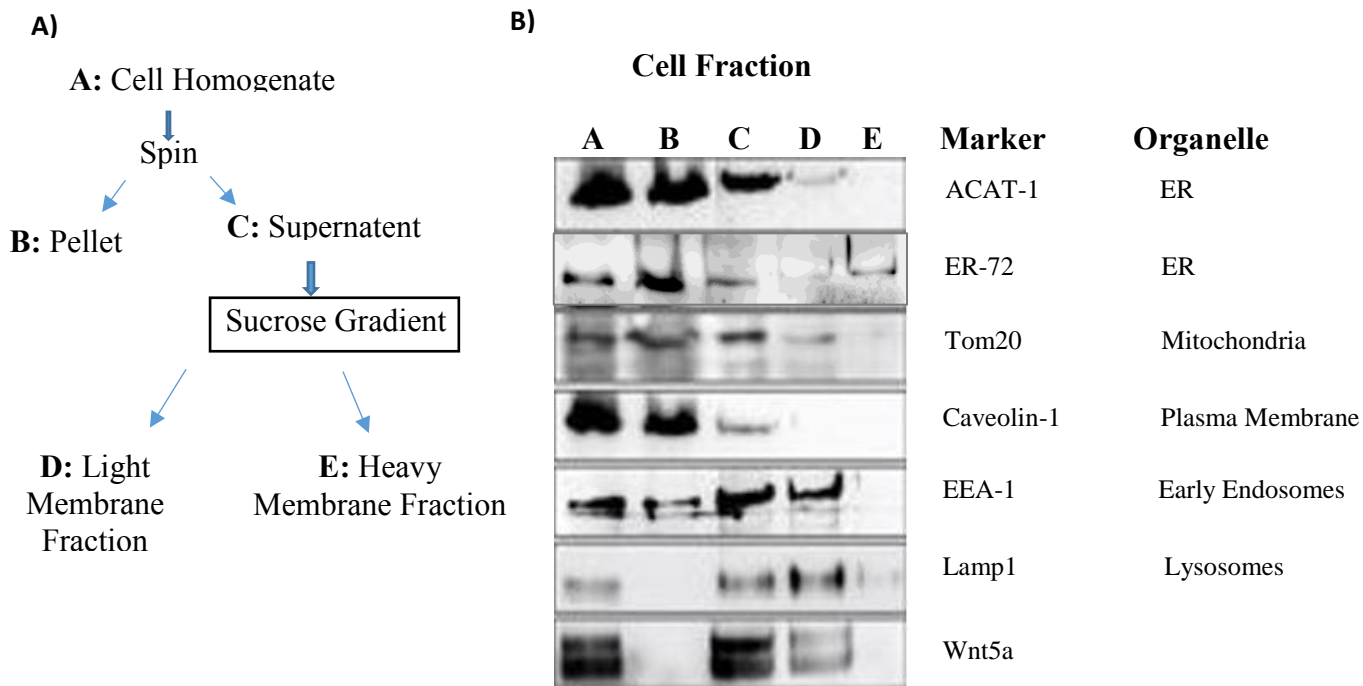


**Figure 26: Decreased ACAT1 expression in MEF LRP1<sup>-/-</sup> cells.** ACAT1 relative mRNA levels in MEFs LRP1<sup>-/-</sup> and controls before (D0) and upon cholesterol accumulation protocol (D10) (n=4 independent experiments).

### ***3.3 Cholesterol quantification in lysosomal and ER fractions***

To measure the membrane cholesterol content in Lamp1 positive compartments we collaborated with Dr. Diane Julien David, UMR 7178, University of Strasbourg. We used a subcellular fractionation approach to isolate LEL membranes from human VSMCs as outlined in Figure 27A. Fractionation was first performed in CMLV cells (**Fig.27B** left panel) as described in (Radhakrishnan *et al.*, 2008). The cell homogenate (designated Fraction A) was subjected to two centrifugation steps in order to separate LELs membranes from other organelles. Centrifugation of the homogenate at 3000xg separates unbroken cells and the heaviest membranes. As assessed by immunoblot analysis of the fractions, a plasma membrane protein marker (Caveolin-1) and ER membrane protein markers (ACAT-1, and ER-72) are mostly retained in the 3000g pellet (Fraction B), whereas significant amounts of all other membrane markers, including the LEL protein marker Lamp1 were present in the 3000xg supernatant (Fraction C). Fraction C was then subjected to centrifugation through a discontinuous sucrose gradient containing 7.5%, 15%, 30% & 45% sucrose. This yielded two distinct bands of membranes (Fractions D and E). Fraction D and E contained both ER membrane protein markers, and no plasma membrane protein marker. The LEL membrane protein Lamp1 along with the early endosomal membrane protein EEA1 were present in Fraction D and almost absent in Fraction E (**Fig. 27B**). Interestingly, Wnt5a concentrated in the Lamp1 positive Fraction D,

indicative of its localization in LELs and in endocytic compartments, as previously described for other Wnt ligands (Taelman *et al.*, 2010). Analysis of cholesterol content of membrane fractions revealed that cholesterol in the fraction enriched in ER membranes (the heavy Fraction E) is decreased in mutant cells compared to controls (**Fig. 27C**). Thus, in the absence of Wnt5a, cholesterol is retained in LEL fractions. Less cholesterol trafficks to the ER, ACAT-1 is down regulated, and SREBP-2 is induced. This supports our hypothesis that Wnt5a is required for cholesterol trafficking from LELs to the ER.



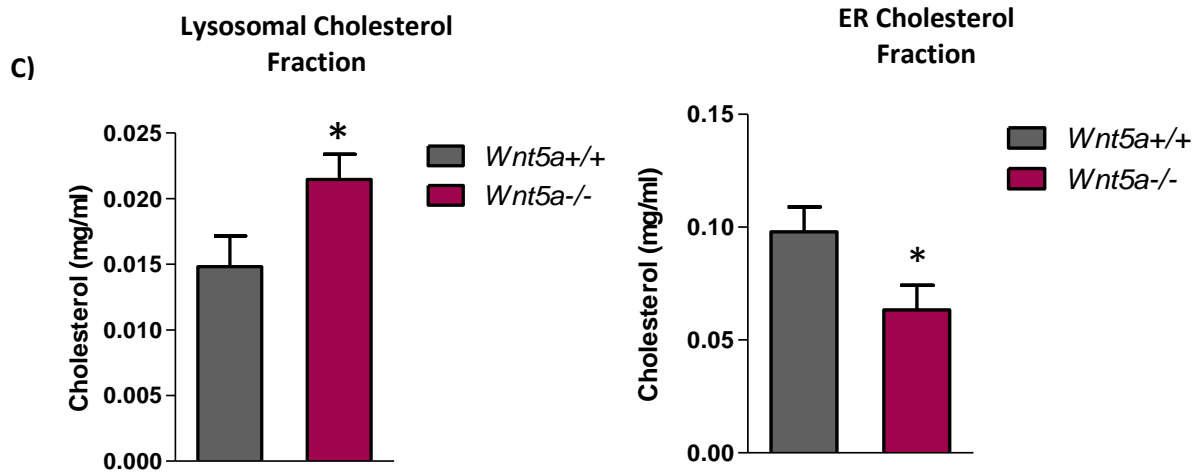


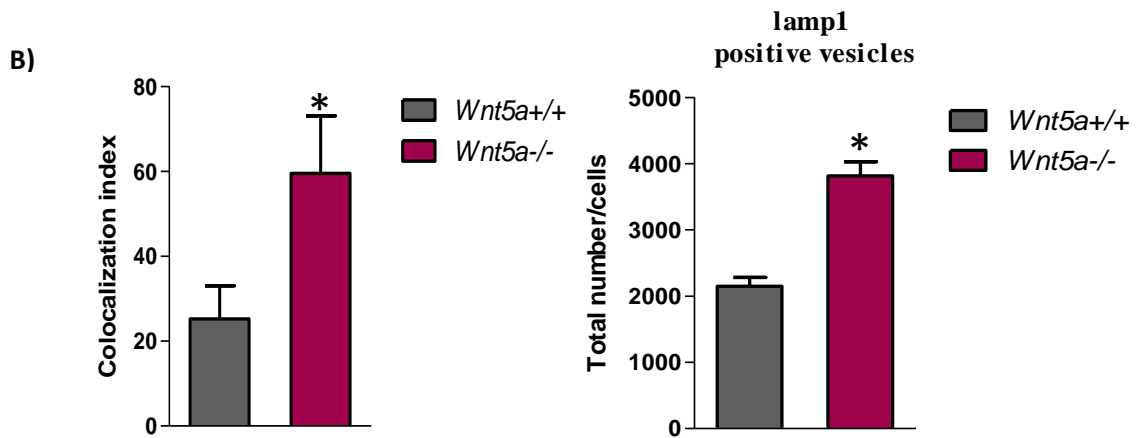
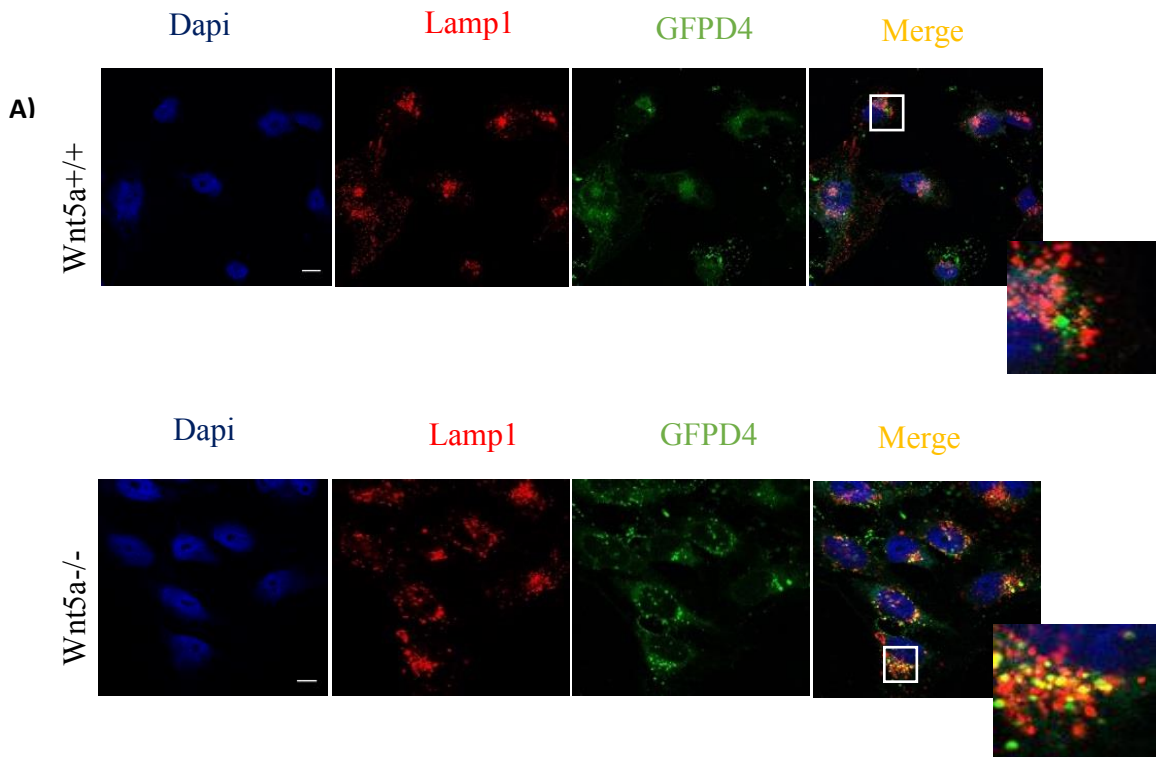
**Figure 27: Cholesterol quantification in lysosomal and ER fractions.** Purification of ER and LELs, elimination of nuclear, mitochondria, plasma, golgi and early endosomal membranes. **A)** Left panel is showing the diagram of LELs membrane fractionation scheme. A-E denote major fractions recovered and analyzed by western blot. **B)** Right panels, CMLVs were treated according to the fractionation scheme and as described in the method section. Cells were disrupted and centrifuged at 3000g. The supernatant was then loaded at the top of a discontinuous sucrose gradient and centrifuged at 100,000g for one hour, yielding two distinct membrane layers. After this step, aliquots representing equal volumes of each fraction (A-E) were subjected to immunoblot analysis for the indicated organelles markers and *Wnt5a*. **C)** Quantification of cholesterol concentrations in heavy (E fraction) membrane fractions from human *Wnt5a*<sup>-/-</sup> VSMCs and *Wnt5a*<sup>+/+</sup>.

## 4 Altered lysosomal function

Next, in collaboration with Catherine Tomasetto and Fabien Alpy we assessed the subcellular sites of cholesterol accumulation and regulation of lysosomal function.

#### ***4.1 Quantification of co-localization of cholesterol in subcellular lysosomal vesicles***

We used confocal imaging to quantify cholesterol inside cells with two specific fluorescent probes: the D4 fragment of perfringolysin O fused to GFP (GFP-D4) (Ohno-Iwashita et al., 2004) and Lamp1 (glycosylated lysosomal membrane protein rich in sialic acid and covers 80% of lysosomal surface along with Lamp-2). Lamp1 and GFP-D4 were received from Fabien Alpy (IGBMC, Illkirch, France). We found that cholesterol-enriched cytosolic vesicles that accumulate in Wnt5a<sup>-/-</sup> VSMCs are Lamp1 (lysosomal associated membrane protein 1) positive endosomal compartments (**Fig. 28A**). As GFP-D4 binds only to membranes containing more than 35 mol% cholesterol (Ohno-Iwashita et al., 2004), these data indicate a massive accumulation of cholesterol in LELs in the absence of Wnt5a. Co-localization studies for GFPD4 positive lamp1 vesicles in cells were performed using a macro in Image-J. Quantification of co-localization between GFP-D4 and Lamp1 show that there is 3X more cholesterol in Lamp1 positive compartments in VSMCs lacking Wnt5a compared to controls upon cholesterol accumulation (**Fig. 28B**). In addition, immunofluorescence analysis indicated that the LELs marker Lamp1 increased substantially in cholesterol-fed mutant cells compared to controls. Western blot analysis of Lamp1 shows a decrease in lamp1 protein expression upon cholesterol treatment in presence of Wnt5a whereas in absence of Wnt5a lamp1 is increasing suggesting that lysosomal function is altered (**Fig. 28C**). Taken together, these data suggest that loss of Wnt5a alters lysosomal function; consequently, cholesterol accumulates in LELs, leading to the increase in LEL size and increased Lamp1 expression.



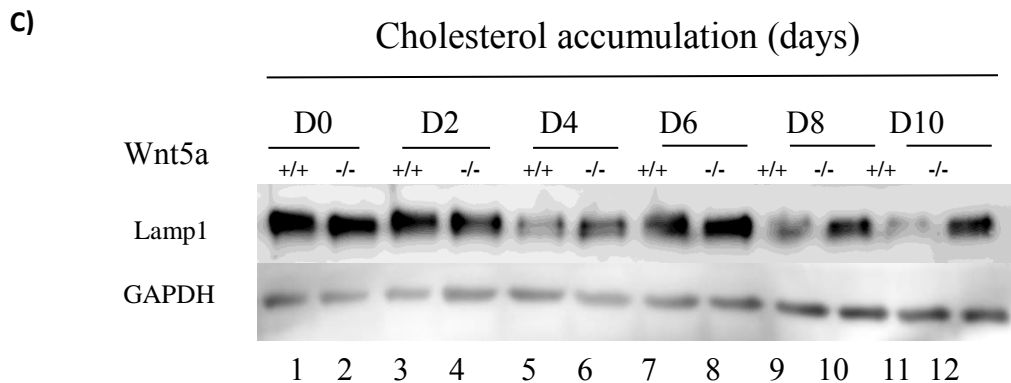


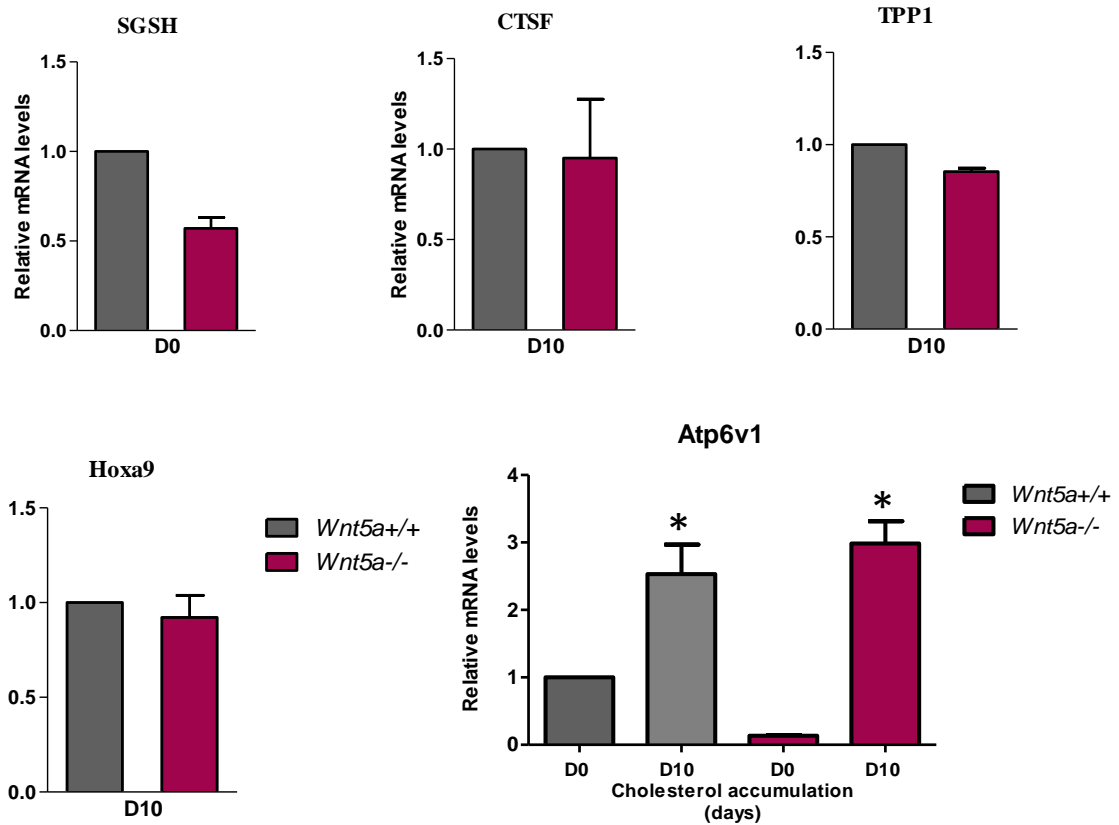
**Figure 28: Cholesterol accumulates in lysosomal vesicles in VSMCs Wnt5a<sup>-/-</sup>.** Human Wnt5a KO (Wnt5a<sup>-/-</sup>) and controls (Wnt5a<sup>+/+</sup>) VSMCs were treated for cholesterol accumulation as described in the method section. **A)** To follow cholesterol accumulation cells were labeled with anti-Lamp1 antibodies (red) a LELs marker, and with the fluorescent cholesterol probe GFP-D4 (green). Nuclei were stained in blue. Merge images of GFP-D4 and Lamp1 signals are shown. Higher magnification (2.5X) images of the area outlined in white are shown on the right. Scale bar, 5 $\mu$ m. **B)** Quantification (n=5 independent experiments) of confocal analysis shows increased colocalization between GFP-D4 (cholesterol) and Lamp1 (LELs) in Wnt5a KO VSMCs (Wnt5a<sup>-/-</sup>) compared to controls (Wnt5a<sup>+/+</sup>). **C)** Western blot analysis of Lamp1 in treated cells.

## 4.2 Regulation of lysosomal function in absence of Wnt5a

A dynamic regulation of lysosomal function was recently demonstrated by the identification of the MiT/TFE transcription factors, which include the transcription factor EB (TFEB), TFEC, TFE3, and MITF (Palmieri *et al.*, 2011; Sardiello *et al.*, 2009). Subsequent investigations showed that TFEB drives the expansion of the lysosomal compartment, lysosomal biogenesis,

and autophagy (Palmieri *et al.*, 2011; Sardiello *et al.*, 2009). To assess whether Wnt5a modulates TFEB activity we measured mRNA levels of its target genes, SGSH, ATP6V, CTSF and TPP1 (Sardiello *et al.*, 2009). In untreated cells as well as in cholesterol-fed cells, no significant change was observed except for ATP6V in the mRNA levels of these genes in the absence of Wnt5a compared to controls (Fig. **29A**). Expression of Hoxa9, a non-TFEB target gene was not affected. This suggested that, in the absence of Wnt5a the increase in Lamp1 expression is due to intralysosomal storage of cholesterol and cholesteryl-ester, and does not depend upon TFEB activation. Increased ATP6V expression levels mark increased lysosomal acidification. Therefore, upon cholesterol feeding for 10 days, VSMCs were labelled with lysotracker red. Lysotracker red dye accumulates in vesicles with acidic pH Wnt5a-VSMCs present more labelling for lysotracker red (Fig.**29B**). This increased acidification of lysosomes might be because of altered lysosomal function in absence of Wnt5a.

A)



B)

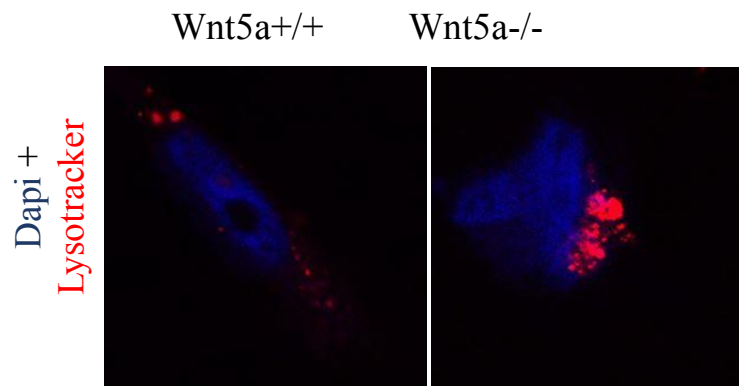


**Figure 29: Regulation of lysosomal function in absence of *Wnt5a*.** A) Relative mRNA levels of the indicated genes in human VSMC *Wnt5a*<sup>-/-</sup> and controls untreated (D0) and treated for cholesterol accumulation (D10) (n=4 independent experiments). Values are means  $\pm$  S.E.M. with  $p < 0.05$  (\*). B) Increased lysotracker red labelling in *Wnt5a*<sup>-/-</sup> VSMCs upon cholesterol accumulation (D10).

## 5. Wnt5a downregulates mTORC1 pathway and triggers autophagy

LELs have emerged as the cellular site where the master growth regulator, mechanistic target of rapamycin complex 1 (mTORC1) is activated. mTORC1 senses nutrient signals inside cells and drives the synthesis of fatty acids and sterols by increasing the expression and proteolytic cleavage of SREBP-1c and SREBP-2 (Owen *et al.*, 2012; Yecies *et al.*, 2011).

### 5.1 Increased mTORC1 phosphorylation in absence of Wnt5a

Given that high mTORC1 activity coincides with low ER cholesterol, high ACAT-1 expression, and activation of SREBP-2 (Eid *et al.*, 2017), we assessed p-mTORC1 levels in Wnt5a<sup>-/-</sup> VSMCs. We found a robust increase of p-mTORC1 and its downstream targets, p-P70S6 and p-4EBP-1, and of p-Akt in the absence of Wnt5a in human VSMCs (Fig.30A). However, Rescue experiments show that treatment of human Wnt5a<sup>-/-</sup> VSMCs with conditioned media enriched in Wnt5a decreased the p-mTORC1 target gene p-P70S6 to control levels, whereas mock media had no effect (Fig.30B).

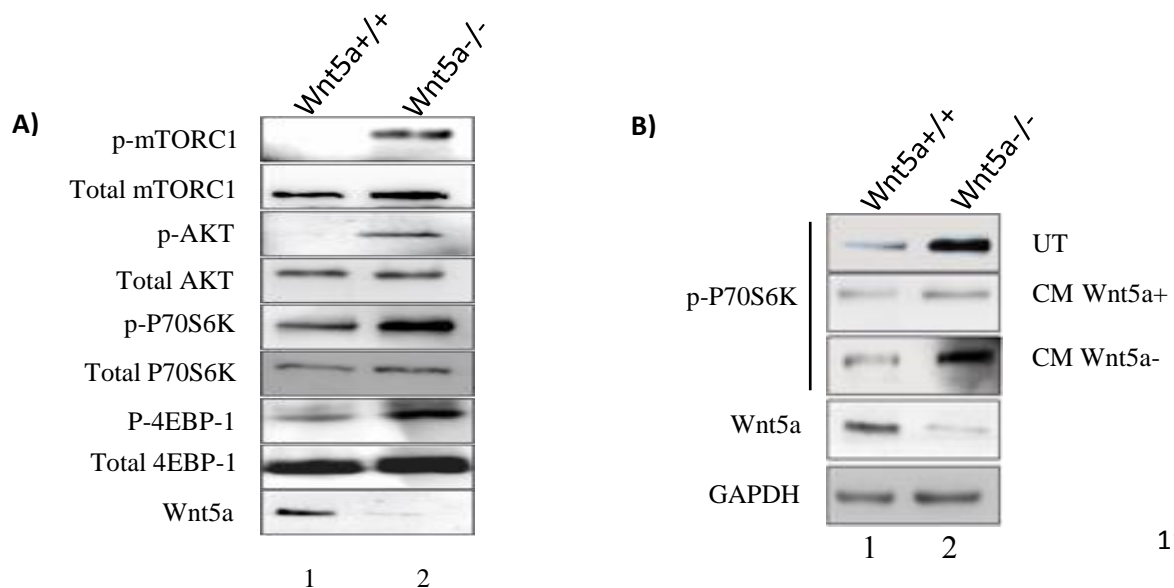


**Figure 30: Increased mTORC1 and its target genes in absence of Wnt5a.** **A)** Western blot analysis of p-mTORC1 (ser2448), total mTORC1, p-Akt (Ser473), total Akt, p-P70S6(Thr389), total P70 S6, p-4EBP-1, total 4EBP-1, and Wnt5a in human Wnt5a KO (Wnt5a<sup>-/-</sup>) and controls (Wnt5a<sup>+/+</sup>) VSMCs upon cholesterol accumulation protocol. **B)** Western blot analysis showing p-P70S6(Thr389) expressions in Wnt5a<sup>-/-</sup> VSMCs untreated (UT) or treated with conditioned medium enriched in Wnt5a (CM Wnt5a<sup>+</sup>) or mock medium (CM Wnt5a<sup>-</sup>).

Marked activation of the PI3K/Akt/mTORC1 pathway in the absence of Wnt5a was also observed in vivo with increased protein levels of p-Akt, p-P70 S6, and p-4EBP1 in aortas from smWnt5a<sup>-</sup> mice compared to controls (Fig.16).

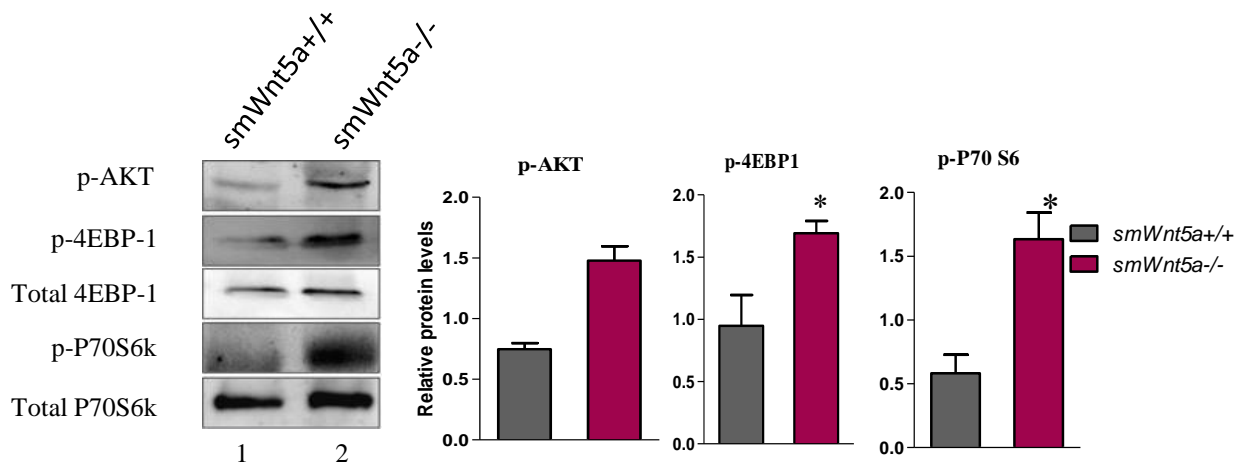


**Figure 31: Increased mTORC1 and its target genes in absence of Wnt5a.** Western blot analysis and quantification of relative protein levels of the indicated genes in aortas from control (smWnt5a<sup>+</sup>) and mutant (smWnt5a<sup>-</sup>) mice (n=3). Values are means  $\pm$  S.E.M. with  $p < 0.05$  (\*),  $p < 0.01$  (\*\*).A), Western blot analysis of p-mTORC1 and total mTORC1

protein levels during the course of cholesterol accumulation in *Wnt5a*<sup>-/-</sup> VSMCs and controls.

## 5.2 Increased phosphorylation of tyrosine kinase in *Wnt5a* absence

Changes in cholesterol levels can alter the activity of signaling pathways originating at the plasma membrane involving phosphoinositide-3 kinase (PI3K) that can activate mTORC1 (Perera and Zoncu, 2016). To test whether *Wnt5a* acts upstream of mTORC1 or directly on mTORC1 we measured PI3K activation in human VSMCs. We found the p85 subunit of PI3K to be highly tyrosine phosphorylated in human *Wnt5a*<sup>-/-</sup> VSMCs compared to controls (**Fig.32A**) and treatment with the PI3K inhibitor Wortmanin inhibited mTORC1 activation in human *Wnt5a*<sup>-/-</sup> VSMCs (**Fig.32B**). This indicates that *Wnt5a* down regulated the PI3K/Akt/mTORC1 pathway in human VSMCs.

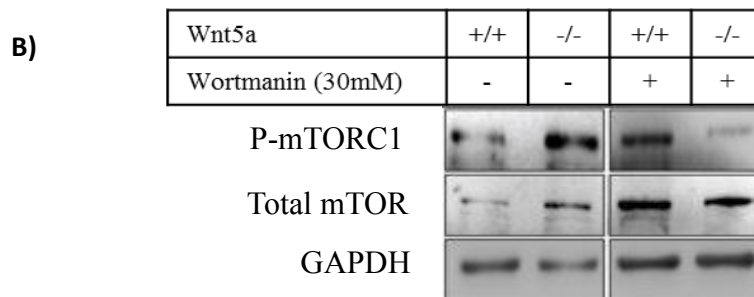
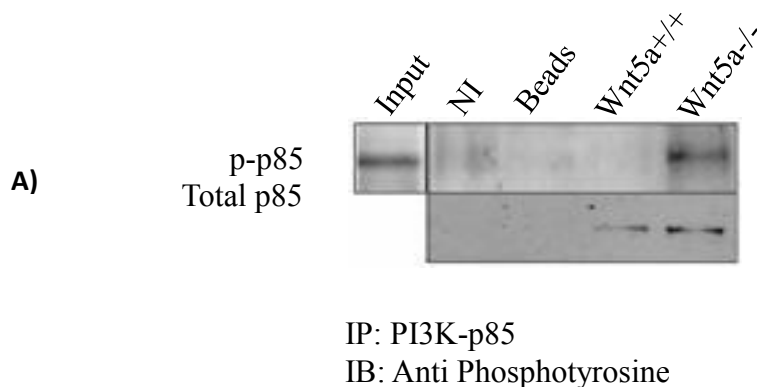


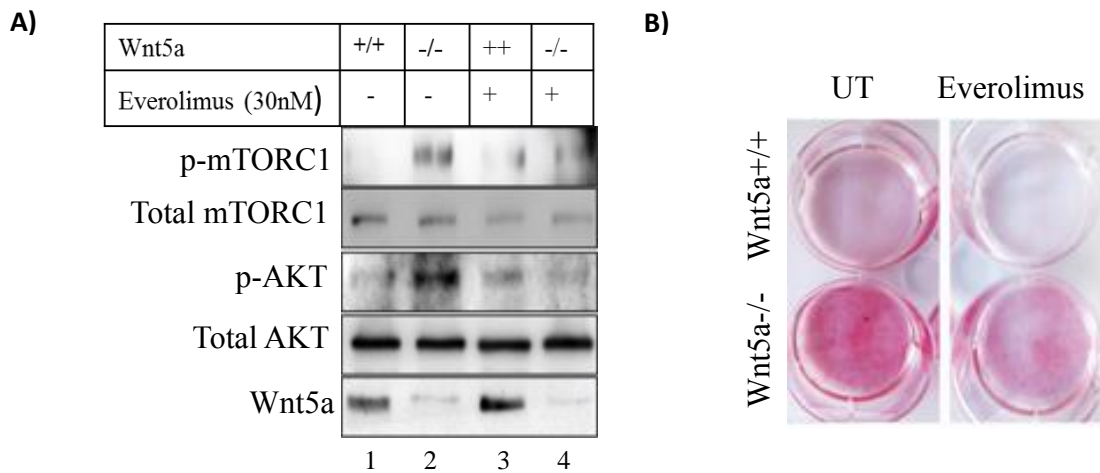
**Figure 32: Wnt5a downregulates PI3Kinase/mTORC1 pathway.** **A)** Immunoprecipitation in Wnt5a<sup>-/-</sup> VSMCs and controls of the PI3K-p85 subunit followed with immunoblotting with anti-phosphotyrosine (4G10) antibodies show the tyrosine-phosphorylated form of p85 (p-p85) in the absence of Wnt5a. NI=non-immune antibodies, Beads = empty beads. Input is from whole cell lysate (n=3). **B)** Western blot analysis showing p-mTORC1, total mTORC1, and GAPDH in Wnt5a<sup>-/-</sup> VSMCs and controls treated with Wortmanin (30nM).

### ***5.3 Effects of LiCl and everolimus on cholesterol trafficking***

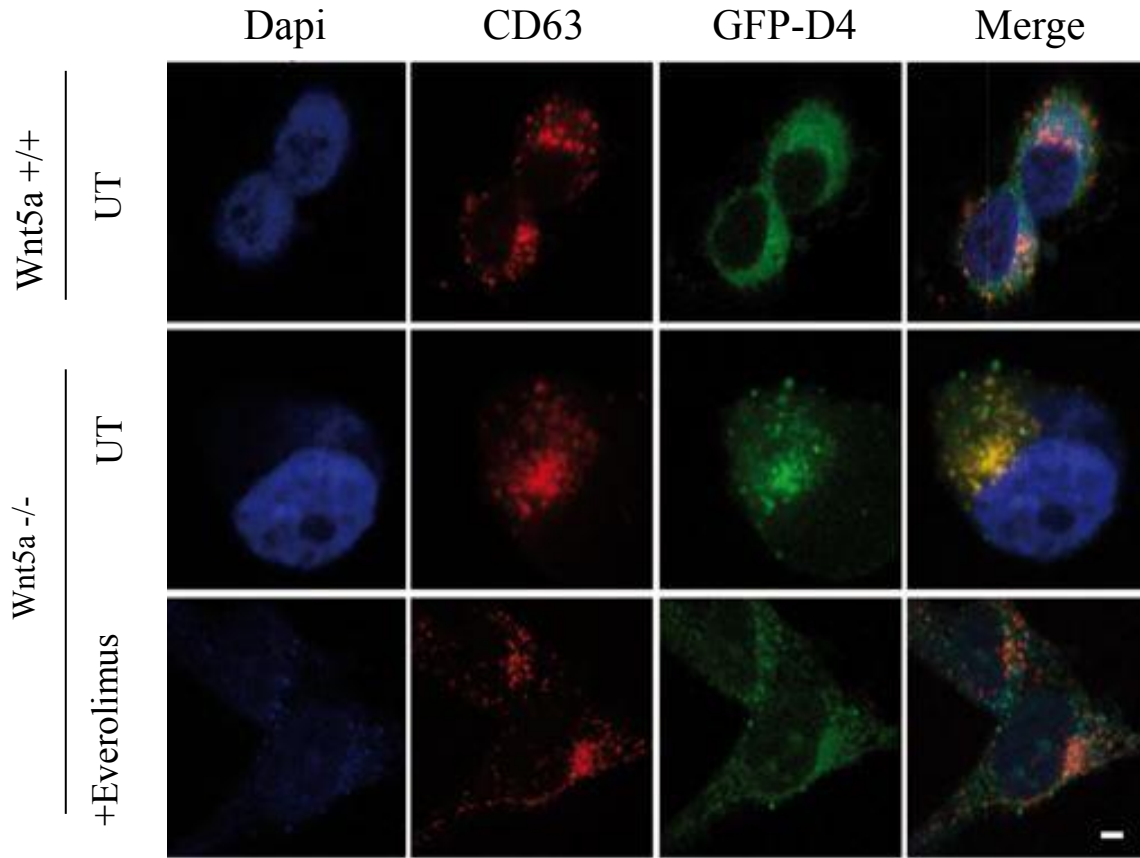
Everolimus®, is an mTORC1 inhibitor prescribed in cancer related indications (Wesolowski *et al.*, 2014). As our results show that phospho-mTORC1 levels are increased in absence of Wnt5a, therefore, we decided to inhibit mTORC1 activity using its inhibitor. We observed that it decreases p-mTORC1 and p-Akt in human Wnt5a<sup>-/-</sup> VSMCs (**Fig. 33A**). Everolimus® treatments decreased cholesterol accumulation in human Wnt5a<sup>-/-</sup> VSMCs (**Fig.33B**), and fully rescued cholesterol trafficking from CD63 positive endosomal compartments to the ER (**Fig.33C**). CD63 is a membrane bound protein highly expressed in lysosomes and endosomes. Thus, loss of Wnt5a coincides with high mTORC1 activity, which is known to block cholesterol egress from LELs and to promote cholesterol accumulation (Eid *et al.*, 2017). Similarly, treatment with the GSK3 inhibitor LiCl (LiCl is an agonist of Wnt5a and a FDA approved treatment of choice for mood disorders and neurodegenerative diseases) (Yao *et al.*, 2018) decreased p-mTORC1 in human Wnt5a<sup>-/-</sup> VSMCs (**Fig.33D**).

The Glycogen Synthase Kinase 3 (GSK3) plays a central role in Wnt- $\beta$ -catenin signaling and Wnt inhibits the GSK3 dependent phosphorylation and degradation of  $\beta$ -catenin (Taelman *et al.*, 2010). To test how Wnt5a regulates

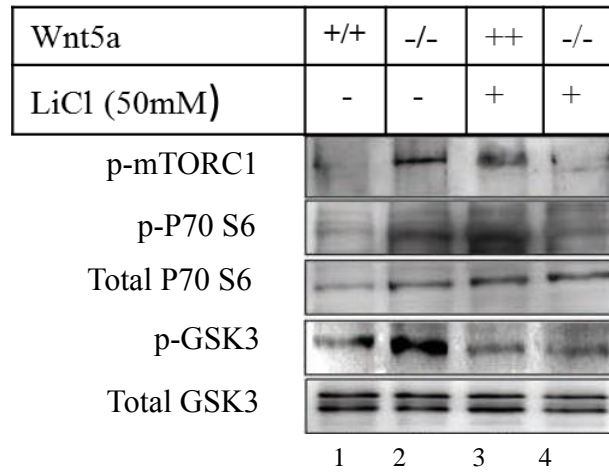
GSK3, we measured p-GSK3 in human *Wnt5a*<sup>-/-</sup> VSMCs and controls. We found that loss of *Wnt5a* activated GSK3 on its catalytic domain (**Fig. 33D**) (Harwood *et al.*, 1995). In agreement to what was previously reported, and showing that *Wnt3a* activates mTORC1 phosphorylation upon treatment with Wnt agonist LiCl, we also observed increased expression of p-mTORC1 and its target p-P70 S6 in control cells (Inoki *et al.*, 2006). However, in our case loss of *Wnt5a* inhibited the increase in p-mTORC1 and p-P70 S6 induced by LiCl (**Fig. 33D**). These data suggested that *Wnt5a* regulates GSK3 in a manner similar to other Wnt ligands, but behave differently than other Wnt ligands in the regulation of mTORC1.



c)



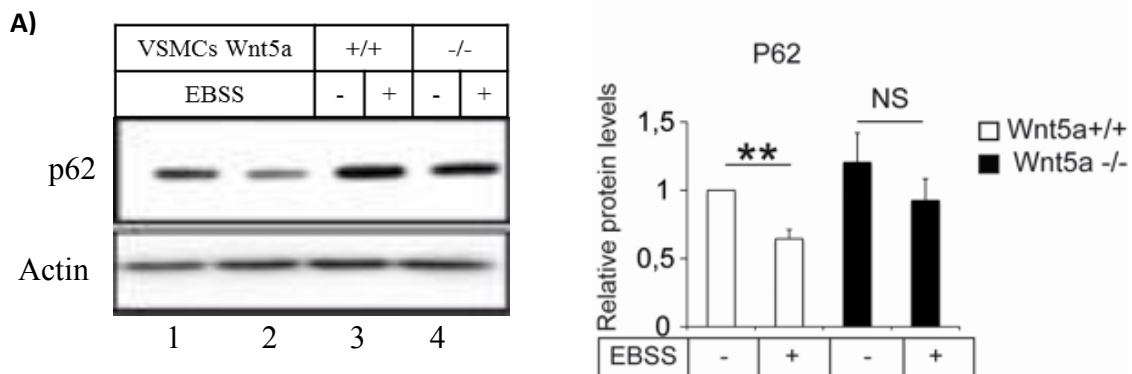
d)



**Figure 33: Cholesterol trafficking rescue by mTORC1 inhibition.** **A)** Western blot analysis showing p-mTORC1, total mTORC1, p-Akt, total Akt, and Wnt5a in Wnt5a<sup>-/-</sup> VSMCs and controls treated with Everolimus® (30nM). **B)** Oil red O staining of Wnt5a<sup>-/-</sup> VSMCs and controls upon 10 days of cholesterol accumulation cocktail plus treatment with the p-mTORC1 inhibitor, Everolimus® (30nM)(+ Everolimus) or vehicle (UT) (n=3). **C)** Confocal analysis showing colocalization (yellow) between GFP-D4 positive vesicle (cholesterol, green) and CD63 (LELs, red) in untreated (UT) and Everolimus (30nM) treated Wnt5a<sup>-/-</sup> VSMCs. **D)** Treatment with the Wnt activator LiCl (50mM).

#### 5.4 Wnt5a promotes autophagy

Since high activity of mTORC1 suppresses autophagy (Eid *et al.*, 2017), we measured protein levels of two major markers of autophagy, P62 and LC3 in human VSMCs in collaboration with Dr. Laurent Martinez, Inserm U1048, Toulouse. Absence of Wnt5a blocks the degradation of P62 (Fig.34A) and of LC3 (Fig.34B) during starvation medium treatments, as well as degradation of P62 during cholesterol accumulation, which indicates autophagy inhibition. Thus, Wnt5a promotes autophagy and facilitates LEL cholesterol egress by inhibiting mTORC1.



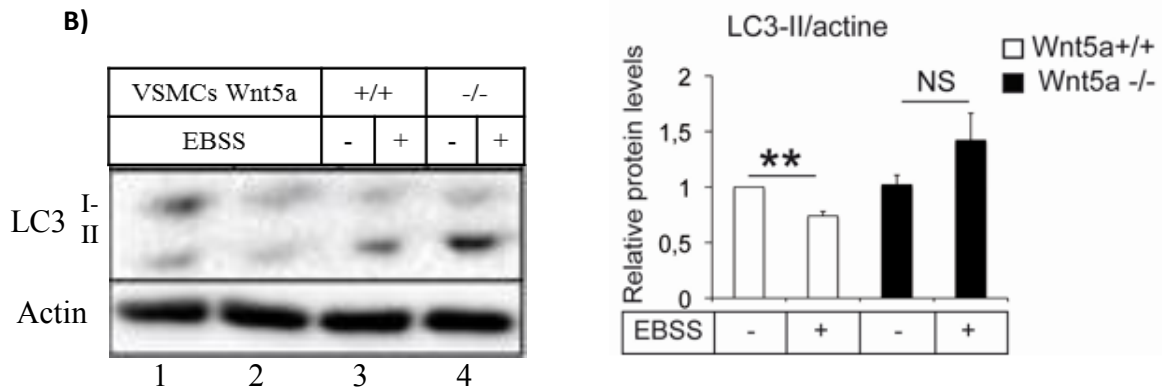


**Figure 34: Wnt5a triggers autophagy.** **A)** Western blot analysis of p62 levels and **B)**, its quantification in human Wnt5a KO (Wnt5a<sup>-/-</sup>) and controls (Wnt5a<sup>+/+</sup>) VSMCs upon starvation medium treatments (n=9). **B)** Western blot analysis of LC3I/II and **D)**, its quantification in human Wnt5a KO (Wnt5a<sup>-/-</sup>) and controls (Wnt5a<sup>+/+</sup>) VSMCs upon starvation medium treatments (n=9).

## 6. Wnt5a physically interacts with cholesterol and NPC proteins.

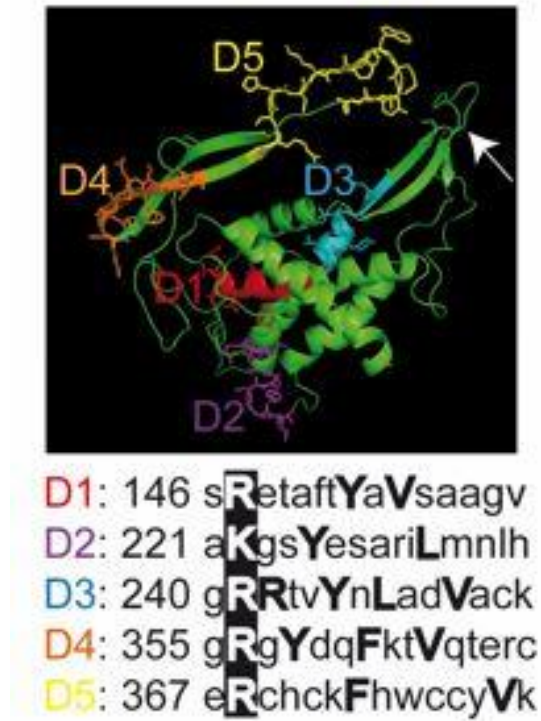
On the basis of our results indicating that Wnt5a interferes with cholesterol trafficking in LELs, a compartment that harbors most of the cholesterol (60%) in the endocytic pathway (Mobius *et al.*, 2003), we examined whether the Wnt5a sequence contains cholesterol-binding motifs.

### 6.1 Wnt5a binding to cholesterol

We identified 5 putative cholesterol recognition amino acid consensus (CARC) motifs that we named D1-5 (Fig. 35A). The consensus CARC

sequence (L/V)-X1-5-Y- X1-5-(K/R) has been described in transmembrane domains of cholesterol-regulated proteins such as caveolins, the Ca<sup>2+</sup> channel Orai-1, and SLC38A9 within the mTORC1 scaffolding complex (Castellano *et al.*, 2017). However, cholesterol-binding domains have also been identified outside the membrane-spanning regions of soluble proteins such as,  $\alpha$ -synuclein, the neural protein associated with Parkinson disease, where they bind cholesterol with low affinity (Fantini *et al.*, 2011). Using the 3D structure of Wnt8 another Wnt ligand that is 33 % homologous to Wnt5a as a template (Janda *et al.*, 2012), we in collaboration with Fabian Alpy *et al.* we modeled *in silico* the 3D structure of Wnt5a and the subsequent localization of CARC motifs (Fig. **35A**). CARC motifs D2, D3, and D4 were found at the periphery of the 3D structure of Wnt5a, accessible to cholesterol, and thus in a biologically relevant position. We next investigated the ability of Wnt5a to bind cholesterol in liposomes reconstituted with phosphatidylcholine, enriched with cholesterol (PC+Chol) or not (PC). Co-sedimentation assays revealed that Wnt5a did not pellet with PC-containing liposomes (Fig. **35B**, lane 4). However, the inclusion of cholesterol in PC-containing liposomes enhanced their association with Wnt5a (Fig. **35B**, lane 2) indicating that Wnt5a binds to cholesterol-enriched membranes.

A)



B)

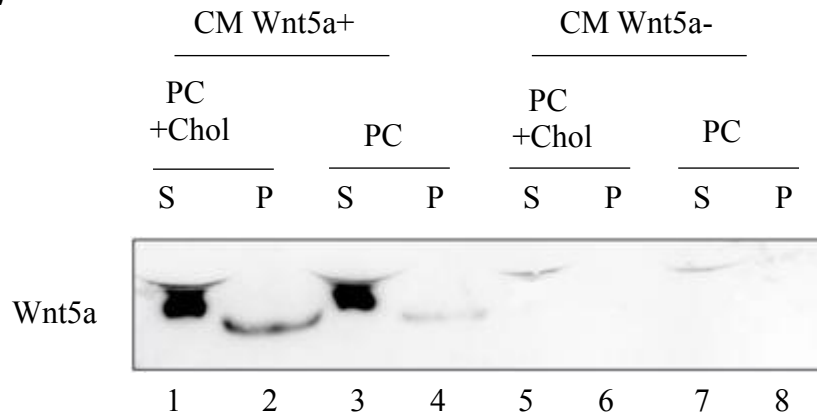
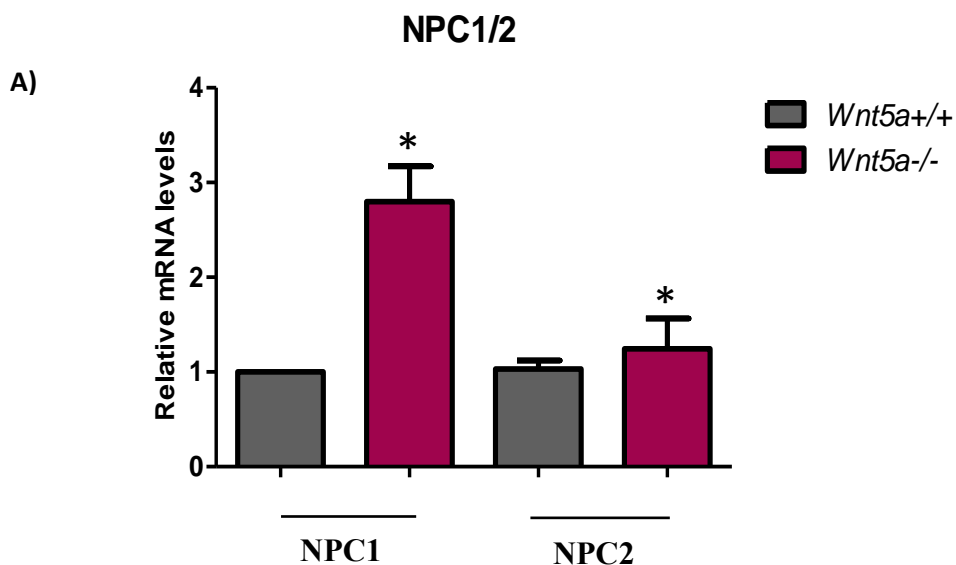


**Figure 35: Wnt5a binds to cholesterol.** A) Predictive 3D structure of Wnt5a and localization of the CARC motifs. The arrow is showing localization for the palmitoleic acid lipid group. The essential Arg within the CARC motifs are boxed in dark. B) Conditioned medium enriched in Wnt5a (CM Wnt5a+) or mock medium (CM Wnt5a-) were incubated with liposomes containing phosphatidylcholine (PC) or phosphatidylcholine + cholesterol

(PC + Chol). Liposomes were sedimented, washed and analyzed by immunoblotting for the presence of Wnt5a. Supernatant (S) and pellets (P) were loaded.

## 6.2 *Wnt5a interacts with NPCs*

In LELs two proteins, NPC1 and NPC2 are crucial for moving cholesterol across the membrane (Infante *et al.*, 2008). We therefore tested whether Wnt5a interacts with NPC1 and NPC2, and measured their mRNA levels in the absence of Wnt5a. We found that mRNA levels of NPC1 and NPC2 increased by 2-3X in *Wnt5a*<sup>-/-</sup> VSMCs compared to control cells (Fig.36A). Moreover, when co-expressed in HEK293T cells, co-immunoprecipitation experiments show that Wnt5a physically interacts with NPC1 and NPC2 (Fig.36B). The immunoprecipitate does not contain the late endosome marker, Lamp1 indicating a direct interaction between Wnt5a and NPC proteins and not a mere coimmunoprecipitation of proteins present in the same membrane complex. We in collaboration with Christine Schaeffer-Reiss, LSMBO, Strasbourg we validated complex membership by mass spectrometry analysis of the interactome and confirmed the specific interaction between Wnt5a and NPC proteins.



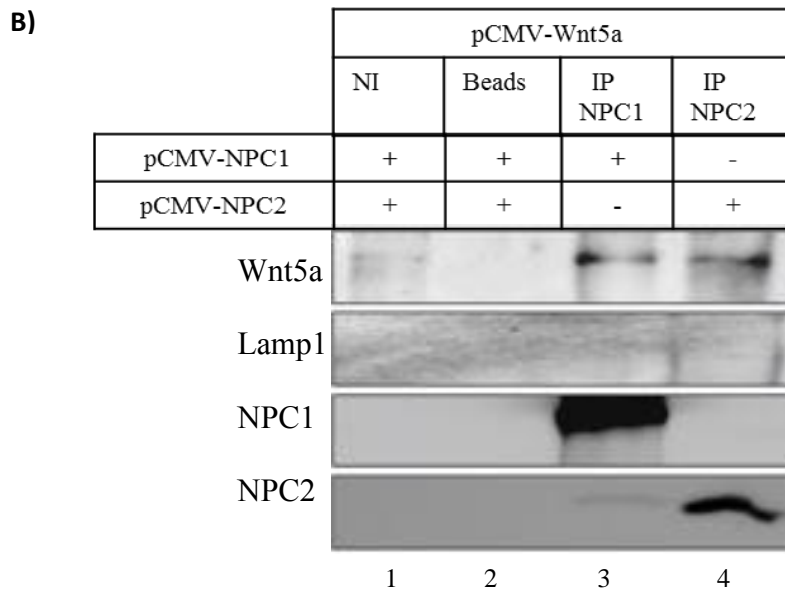


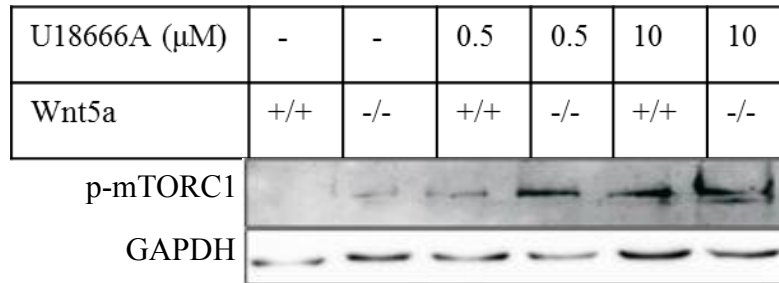
**Figure 36: Wnt5a interacts with NPC proteins.** **A)** Relative transcript levels of NPC1 and NPC2 in presence or absence of Wnt5a in human Wnt5a KO (Wnt5a<sup>-/-</sup>) and controls (Wnt5a<sup>+/+</sup>) VSMCs. **B)** HEK293 cells were co-transfected with either pCMV-Wnt5a and pCMV-NPC1 or pCMV-Wnt5a and pCMV-NPC2 expression plasmids. Immunoprecipitations of NPC1 (lane 3) or with NPC2 (lane 4), followed with immunoblotting with Wnt5a show that Wnt5a interacts with both NPC proteins. Absence of Lamp1 in complexes indicates that these interactions are specific. NI=non-immune antibodies, Beads=empty beads.

### ***6.3 Wnt5a counteracts activation of mTORC1 mediated by U18666A***

The U18666A compound is a cholesterol transport-inhibiting agent, used to mimic NPC1 deficiency, which causes the accumulation of cholesterol in cells (Lu *et al.*, 2015). Treatments of human Wnt5a<sup>-/-</sup> VSMCs with increasing

amounts of U18666A boosted the effects of Wnt5a deficiency on activated mTORC1 (Fig.37A). Interestingly, we found that in human Wnt5a<sup>-/-</sup> VSMCs, Wnt5a-enriched conditioned medium decreased mTORC1 activity induced by U18666A treatments, whereas mock medium had no effect (Fig.37B). Thus, loss of Wnt5a or NPC1 inhibition has a similar effect on mTORC1 activation and cholesterol trafficking, and Wnt5a counteracts the activation of mTORC1 mediated by U18666A-induced NPC1 inhibition.

**A)**



**B)**

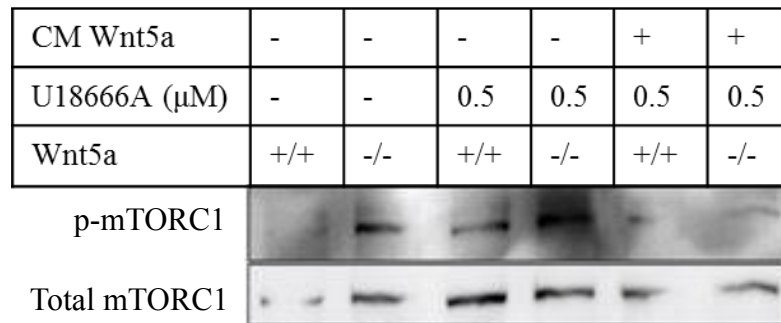
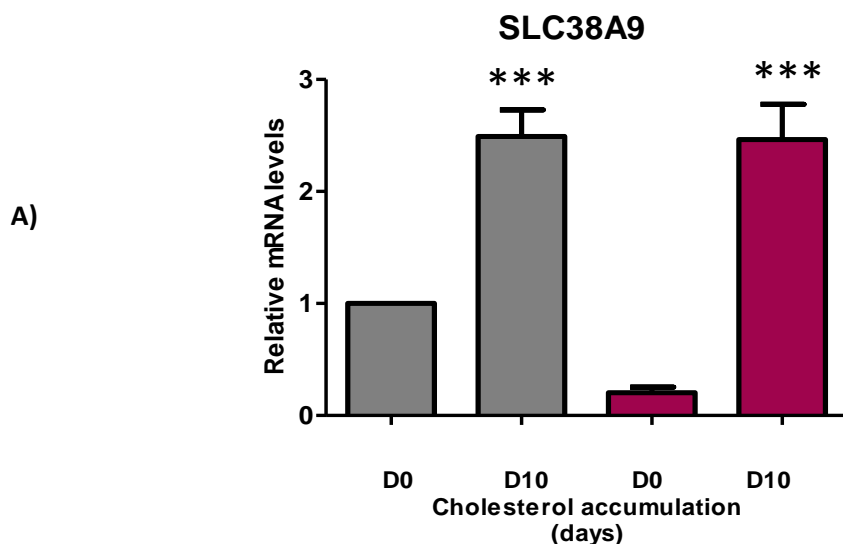


**Figure 37: Wnt5a counteracts U18666A mediated mTORC1 upregulation. A)** Effects of increasing amounts of the U18666A compound on the phosphorylation of mTORC1 in human VSMCs Wnt5a KO (-/-) and control (+/+). **B)** Effects of the U18666A compound on the phosphorylation of mTORC1 in presence of control medium (CM Wnt5a-) or Wnt5a enriched condition medium (CM Wnt5a+) in human Wnt5a KO (-/-) and control VSMCs (+/+).

#### 6.4 Increased expression of SLC38A9 in absence of Wnt5a

SLC38A9 is a lysosomal membrane protein that regulates the transport of amino acids and cholesterol at lysosomal membrane (Castellano *et al.*, 2017) (Wang *et al.*, 2015). Lysosomal cholesterol controls mTORC1 activation via SLC38A9-NPC1 complex (Brian *et al.*, 2017). As Wnt5a and SLC38A9 both bind to NPC1 and since mTORC1 senses cholesterol via SLC38A9, we measured expression levels of SLC38A9 in VSMCs. In untreated cells, mRNA levels of SLC38A9 were robustly increased in Wnt5a<sup>-/-</sup> VSMCs compared to control cells (Fig. 38A). These effects are even more pronounced upon cholesterol accumulation. As it has been previously shown that NPC1 physically interacts with SLC38A9 (Castellano *et al.*, 2017). We tested whether Wnt5a may also physically interacts with SLC38A9.

HEK 293 cells transfected with pCMV-Wnt5a and Mock were immunoprecipitated with SLC38A9 antibody, followed with immunoblotting with Wnt5a. In our hands, we were unable to find a physical interaction between SLC38A9 and Wnt5a. We found a band corresponding in size to Wnt5a. however, immunoblotting with SLC38A9 did not revealed its presence strongly suggesting that Wnt5a band were not specific.



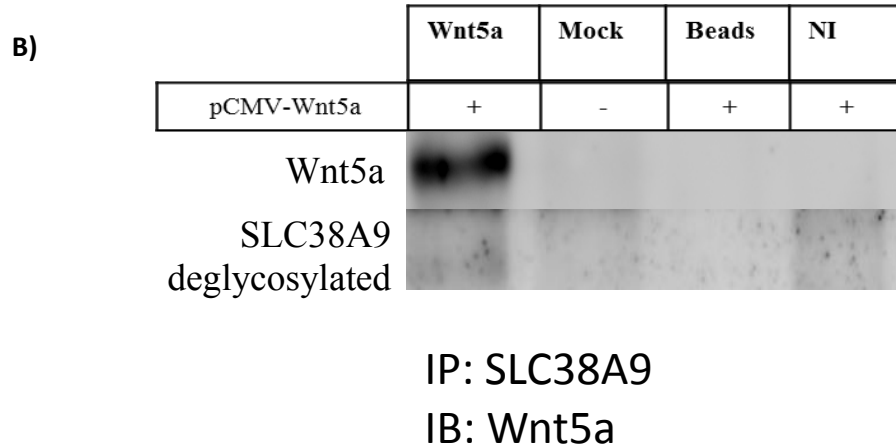


**Figure 38: Significant increase in SLC38A9 expression in absence of Wnt5a. A)** Relative transcript levels of SLC38A9 in human Wnt5a KO (-/-) and control VSMCs (+/+). **B)** HEK293 cells were transfected with either pCMV-Wnt5a and Mock expression plasmids. Immunoprecipitations of SLC38A9, followed with immunoblotting with Wnt5a show that Wnt5a interacts with SLC38A9. Immunoblot for SLC38A9 donot shows the band for SLC38A9. NI=non-immune antibodies, Beads=empty beads.

# Results // Part-II

## **Loss of adaptor protein ShcA in endothelial cells protects against atherosclerotic lesion formation.**

I participated in another research project in our lab that studied the role of the adaptor protein ShcA in atherosclerosis. ShcA binds to the cytoplasmic tail of tyrosine kinase receptor and low density lipoprotein related receptor (LRP1) (Lai & Pawson, 2000). ShcA protein exists in 03 isoforms 46, 52 & 66 kDa (Napoli *et al.*, 2003). It is involved in embryogenesis and functions in adult cardiac development. It has been described previously that ShcA is responsible for the monocyte derived macrophage infiltration at the lesion site and LDL oxidation (E. Woldt *et al.*, 2011). Its p66 isoform also protects against foam cell formation and atherosclerosis development (Napoli *et al.* 2003). However, the cellular mechanisms for the role of ShcA in vascular wall were not clearly defined. To study the mechanisms involved we knocked down ShcA in endothelia cells in mice using Cre/lox system. Our results show that ShcA induces the expression of ICAM-1 and adhesion of macrophage cells, decreases eNOS expression and promotes atherosclerosis lesion development.

In presence of ShcA, expression of NF- $\kappa$ B which is an activator of adhesion molecules is decreased. However, ShcA induces an increase in ICAM-1 expression by an indirect activation of Zeb1. Zeb1 is a transcriptional repressor for adhesion molecules. In presence of ShcA, Zeb1 binds to Hippo-pathway effector YAP resulting in the increased nuclear translocation of YAP. This switches Zeb1 from a repressor to an activator of transcription, thus increasing ICAM-1 expression which leads to increased monocyte-macrophage adhesion at the lesion site.

Endothelial nitric oxide synthase (eNOS) is a target of Akt. Akt can causes phosphorylation and activation of eNOS, therefore, inhibiting LDL oxidation (Dimmeler *et al.*, 1999). ShcA down regulates eNOS by decreasing the phosphorylation of AKT. It compromise vascular homeostasis, promote LDL oxidation and atherosclerosis development.

In conclusion, ShcA induces Zeb1 mediated increase in ICAM1 expression and decreasing nitric oxide production respectively, thereby leading to atherosclerosis development.

# SCIENTIFIC REPORTS



Correction: Author Correction

OPEN

## Loss of the adaptor protein ShcA in endothelial cells protects against monocyte macrophage adhesion, LDL-oxidation, and atherosclerotic lesion formation

Antoine Abou-Jaoude<sup>1</sup>, Lise Badiqué<sup>1</sup>, Mohamed Mlih<sup>1</sup>, Sara Awan<sup>1</sup>, Sunning Guo<sup>1</sup>, Alexandre Lemle<sup>1</sup>, Clauda Abboud<sup>1</sup>, Sophie Foppolo<sup>1</sup>, Lionel Host<sup>1</sup>, Jérôme Terrand<sup>1</sup>, Hélène Justiniano<sup>1</sup>, Joachim Herz<sup>2</sup>, Rachel L. Matz<sup>1</sup> & Philippe Boucher<sup>1</sup> 

ShcA is an adaptor protein that binds to the cytoplasmic tail of receptor tyrosine kinases and of the Low Density Lipoprotein-related receptor 1 (LRP1), a trans-membrane receptor that protects against atherosclerosis. Here, we examined the role of endothelial ShcA in atherosclerotic lesion formation. We found that atherosclerosis progression was markedly attenuated in mice deleted for ShcA in endothelial cells, that macrophage content was reduced at the sites of lesions, and that adhesion molecules such as the intercellular adhesion molecule-1 (ICAM-1) were severely reduced. Our data indicate that transcriptional regulation of ShcA by the zinc-finger E-box-binding homeobox 1 (ZEB1) and the Hippo pathway effector YAP, promotes ICAM-1 expression independently of p-NF- $\kappa$ B, the primary driver of adhesion molecules expressions. In addition, ShcA suppresses endothelial Akt and nitric oxide synthase (eNOS) expressions. Thus, through down regulation of eNOS and ZEB1-mediated ICAM-1 up regulation, endothelial ShcA promotes monocyte-macrophage adhesion and atherosclerotic lesion formation. Reducing ShcA expression in endothelial cells may represent an obvious therapeutic approach to prevent atherosclerosis.

Atherosclerosis involves multiple processes such as endothelial dysfunction, inflammation and cell proliferation. It coincides with subendothelial low-density lipoprotein (LDL) accumulation. The pro-oxidative environment favors oxidation of LDL and oxidized LDL (oxLDL) activate endothelial cells which overexpress adhesion molecules E-selectin, VCAM-1 and ICAM-1<sup>1</sup>. Thus, activation of these signaling pathways in endothelial cells is a key mechanism in the development of atherosclerotic lesions, and controlling endothelial dysfunction could reduce the progression of the disease.

ShcA is a cytosolic adaptor protein<sup>2</sup> that binds to the cytoplasmic tail of receptor tyrosine kinases (RTKs). Germ line deletion of the ShcA gene in mice leads to lethality at embryonic day 12, demonstrating an essential, but still undefined, role during development<sup>3</sup>. In adults and in embryos, ShcA regulates several important physiological processes. For instance, it signals in pathways such as IGF-I or PDGF $\beta$ , which are involved in proliferation/differentiation decisions<sup>2,4-6</sup>. These signals converge to Ras/MAP kinase and Akt/mTOR pathways. ShcA also binds to the tyrosine-phosphorylated form of the second NPxY motif within the tail of Low-density lipoprotein (LDL) receptor-Related Protein-1 (LRP1), an ubiquitously expressed transmembrane receptor that belongs to the LDL receptor gene family<sup>7</sup>. LRP1 is involved in lipoproteins endocytosis and in the control of intracellular signaling pathways. Mice lacking LRP1 in vascular smooth muscle cells (vSMCs) are characterized by a susceptibility to develop atherosclerosis. The lesions are associated with increased PDGF $\beta$  and TGF $\beta$  signaling that activate

<sup>1</sup>CNRS, UMR 7213, University of Strasbourg, 67401, Illkirch, France. <sup>2</sup>Department of Molecular Genetics, University of Texas Southwestern Medical Center, Dallas, TX, USA. Antoine Abou-Jaoude and Lise Badiqué contributed equally to this work. Philippe Boucher and Rachel L. Matz jointly supervised to this work. Correspondence and requests for materials should be addressed to R.L.M. (email: [rachel.matz-westphal@unistra.fr](mailto:rachel.matz-westphal@unistra.fr)) or P.B. (email: [philippe.boucher@unistra.fr](mailto:philippe.boucher@unistra.fr))

vSMCs proliferation<sup>8</sup>, and decreased Wnt5a signaling that stimulates foam cell formation<sup>9,10</sup>. The PDGF receptor and LRP1 co-immunoprecipitate and LRP1 is a substrate for PDGF-dependent tyrosine kinases<sup>8,11,12</sup>. Thus, by binding to LRP1, ShcA might play an important role in atherosclerotic lesions development.

ShcA is expressed in the cardiovascular system early during embryogenesis and in adults, and controls heart development<sup>3</sup>. In the heart, by binding to integrins or dystrophin, it links the extracellular matrix (ECM) to the cytoskeleton and the contractile apparatus<sup>2,13</sup>. In the vascular wall, the role of ShcA is not well defined. The mammalian ShcA protein has 3 isoforms of 46, 52 and 66 kDa and previous studies showed that mice lacking the p66 isoform had reduced tissue oxidative stress, foam cell and early atherosclerotic lesion formation when fed a high fat diet<sup>14</sup>. However, the molecular and cellular mechanisms of this phenotype remain largely unknown. In particular, it does not indicate in which vascular cell type ShcA deletion would be atheroprotective. We previously reported that the deletion of ShcA in vSMCs did not modify the development of atherosclerotic lesions in mice fed an atherogenic diet<sup>13</sup>. Here, to study the role of ShcA in atherosclerosis and vascular remodeling, we suppressed its expression specifically in endothelial cells using the Cre/lox system.

## Results

**Specific deletion of ShcA in endothelial cells protects from atherosclerosis.** We generated Tie2Cre+/ShcA<sup>flox/flox</sup> mice, in which ShcA is selectively ablated in endothelial cells, by inter-crossing Tie2Cre transgenic mice with floxed ShcA animals<sup>13</sup> (ShcA<sup>flox/flox</sup>). To increase atherosclerosis susceptibility, Tie2Cre+/ShcA<sup>flox/flox</sup> animals were maintained on a LDL receptor-deficient background (LDLR<sup>-</sup>), fed an atherogenic diet, and are hereafter referred to as endoShcA<sup>-</sup>. Western blot analysis of ShcA in endothelial cells isolated from aortas of endoShcA<sup>-</sup> and endoShcA<sup>+</sup> (control) mice confirmed the deletion of ShcA (Fig. 1A). Absence of ShcA expression in endothelial cells had no significant effect on plasma cholesterol ( $48.3 \pm 10.1$  mmol/l in endoShcA<sup>-</sup> mice vs  $41.2 \pm 3.3$  mmol/l in controls) or triglyceride levels ( $2.5 \pm 0.1$  mmol/l in endoShcA<sup>-</sup> mice vs  $2.9 \pm 0.9$  mmol/l in controls), in mice fed an atherogenic diet for 24 weeks. However, when fed an atherogenic diet atherosclerotic lesions were two times smaller in endoShcA<sup>-</sup> mice than in age-matched control mice (endoShcA<sup>+</sup>) as demonstrated by Sudan IV staining and *en face* analysis of the whole aortas (Fig. 1B,C), and histological analysis (Fig. 1D, top panels). The reduced atherosclerotic lesion size was similar in male and female mice (data not shown). During atherosclerosis, infiltration of foamy macrophages and vascular smooth muscle cells plays a crucial role. Whereas histological analysis of the arterial wall in large vessels such as thoracic aortas revealed an accumulation of CD-68-positive macrophage foam cells within the core of the atherosclerotic plaques in control mice (Fig. 1D, bottom panels), almost no CD68-positive macrophage-foam cells accumulated in endoShcA<sup>-</sup> aortas (Fig. 1D, bottom panels). This decreased number of macrophage foam cells in the atherosclerotic plaques indicates that ShcA expression in endothelial cells promotes CD-68-positive macrophage cell infiltration and/or foam cell formation.

**Deletion of ShcA in endothelial cells protects from intracellular lipid accumulation and foam cell formation.** To study the role of endothelial ShcA on intracellular lipid accumulation and foam cell formation, human endothelial cells (EA.hy 926 cell line) down regulated for p66, p52 and p46 ShcA isoforms and control cells were co-cultured in presence of THP-1 monocyte-derived macrophages stimulated with oxidized low-density lipoprotein to induce foam cell formation. Deletion of three isoforms of ShcA in endothelial cells significantly decreases the ox LDL uptake of macrophages and foam cell formation as evidenced by Oil-Red-O staining (Fig. 2A). Quantification analysis upon Oil-Red-O staining showed half neutral lipid accumulation in the absence of endothelial ShcA (Fig. 2B). These data indicate that endothelial ShcA promotes lipid accumulation in macrophages and foam cell formation.

**Decrease of ICAM-1 expression in the absence of ShcA.** Recruitment of monocytes and their endothelial cell adhesion occurs through intercellular adhesion molecule 1 (ICAM-1), vascular cell adhesion molecule 1 (VCAM-1), and E-selectin, secreted by inflamed or damaged endothelium. Among these, the key molecule ICAM-1, a member of the adhesion immunoglobulin super family<sup>15</sup>, displays an important role in the development of atherosclerosis. For instance, deficiency in ICAM-1 was shown to disable monocyte-endothelial cell adhesion leading to reduce atherosclerotic lesion size in apoE<sup>-/-</sup> mice<sup>16</sup>. To test whether decreased accumulation of CD-68-positive foam cells was due to decreased expression of ICAM-1 in endothelial cells, we measured its mRNA and protein levels in EA.hy 926 endothelial cells down regulated for p66, p52 and p46 ShcA isoforms and in control cells. We found a marked decrease of ICAM-1 protein (Fig. 2C,D) and mRNA levels (Fig. 2E) in the absence of ShcA. VCAM-1 mRNA, and E-selectin mRNA and protein levels were also decreased (Fig. 2C-E).

**Deletion of the p66 isoform of ShcA in endothelial cells is not sufficient to protect from intracellular lipid accumulation and foam cell formation.** Since genetic deletion of the p66 isoform of ShcA reduces oxLDLuptake and early atherosclerotic plaque formation in apolipoprotein E<sup>-/-</sup> fed a high fat diet<sup>14,17</sup>, we next wanted to test whether deletion of the p66 isoform in endothelial cells is sufficient to protect from intracellular lipid accumulation and foam cell formation. When EA.hy 926 endothelial cells down regulated for the p66 isoform of ShcA were co-cultured in presence of THP-1 monocyte-derived macrophages stimulated with oxidized low-density lipoprotein to induce foam cell formation, we found a modest decrease in foam cell formation as evidenced by Oil-Red-O staining (Fig. 3A). Quantification analysis showed a 20% decrease in neutral lipid accumulation in the absence of p66 ShcA (Fig. 3B). These results suggest that three isoforms of ShcA are required for efficient intracellular lipid accumulation and foam cell formation. We also tested whether deletion of the p66 ShcA isoform decreased expression of adhesion molecules. We found a marked decrease of ICAM-1 protein (Fig. 3C,D) and mRNA levels (Fig. 3E) in EA.hy 926 endothelial cells down regulated for the p66 isoform of ShcA compared to control cells. However, VCAM-1 protein levels were only moderately decreased, whereas VCAM-1

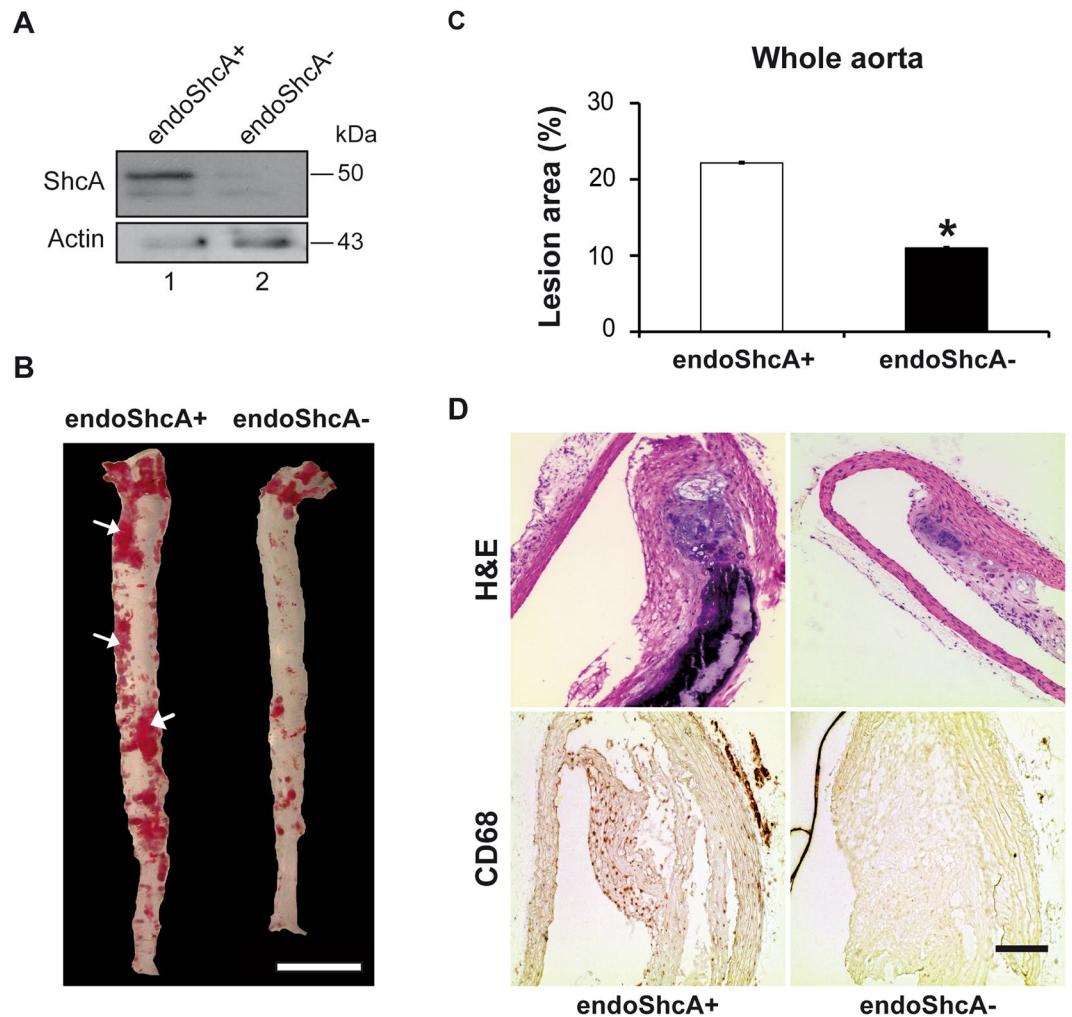


**Figure 1.** Absence of ShcA in endothelial cells protects from atherosclerotic lesion formation. Atherosclerosis in mice lacking ShcA in vascular endothelial cells and fed a cholesterol-rich diet. Western blotting of ShcA in endothelial cells isolated and pooled from aortas of endoShcA<sup>-</sup> and endoShcA<sup>+</sup> mice ( $n = 5$  mice for each genotype) (A). Opened and Sudan IV-stained aortas from endoShcA<sup>-</sup> mice and controls (endoShcA<sup>+</sup>). Arrows show lipid-laden (Sudan-positive) atherosclerotic lesions; Scale bar, 0.5 cm (B). Quantification of atherosclerotic lesion size in whole aortas from endoShcA<sup>-</sup> ( $n = 5$ ) and control ( $n = 5$ ) mice (C). Hematoxylin and eosin (H&E) and CD68 staining of the lesions in thoracic aortas from endoShcA<sup>-</sup> and endoShcA<sup>+</sup> mice. Scale bar, 20  $\mu$ m (D). Data are represented as mean  $\pm$  SEM. \* $P < 0.05$ , two-tailed unpaired Student's *t*-test.

mRNA as well as E-selectin mRNA and protein levels remained unchanged (Fig. 3D,E). Thus, in endothelial cells p46, p52 and p66 ShcA play an important role in expression of adhesion molecules and in the interaction between endothelial cells and monocytes, leading to monocyte recruitment and subsequent development of atherosclerosis.

**Increase in p-NF- $\kappa$ B expression in ShcA<sup>-/-</sup> endothelial cells.** We next wanted to determine how ShcA regulates ICAM-1 expression in endothelial cells. The nuclear form of the NF-kappa B transcription factor (NF- $\kappa$ B) binds to DNA as a heterodimer of a 50 kDa (p50) and 65 kDa (p65) polypeptide<sup>18</sup>. Once phosphorylated, the transcription factor NF- $\kappa$ B is the major driver of *VCAM-1*, *ICAM-1* and *E-selectin* expression<sup>18</sup>. Surprisingly, treatment of endothelial cells with siRNA against ShcA triggered the phosphorylation of the p65 subunit of NF- $\kappa$ B (Fig. 4A,B) and increases the expression of its endogenous activator IKK $\beta$  (Fig. 4A,C)<sup>19</sup>. To determine whether NF- $\kappa$ B is activated in the absence of ShcA, we measured its nuclear translocation and activation of its target gene MCP1<sup>20,21</sup>. We found that in EA.hy 926 endothelial cells down regulated for ShcA (siShcA), p-NF- $\kappa$ B accumulated in the nucleus (Fig. 4D) and activated MCP1 (Fig. 4E) when compared to control cells (siCtrl). This suggests that, in the absence of ShcA regulation of adhesion molecules expression levels is independent of NF- $\kappa$ B.

**Decrease in ShcA expression activates nuclear translocation of the transcription factor ZEB1 and decreases the nuclear translocation of YAP.** It was previously reported that the transcription factor zinc-finger E-box-binding homeobox 1 (ZEB1) bound the ZEB1-binding sites of ShcA promoter in epithelial cells<sup>22</sup>. In addition, ZEB1 has at least one putative binding site on the p46/p52 isoforms promoter at the position

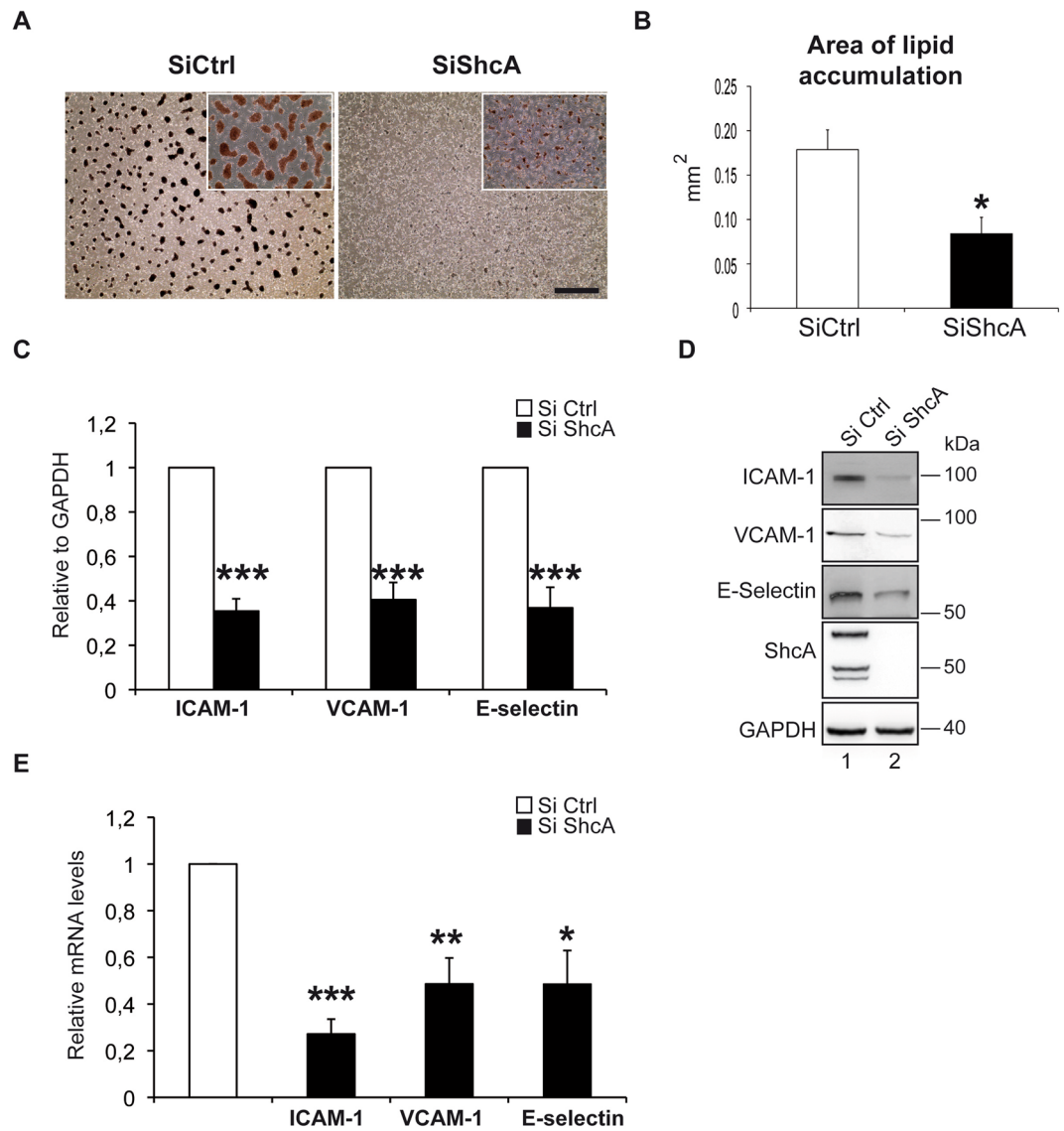


**Figure 2.** Expression of the three isoforms of ShcA in endothelial cells is required for foam cells formation, macrophage adhesion, and ICAM-1 expression. Accumulation of lipids in THP1-derived macrophages treated with oxidized LDL in the absence or presence of the three isoforms of ShcA in EA.hy 926 endothelial cells. Cells were stained with Oil/RedO. Representative microscopic fields. The subpanels on the right are higher magnification (2.5 $\times$ ) images. SiCtrl and SiShcA panels are same magnifications, and scale bare is 5  $\mu$ m (A). Quantification of lipid accumulation upon Oil/RedO staining in THP1-derived macrophages treated with oxidized LDL in the absence (n = 5) or presence (n = 5) of ShcA in EA.hy 926 endothelial cells. Oil/RedO positive regions were manually outlined and the quantification of outlined regions was determined with Image J as described in the methods section (B). Quantification by western blot of indicated genes in EA.hy 926 endothelial cells down regulated for ShcA (siShcA) (n = 3) and in control cells (siCtrl) (n = 3) (C). Western blot analysis of ICAM-1, VCAM-1, E-Selectin, ShcA, and GAPDH expressions in EA.hy 926 endothelial cells down regulated for ShcA (siShcA) and in control cells (siCtrl) (D). mRNA of the indicated genes measured by Real Time PCR in EA.hy 926 endothelial cells down regulated for ShcA (siShcA) (n = 3) and in control cells (n = 3) transfected with siControl (siCtrl) (E). All data are represented as mean  $\pm$  SEM. \* $P$  < 0.05, \*\* $P$  < 0.01, \*\*\* $P$  < 0.001, two-tailed unpaired Student's t-test.

– 830 (Eukaryote promoter and GP miner databases). Thus, we next thought to assess the nuclear translocation of ZEB1 in EA.hy 926 endothelial cells treated with siShcA and in control cells. Using immuno-fluorescence (Fig. 5A) and cell fractionation experiments (Fig. 5B), we found, a marked increase in cytosolic expression and nuclear translocation of ZEB1 in siShcA-treated endothelial cells *versus* control cells indicating that ShcA is required for down regulation of ZEB1 expression. To evaluate the impact of reducing ZEB1 levels on ShcA and ICAM-1 expressions, we measured ShcA and ICAM-1 mRNA levels upon siZEB1 treatment. Interestingly, down regulation of ZEB1 decreased both ShcA and ICAM-1 mRNA and protein levels (Fig. 5C–D). Knockdown of ZEB1 similarly decreased p66 ShcA mRNA levels (data not shown). These data indicate that ShcA and ZEB1

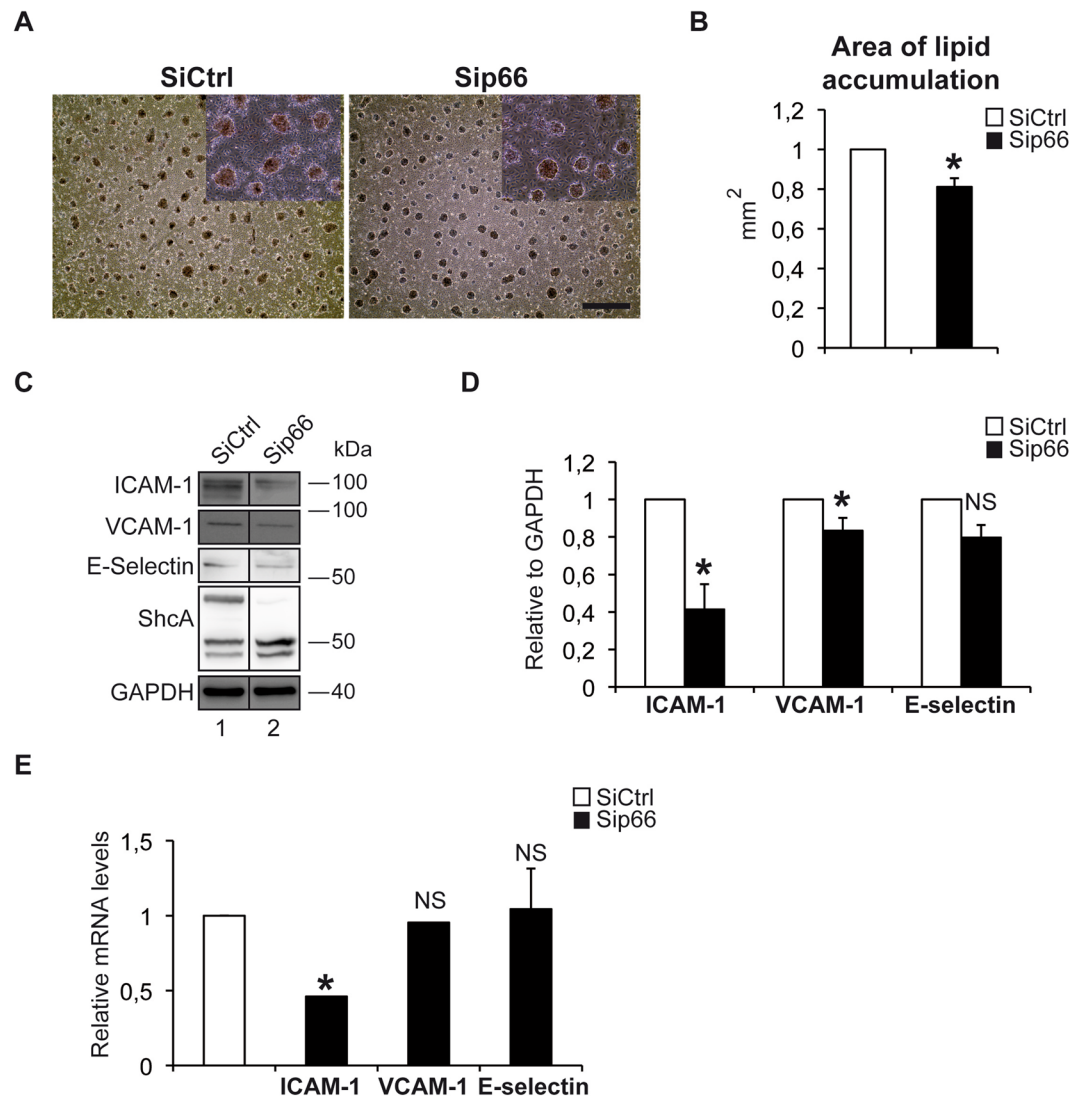


**Figure 3.** Deletion of p66ShcA down regulates ICAM-1 expression in endothelial cells, but does not decrease ox LDL uptake of THP-1 monocyte-derived macrophages and foam cell formation. Accumulation of lipids in THP1-derived macrophages treated with oxidized LDL in the absence or presence of p66ShcA in EA.hy 926 endothelial cells. Cells were stained with Oil/RedO. Representative microscopic fields. The subpanels on the right are higher magnification (2.5 $\times$ ) images. SiCtrl and p66SiShcA panels are same magnifications, and scale bar is 5  $\mu$ m (A). Quantification of lipid accumulation upon Oil/RedO staining in THP1-derived macrophages treated with oxidized LDL in the absence (n = 5) or presence (n = 5) of p66ShcA in EA.hy 926 endothelial cells. Oil/RedO positive regions were manually outlined and the quantification of outlined regions was determined with Image J as described in the methods section (B). Western blot analysis (C) and quantification of western blot analysis of ICAM-1 in EA.hy 926 endothelial cells down regulated for p66ShcA and in controls (D). RT-PCR of the indicated genes in EA.hy 926 endothelial cells down regulated for p66ShcA and in controls (E). Error bars, s.e.m. \* $P < 0.05$ , NS = non significant.

are required for ICAM-1 transcriptional regulation, whereas ShcA down regulates ZEB1 expression through a negative feedback mechanism. Mechanistically, ZEB1 function as a transcriptional repressor<sup>23</sup>. However, depending upon the recruitment of a different set of co-factors, direct transcriptional activation by ZEB1 has also been reported for a few target genes<sup>24,25</sup>. For instance, ZEB1 directly binds to YAP to stimulate transcription<sup>24</sup>. Since ShcA is required for nuclear translocation of YAP<sup>26</sup>, ShcA might recruit YAP in the nucleus to switch ZEB1 from a repressor to a transcriptional activator, thereby up-regulating ICAM-1 expression. To test this, we performed cell fractionation assays in EA.hy 926 endothelial cells and found a decrease in nuclear expression of YAP in ShcA knockdown cells compared to controls (Fig. 5B). This strongly suggests that a ZEB1/YAP complex, most likely through binding to ShcA promoters, promotes ShcA-mediated up regulation of ICAM-1 expression.

**Increased p-Akt that activates eNOS, decreases LDL oxidation and recruitment of monocytes.** In endothelial cells, Akt can phosphorylate and activate endothelial nitric oxide synthase (eNOS) which

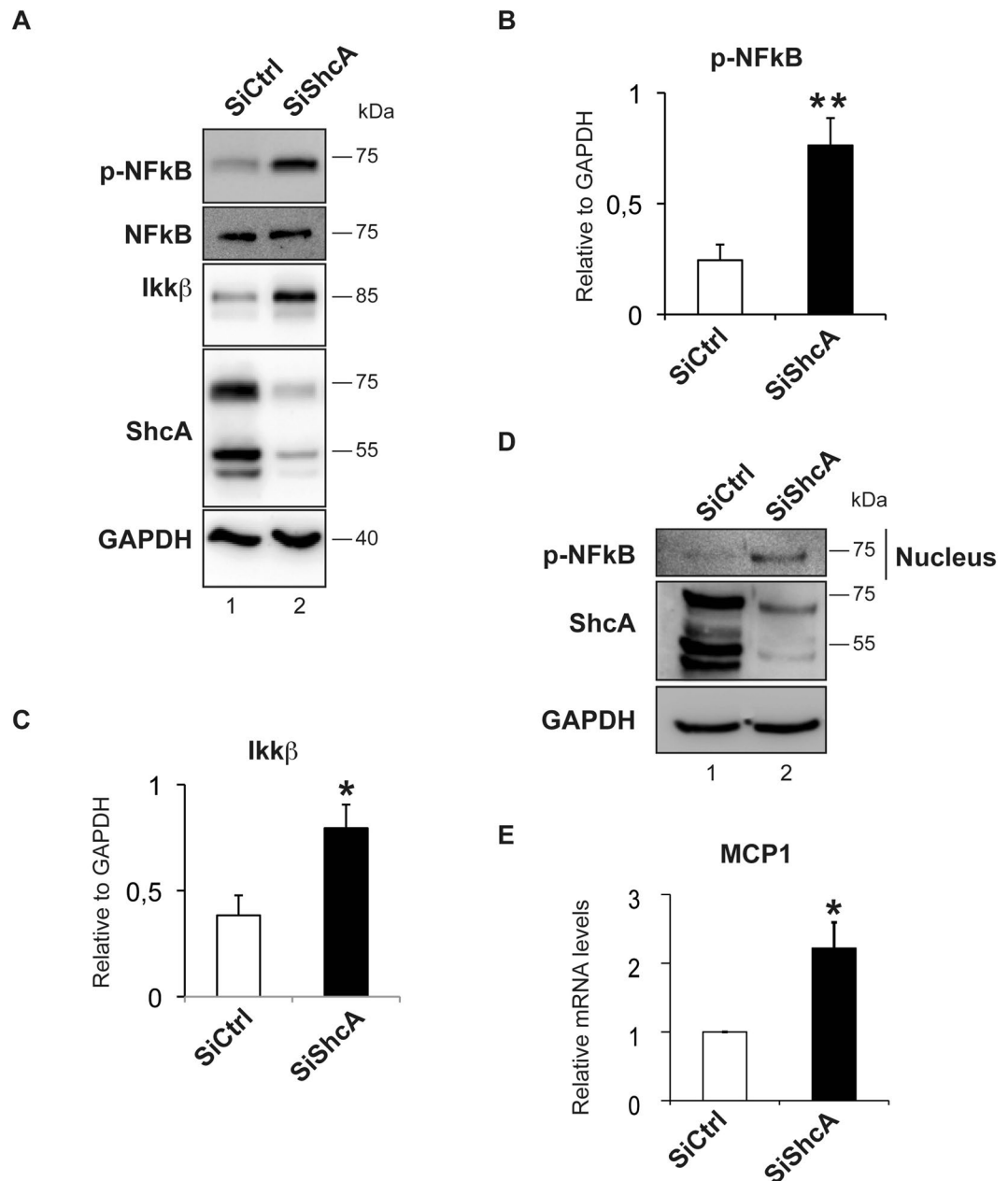


**Figure 4.** ShcA in endothelial cells triggers ICAM-1 expressions independently of NF- $\kappa$ B. Western blot analysis of the p65 subunit of NF- $\kappa$ B phosphorylated at the Ser536 residue (p-NF- $\kappa$ B), total NF- $\kappa$ B p65 (NF- $\kappa$ B), IKK $\beta$ , ShcA and GAPDH in whole cell lysate from EA.hy 926 endothelial cells down regulated for the three isoforms of ShcA (siShcA) and in controls cells (siCtrl) (A). Quantification by western blot of the p65 subunit of p-NF- $\kappa$ B protein levels ( $n = 6$ ) (B) and of IKK $\beta$  protein levels ( $n = 7$ ) in whole cell lysate (C). Western blot measurement of p-NF $\kappa$ B nuclear accumulation in EA.hy 926 endothelial cells down regulated for ShcA (siShcA) compared to controls cells (siCtrl) (representative from  $n = 3$  separated experiments) (D). The increase in nuclear translocation of p-NF $\kappa$ B in EA.hy 926 endothelial cells down regulated for ShcA is accompanied by an increase in its target gene mRNA levels, MCP1 ( $n = 5$  for each genotype) (E). All data are represented as mean  $\pm$  SEM. \* $P < 0.05$ , \*\* $P < 0.01$ , two-tailed unpaired Student's t-test.

inhibits LDL oxidation<sup>27</sup>. As loss of eNOS activity is an established contributor to endothelial dysfunction<sup>28</sup> and endothelium-derived NO plays a vital role in the prevention of atherosclerosis<sup>29</sup>, we explored whether absence of ShcA increased eNOS activation. In EA.hy 926 endothelial cells down regulated for ShcA we found an increase in p-Akt protein levels (Fig. 6A,B) and its target gene p-mTOR (Fig. 6A)<sup>30</sup>, accompanied by a marked increased in eNOS phosphorylation (Fig. 6A,B). Densitometric analysis confirmed these data (Fig. 5B). Interestingly, immunohistochemistry analysis show that mice lacking ShcA in vascular endothelial cells (endoShcA<sup>-</sup>) and fed a cholesterol-rich diet expressed a larger amount of p-eNOS than control mice (Fig. 6C). Furthermore, they also expressed less ICAM-1 in vascular endothelial cells than controls (Fig. 6C). Thus, through inhibition of eNOS,

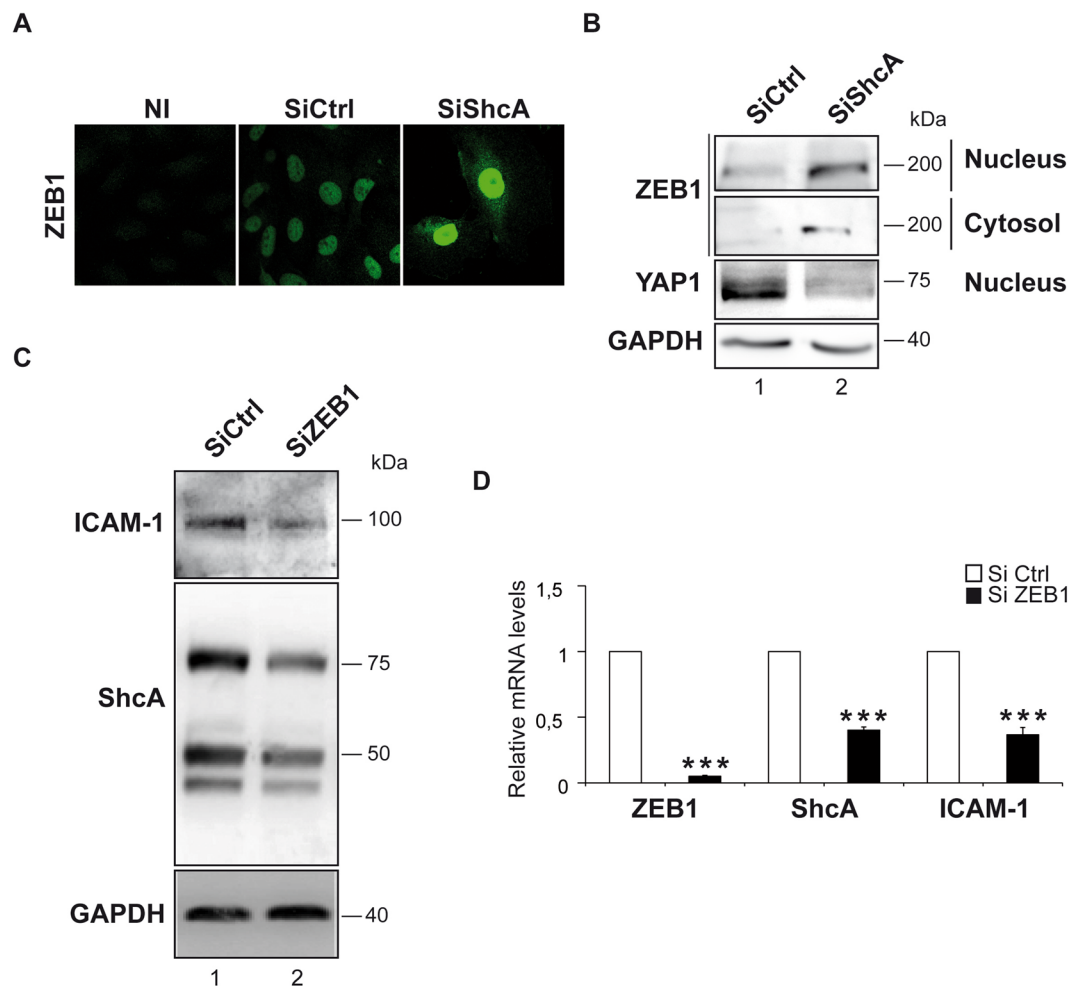


**Figure 5.** The absence of ShcA increased ZEB1 nuclear translocation and decreased YAP nuclear translocation. To follow accumulation of ZEB1 in the nucleus, EA.hy 926 endothelial cells down regulated for the three isoforms of ShcA (siShcA) and control cells (siCtrl) were labeled with anti-ZEB1 and analyzed by confocal images (A). Western blot analysis of the indicated genes in cytosol and nuclear fractions from EA.hy 926 endothelial cells down regulated for the three isoforms of ShcA (siShcA) and control cells (siCtrl) ( $n = 4$ ) (B). Western blot analysis of ShcA and ICAM1 in whole cell lysates from EA.hy 926 endothelial cells down regulated for ZEB1 (siZEB1) ( $n = 3$ ) and control cells ( $n = 3$ ) (siCtrl) (C). ZEB1, ShcA and ICAM1 mRNA levels analyzed by Real Time PCR in EA.hy 926 endothelial cells down regulated for ZEB1 (siZEB1) ( $n = 3$ ) and control cells ( $n = 3$ ) (siCtrl) (D). NI, non-immun antibody. Data are represented as mean  $\pm$  SEM. \*\*\* $P < 0.001$ , two-tailed unpaired Student's t-test.

increased expression of ICAM-1, and increased LDL oxidation, and by promoting maladaptive monocyte-derived macrophage adhesion, endothelial ShcA contributes to atherosclerotic lesion formation.

## Discussion

Our data indicate that three isoforms of endothelial ShcA protein play a pivotal role in the pathophysiology of atherosclerosis by triggering monocyte-derived macrophages infiltration and LDL oxidation. Previous genetic ablation studies suggested an important role for ShcA in the regulation of fat accumulation<sup>31</sup>. Other studies reported that constitutive mutation of p66Shc gene, one of the three isoforms encoded by the mammalian ShcA locus, decreased atherosclerotic lesion size in mice fed a high-fat diet<sup>14,32</sup>. Interestingly, lesions from p66 (Shc<sup>-/-</sup>) mice had less macrophage-derived foam cells than wild type mice, and decreased proatherogenic factors, including oxLDL, but, the mechanism was unknown. *In vitro*, p66 Shc is involved in oxLDL uptake<sup>17</sup>. Here, we report that all three isoforms of ShcA are required to decrease eNOS expression levels, to increase ICAM-1 expression, and promote cell adhesion molecules and atherosclerosis.

Our study also reveals a complex interaction between ShcA and ZEB1 that promotes adhesion molecules expression in EA.hy 926 endothelial cells. In absence of ShcA, ICAM-1 and other adhesion proteins are down regulated. Interestingly, we found that NF- $\kappa$ B, the primary driver of adhesion protein expression is upregulated in the absence of ShcA. This would suggest that ShcA upregulated adhesion protein expression through a mechanism independent of NF- $\kappa$ B. Since ZEB1 binds to the E-box consensus sequence CACCT present in the p66

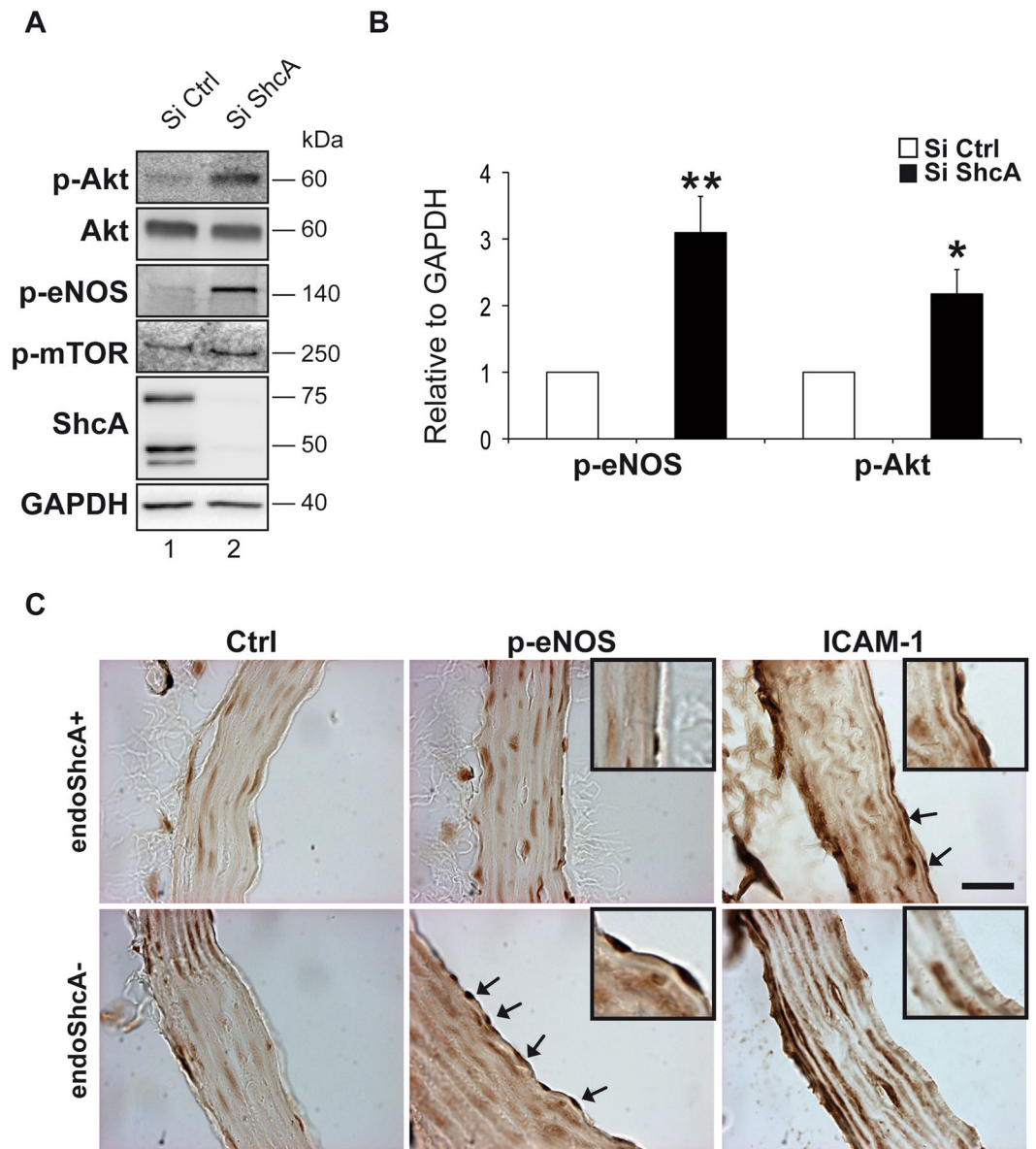


**Figure 6.** The decrease in ICAM-1 protein expression correlates with increased p-Akt and p-eNOS protein levels in endothelial cells deficient for ShcA. Western blot analysis of whole cell lysates from EA.hy 926 endothelial cells down regulated for the three isoforms of ShcA and in control cells using using phospho-eNOS (Ser1177) (p-eNOS), phospho-Akt (Ser473) (p-Akt), phospho-mTOR (Ser2448) (p-mTOR), Akt, ShcA, and GAPDH antibodies (A). Quantification of western blot analysis of p-eNOS and p-Akt in EA.hy 926 endothelial cells down regulated for ShcA and in controls ( $n = 8$  separated experiments) (B). Representative immunohistochemistry experiment for expression of p-eNOS and ICAM-1 in mice lacking ShcA in vascular endothelial cells (endoShcA<sup>-</sup>) ( $n = 2$ ) or control mice (endoShcA<sup>+</sup>) ( $n = 2$ ) fed a cholesterol-rich diet as described in the method section. Decreased ShcA expression in endothelial cells of mice (endoShcA<sup>-</sup>) greatly increased expression of p-eNOS protein (arrows), as well as decreased expression of ICAM-1 (arrows) in these cells, compared to controls (endoShcA<sup>+</sup>). Non-immune antibodies (Ctrl), the subpanels on the right are higher magnification ( $2.5\times$ ) images of vascular endothelial cells. Scale bar,  $20\ \mu\text{m}$  (C). Data are represented as mean  $\pm$  SEM. \* $P < 0.05$ , \*\* $P < 0.01$ , two-tailed unpaired Student's t-test.

promoter<sup>22</sup>, and that such sequences are also present on the p46/p52 isoforms promoter, we tested whether ZEB1 activated ShcA in EA.hy 926 endothelial cells. We found that upon siZEB1 treatments, ShcA and ICAM-1 are markedly down regulated indicating that ZEB1 induces ShcA expression. In addition, ShcA knockdown is accompanied by an increase in ZEB1 expression levels and its nuclear localization in endothelial cells. This would represent an adaptive response to ShcA loss and a negative feedback loop between ShcA and ZEB1 in endothelial cells. Such a negative feedback mechanism was already described in lung epithelial cancer cells where p66Shc deficiency enhanced the expression of ZEB1 and consequently decreased E-cadherin<sup>22</sup>.

ZEB1 is a transcriptional repressor of epithelial genes such as E-cadherin<sup>23</sup>. However, ZEB1 can also behave as an activator depending on its interaction with co-factors<sup>24</sup>. Indeed, by binding to the Hippo-pathway effector YAP (Yes-associated protein), ZEB1 switches from a repressor to an activator of transcription<sup>24</sup>. Here we found that in the absence of ShcA, YAP protein expression decreased in the nucleus. This strongly suggests that ShcA participate in the dual function of ZEB1. By promoting YAP nuclear translocation ShcA switches ZEB1 function from a repressor to an activator of transcription, thereby promoting ICAM-1 expression. However, we cannot exclude that interactions with other transcription factors may also confer the transcriptional co-activation by ZEB1.

Here, we also found that upon ShcA knockdown, the transcription factor NF- $\kappa$ B is induced and translocated to the nucleus. This would stimulate inflammation, recruitment of multiple immune cells including macrophages, and promote atherosclerosis. Since NF- $\kappa$ B increases ZEB1 nuclear translocation, which in turn behaves as a repressor of E-cadherin<sup>33</sup>, similarly, in the absence of ShcA, NF- $\kappa$ B might repress ICAM-1 expression through increased ZEB1 nuclear translocation. Thus, whereas NF- $\kappa$ B stimulates inflammation, the increase in NF- $\kappa$ B can be not only limited to negative effects on atherosclerosis.

Previous studies reported that LDL cholesterol upregulates the expression of human endothelial p66Shc via hypomethylation of CpG dinucleotides in the p66Shc promoter<sup>34</sup>, and that epigenetic upregulation of the p66Shc isoform of ShcA mediates increase in ICAM-1 expression<sup>34</sup>. This suggest that at least two independent mechanisms up regulate ShcA and the corresponding increase in ICAM-1 expression in endothelial cells, one involving hypomethylation of the promoter, another one involving transcriptional up regulation and nuclear translocation of ZEB1.

Endothelium-derived NO has also a crucial role in the local regulation of vascular homeostasis. A decrease in the bioavailability of NO aggravates the development of atherosclerotic lesions<sup>35</sup>. NO *per se* suppresses LDL oxidation and macrophage accumulation<sup>36</sup>. eNOS is an Akt target and the activation of eNOS by Akt is one of the most important physiological effects of Akt on cell attachment in endothelial cells<sup>27</sup>. Here we found that p-Akt is decreased when ShcA is expressed. This results by decreased eNOS levels, LDL oxidation, inflammation and atherosclerosis in mice.

In conclusion, we found that ShcA promotes a ZEB1-mediated increase of ICAM-1 expression, favor monocyte-derived macrophages adhesion, intracellular lipid accumulation and foam cell formation while simultaneously decreasing vascular NO production, events that would contribute to endothelial dysfunction commonly seen during atherosclerosis.

## Methods

**Mice.** All animal experimentations and procedures were approved by the Institutional Animal Care and Use Committee (IACUC) of University of Strasbourg, France, and performed conform to the guidelines from Directive 2010/63/EU of the European Parliament on the protection of animals used for scientific purposes. C57/B6 mice carrying a ShcA allele into which loxP sites are integrated have been generated by gene targeting in embryonic stem cells. LoxP sites have been introduced upstream of exon 2 and downstream of exon 7 (ShcA<sup>lox/lox</sup>)<sup>13</sup>. Cre-mediated recombination resulted in deletion of a 2-kb fragment containing the sequence encoding the PTB domain required for binding to phosphorylated receptors and for signaling activity. Endothelial cells specific p66, p52 and p46 ShcA inactivation was achieved by crossing transgenic mice carrying the Tie2-Cre transgene (a kind gift from Masashi Yanagisawa, University of Texas Southwestern Medical Center, at Dallas) with ShcA<sup>lox/lox</sup> mice. In order to increase susceptibility to spontaneous atherosclerotic lesion development, these animals were crossed to LDL receptor knock out mice (LDLR<sup>-/-</sup>). Genotyping of the wild type and ShcA mutant mice by polymerase chain reaction (PCR) was performed as described<sup>37</sup> using primers specific for ShcA (Primers available upon request). Animals were maintained on a 12-h light/12-h dark cycle. For *in vivo* analysis, 4 males and 1 female of three to four months old were used for each genotype, fed a Paigen diet during six months, and analyzed for atherosclerotic lesions as described previously<sup>8</sup>. For the isolation of tissue for further analysis, the agents used for euthanasia were ketamine (750 mg/kg) and xylazine (50 mg/kg), intraperitoneally.

**Purification of lipoproteins.** LDLs were isolated from South-American sourced Fetal Bovine serum by density gradient centrifugation. LDLs were dialyzed for 48 hours in a solution of NaCl 150 mM and 0.24 mM disodium EDTA, pH 7.4. LDLs were then centrifuged for 30 minutes, 4°C at 10,000 RPM and filtered through a 0.22  $\mu$ m filter. Concentrations were determined by the Lowry method.

**Oxidation of LDLs.** LDLs were added at a concentration of 600  $\mu$ g/ml in RPMI 1640 medium supplemented with 10% South-American sourced FBS. Copper sulfide (SIGMA) was dissolved in RPMI medium, filtered through a 0.22  $\mu$ m filter and added to the LDL solution to a final concentration of 10  $\mu$ M. The resulting solution was incubated at 37°C for 48 hours.

**Cells.** Aortic endothelial cells isolation: Thoracic and abdominal aortas were carefully dissected from 3 months old control and Tie2Cre+/ShcAlox/lox mice. The endothelial layer was removed immediately after dissection by intraluminal perfusion with 0.5% 3-[(3-cholamidopropyl)dimethylammonio]-1 propane sulphonate (CHAPS) in Physiological salt solution (PSS) for 20 s followed by repeated washing with PSS. The washed endothelial layers from 5 mice were collected, pooled and submitted to SDS-polyacrylamide gel electrophoresis and immunoblot analysis according to standard procedures.

Human EA.hy 926 endothelial cells (a kind gift from Dr Sophie Martin, UMR CNRS 7213, University of Strasbourg) were seeded in 6-well-plates at 120,000 cells/well in DMEM medium supplemented with 10% FBS and 2 mM L-Glutamine, and were placed in a 37°C incubator with humidified atmosphere containing 5% CO<sub>2</sub> as described<sup>38,39</sup>. 24 hours after seeding, cells were transfected with either scrambled siRNA, siRNA against p66, p52 and p46 isoforms of ShcA (Dharmacon) or siRNA against the p66 isoform of ShcA<sup>40</sup> (Dharmacon, custom siRNA,

5'-GAAUGAGUCUCUGUCAUCGUU-3') at a final concentration of 100 nM using lipofectamine 3000. 48 hours post-transfection, DMEM medium was replaced with the LDL oxidation solution containing THP-1 (a kind gift from Prof Florence Toti, UMR CNRS 7213, University of Strasbourg) Macrophage cells at  $2.10^6$  cells/well. Phorbol myristate acetate (PMA) was added at a concentration of 50 ng/ml to induce macrophage differentiation. Cells were then incubated at 37 °C, 5%CO<sub>2</sub> for 48 hours.

Control EA.hy 926 endothelial cells transfected with scrambled siRNAs or siShcA were incubated in the same conditions but in a medium that did not contain oxidized LDLs. At the same time,  $2.10^6$  cells/well THP-1 cells were incubated in the same conditions for 48 hours and used as positive control. 48 hours later, wells were stained using Oil/RedO staining. We controlled siRNA transfection efficiency using Western Blotting and/or Real Time PCR. Each experiment was repeated 5 times for statistical significance. For quantitative analysis, images taken through the microscope were processed using ImageJ. Regions formed by the accumulation of foam cells were manually outlined and the quantification of outlined region was determined by ImageJ.

**Lipid Staining.** The cells were fixed with 10% Paraformaldehyde for 30 minutes, washed twice with phosphate-buffered saline (PBS) buffer, pH = 7.4, and stained with a saturated concentration of oil red O for a minimum of 30 minutes. Cells were then washed twice with PBS buffer and LDL accumulation by THP1 cells was observed under microscopy; representative images of whole wells were taken for further analysis.

**Gene expression analysis.** RNA was isolated using TRIzol reagent (Sigma, St Louis, Mo) according to the manufacturer's instructions. 50 ng of RNA were converted to cDNA using the High-capacity cDNA Archive kit (Applied Biosystems, Foster City, CA). PCR amplification was performed using SYBRGreen PCR master mix (Kappa biosystems, Wilmington, MA) according to the manufacturer's instructions. Primers sequences are available upon request.

**Histology experiments.** For immunostaining and histology experiments, mice were transcardially perfused with a 4% paraformaldehyde solution in phosphate buffered saline. Entire aortas were fixed with 4% paraformaldehyde in phosphate-buffered saline, embedded in paraffin, and cut in 5 µm slices as described<sup>37</sup>. Sections were stained with hematoxylin and eosin as described<sup>37</sup>.

**Western blot.** Whole cell extracts were fractionated by SDS-PAGE and transferred to a nitrocellulose membrane using a transfer apparatus according to the manufacturer's protocols (Bio-Rad). After incubation with 5% BSA TBST (10 mM Tris, pH 8.0, 150 mM NaCl, 0.5% Tween 20) for 60 min at room temperature, the membrane was incubated at 4 °C overnight with primary antibodies directed against ShcA (Upstate), ICAM-1 (Abcam), VCAM-1 (Abcam), CD62E (E-selectin) (Abcam), NFκB p65 (Cell Signaling Technology), p-NFκB p65 (S536) (Cell Signaling Technology), Ikkbeta (Cell Signaling Technology), p-eNOS (S1177) (Cell Signaling Technology), P-mTOR (S2448) (Cell Signaling Technology), AREB6 (ZEB1) (Abcam), YAP1 (Santa Cruz), p-Akt (S473) (Cell Signaling Technology), Akt (Cell Signaling Technology), Actin (Sigma, St Louis, Mo) or GAPDH (Sigma, St Louis, Mo). Membranes were then washed five times for 5 min and incubated with a 1:10000 dilution of horseradish peroxidase-conjugated anti-mouse or anti-rabbit antibodies (Santa Cruz) for 1 h at room temperature. Blots were washed with TBST five times and developed with the ECL system according to the manufacturer's protocols (BIO RAD Clarity™ Western ECL Substrate). Clarity™ western ECL substrate allowed visualization of protein expression using ImageQuant™ LAS 4000 Imaging System (Amersham). Optical densitometry was performed with Adobe PhotoshopCS and Image J normalizing bands intensity for GAPDH.

**Cell fractionation.** For cell fractionation, monolayers of human endothelial cells (EAhy) were transfected with either scramble siRNA or siRNA against ShcA (Dharmacon) (100 nM). 48 hours post-transfection, cells were then fractionated as previously described<sup>41</sup>.

**Confocal Microscopy.** EAhy cells were seeded on glass slides, 24 hours later, they were treated with either scramble siRNA or siRNA against ShcA. 48 hours post-transfection, the cells were fixed with paraformaldehyde, and incubated with anti-ZEB1 or anti-IgG control primary antibodies and Alexa Fluor 488 secondary antibodies. Immunofluorescence-labeled cells were analyzed using a Leica TSC SPE confocal microscope with the ×63 oil immersion objective.

**Statistical analysis.** Values are reported as mean ± SEM of at least triplicate determinations. Statistical significance ( $P < 0.05$ ) was determined using an unpaired Student's *t* test (GraphPad Prism, *Abacus Concepts, Berkeley, CA*). *P*-values  $< 0.05$ ,  $< 0.01$ , and  $< 0.001$  are identified with 1, 2, 3 asterisks, respectively. ns:  $p > 0.05$ .

## References

- Mestas, J. & Ley, K. Monocyte-endothelial cell interactions in the development of atherosclerosis. *Trends in cardiovascular medicine* **18**, 228–232 (2008).
- Wills, M. K. & Jones, N. Teaching an old dogma new tricks: twenty years of Shc adaptor signalling. *The Biochemical journal* **447**, 1–16 (2012).
- Lai, K. M. V. & Pawson, T. The ShcA phosphotyrosine docking protein sensitizes cardiovascular signaling in the mouse embryo. *Gene Dev* **14**, 1132–1145 (2000).
- Demoor, M. *et al.* Cartilage tissue engineering: molecular control of chondrocyte differentiation for proper cartilage matrix reconstruction. *Biochimica et biophysica acta* **1840**, 2414–2440 (2014).
- Wang, Y. *et al.* IGF-1R signaling in chondrocytes modulates growth plate development by interacting with the PTHrP/Ihh pathway. *Journal of bone and mineral research: the official journal of the American Society for Bone and Mineral Research* **26**, 1437–1446 (2011).
- Jonquoy, A. *et al.* A novel tyrosine kinase inhibitor restores chondrocyte differentiation and promotes bone growth in a gain-of-function *Fgfr3* mouse model. *Human molecular genetics* **21**, 841–851 (2012).

7. van de Sluis, B., Wijers, M. & Herz, J. News on the molecular regulation and function of hepatic low-density lipoprotein receptor and LDLR-related protein 1. *Curr Opin Lipidol* (2017).
8. Boucher, P., Gotthardt, M., Li, W. P., Anderson, R. G. W. & Herz, J. LRP: Role in vascular wall integrity and protection from atherosclerosis. *Science* **300**, 329–332 (2003).
9. Woldt, E. *et al.* The nuclear hormone receptor PPAR gamma counteracts vascular calcification by inhibiting Wnt5a signalling in vascular smooth muscle cells. *Nat Commun* **3** (2012).
10. Terrand, J. *et al.* LRP1 Controls Intracellular Cholesterol Storage and Fatty Acid Synthesis through Modulation of Wnt Signaling. *Journal of Biological Chemistry* **284**, 381–388 (2009).
11. Loukinova, E. *et al.* Platelet-derived growth factor (PDGF)-induced tyrosine phosphorylation of the low density lipoprotein receptor-related protein (LRP) - Evidence for integrated co-receptor function between LRP and the PDGF. *Journal of Biological Chemistry* **277**, 15499–15506 (2002).
12. Boucher, P. *et al.* Platelet-derived growth factor mediates tyrosine phosphorylation of the cytoplasmic domain of the low density lipoprotein receptor-related protein in caveolae. *Journal of Biological Chemistry* **277**, 15507–15513 (2002).
13. Mliih, M. *et al.* The Src Homology and Collagen A (ShcA) Adaptor Protein Is Required for the Spatial Organization of the Costamere/Z-disk Network during Heart Development. *Journal of Biological Chemistry* **290**, 2419–2430 (2015).
14. Napoli, C. *et al.* Deletion of the p66Shc longevity gene reduces systemic and tissue oxidative stress, vascular cell apoptosis, and early atherogenesis in mice fed a high-fat diet. *Proc Natl Acad Sci USA* **100**, 2112–2116 (2003).
15. Hopkins, A. M., Baird, A. W. & Nusrat, A. ICAM-1: targeted docking for exogenous as well as endogenous ligands. *Adv Drug Deliv Rev* **56**, 763–778 (2004).
16. Nakashima, Y., Raines, E. W., Plump, A. S., Breslow, J. L. & Ross, R. Upregulation of VCAM-1 and ICAM-1 at atherosclerosis-prone sites on the endothelium in the ApoE-deficient mouse. *Arterioscler Thromb Vas* **18**, 842–851 (1998).
17. Shi, Y. *et al.* Oxidized low-density lipoprotein activates p66Shc via lectin-like oxidized low-density lipoprotein receptor-1, protein kinase C-beta, and c-Jun N-terminal kinase kinase in human endothelial cells. *Arterioscler Thromb Vasc Biol* **31**, 2090–2097 (2011).
18. Chen, C. C., Rosenbloom, C. L., Anderson, D. C. & Manning, A. M. Selective inhibition of E-selectin, vascular cell adhesion molecule-1, and intercellular adhesion molecule-1 expression by inhibitors of I kappa B-alpha phosphorylation. *J Immunol* **155**, 3538–3545 (1995).
19. Israel, A. The IKK complex, a central regulator of NF-kappaB activation. *Cold Spring Harb Perspect Biol* **2**, a000158 (2010).
20. Ishikado, A. *et al.* Soy phosphatidylcholine inhibited TLR4-mediated MCP-1 expression in vascular cells. *Atherosclerosis* **205**, 404–412 (2009).
21. Xing, L. & Remick, D. G. Promoter elements responsible for antioxidant regulation of MCP-1 gene expression. *Antioxid Redox Signal* **9**, 1979–1989 (2007).
22. Li, X. *et al.* Negative feedback loop between p66Shc and ZEB1 regulates fibrotic EMT response in lung cancer cells. *Cell Death Dis* **6**, e1708 (2015).
23. Vandewalle, C., Van Roy, F. & Berx, G. The role of the ZEB family of transcription factors in development and disease. *Cell Mol Life Sci* **66**, 773–787 (2009).
24. Lehmann, W. *et al.* ZEB1 turns into a transcriptional activator by interacting with YAP1 in aggressive cancer types. *Nat Commun* **7**, 10498 (2016).
25. Gheldof, A., Hulpiau, P., van Roy, F., De Craene, B. & Berx, G. Evolutionary functional analysis and molecular regulation of the ZEB transcription factors. *Cell Mol Life Sci* **69**, 2527–2541 (2012).
26. Wu, R. F. *et al.* p66Shc couples mechanical signals to RhoA through FAK-dependent recruitment of p115-RhoGEF and GEF-H1. *Mol Cell Biol* (2016).
27. Dimmeler, S. *et al.* Activation of nitric oxide synthase in endothelial cells by Akt-dependent phosphorylation. *Nature* **399**, 601–605 (1999).
28. Heitzer, T., Schlinzig, T., Krohn, K., Meinertz, T. & Munzel, T. Endothelial dysfunction, oxidative stress, and risk of cardiovascular events in patients with coronary artery disease. *Circulation* **104**, 2673–2678 (2001).
29. Knowles, J. W. *et al.* Enhanced atherosclerosis and kidney dysfunction in eNOS(–/–)ApoE(–/–) mice are ameliorated by enalapril treatment. *J Clin Invest* **105**, 451–458 (2000).
30. Wullschleger, S., Loewith, R. & Hall, M. N. TOR signaling in growth and metabolism. *Cell* **124**, 471–484 (2006).
31. Woldt, E. *et al.* Differential signaling by adaptor molecules LRP1 and ShcA regulates adipogenesis by the insulin-like growth factor-1 receptor. *The Journal of biological chemistry* **286**, 16775–16782 (2011).
32. Martin-Padura, I. *et al.* p66Shc deletion confers vascular protection in advanced atherosclerosis in hypercholesterolemic apolipoprotein E knockout mice. *Endothelium* **15**, 276–287 (2008).
33. Chua, H. L. *et al.* NF-kappaB represses E-cadherin expression and enhances epithelial to mesenchymal transition of mammary epithelial cells: potential involvement of ZEB-1 and ZEB-2. *Oncogene* **26**, 711–724 (2007).
34. Kim, Y. R. *et al.* Epigenetic upregulation of p66shc mediates low-density lipoprotein cholesterol-induced endothelial cell dysfunction. *Am J Physiol Heart Circ Physiol* **303**, H189–196 (2012).
35. Moroi, M. *et al.* Interaction of genetic deficiency of endothelial nitric oxide, gender, and pregnancy in vascular response to injury in mice. *J Clin Invest* **101**, 1225–1232 (1998).
36. Ahmed, A. *et al.* Angiotensin-2 confers Atheroprotection in apoE–/– mice by inhibiting LDL oxidation via nitric oxide. *Circ Res* **104**, 1333–1336 (2009).
37. Boucher, P., Gotthardt, M., Li, W. P., Anderson, R. G. & Herz, J. LRP: role in vascular wall integrity and protection from atherosclerosis. *Science* **300**, 329–332 (2003).
38. Schmitz, B. *et al.* Increased monocyte adhesion by endothelial expression of VCAM-1 missense variation *in vitro*. *Atherosclerosis* **230**, 185–190 (2013).
39. Wang, Y. *et al.* An extract from medical leech improve the function of endothelial cells *in vitro* and attenuates atherosclerosis in ApoE null mice by reducing macrophages in the lesions. *Biochem Biophys Res Commun* **455**, 119–125 (2014).
40. Kisielow, M., Kleiner, S., Nagasawa, M., Faisal, A. & Nagamine, Y. Isoform-specific knockdown and expression of adaptor protein ShcA using small interfering RNA. *Biochem J* **363**, 1–5 (2002).
41. El Asmar, Z. *et al.* Convergent Signaling Pathways Controlled by LRP1 (Receptor-related Protein 1) Cytoplasmic and Extracellular Domains Limit Cellular Cholesterol Accumulation. *The Journal of biological chemistry* **291**, 5116–5127 (2016).

## Acknowledgements

We are grateful to Daniel Metzger (IGBMC, University of Strasbourg) for critical reading of the manuscript, Véronique Bruban (UMR CNRS 7213, University of Strasbourg) for technical assistance, Masashi Yanagisawa (University of Texas Southwestern Medical Center, at Dallas) for kindly providing us with the Tie2Cre mice, Sophie Martin (UMR CNRS 7213, University of Strasbourg) for Human endothelial cells (EAhy), Florence Toti (UMR CNRS 7213, University of Strasbourg) for providing us with THP-1 cells, and Irwin Davidson (IGBMC, University of Strasbourg) for YAP antibodies. This work was supported by grants from Fondation de France, Fondation pour la Recherche Médicale (FRM), the Agence Nationale de la Recherche (ANR-06-Physio-032-01

and ANR-09-BLAN-0121-01), National Institutes of Health Grants HL063762, NS093382 and AG053391 (to J.H.), the Consortium for Frontotemporal Dementia Research, and the Bright Focus Foundation.

### Author Contributions

P.B. and R.L.M. designed the project and supervised the entire study. P.B. wrote the manuscript. A.A.J. and L.B. conducted most of the *in vivo* studies and all the *in vitro* studies, gene expression and immunostaining assays, and revised the manuscript, R.L.M. created the colony of endoShcA mice, conducted the Paigen *in vivo* study, and with J.H. participated in the discussion of the results and revised the manuscript, M.M., L.H., S.A., S.G., A.L., C.A., and H.J. performed the quantification of lipids in the plasma, the immunostaining, RT-PCR and western blots analysis, J.T. performed some immunostaining assays and gene expression assays and contributed to the design of the project, S.F. participated in the *in vitro* studies and J.H. critically revised the manuscript.

### Additional Information

**Supplementary information** accompanies this paper at <https://doi.org/10.1038/s41598-018-22819-3>.

**Competing Interests:** The authors declare no competing interests.

**Publisher's note:** Springer Nature remains neutral with regard to jurisdictional claims in published maps and institutional affiliations.



**Open Access** This article is licensed under a Creative Commons Attribution 4.0 International License, which permits use, sharing, adaptation, distribution and reproduction in any medium or format, as long as you give appropriate credit to the original author(s) and the source, provide a link to the Creative Commons license, and indicate if changes were made. The images or other third party material in this article are included in the article's Creative Commons license, unless indicated otherwise in a credit line to the material. If material is not included in the article's Creative Commons license and your intended use is not permitted by statutory regulation or exceeds the permitted use, you will need to obtain permission directly from the copyright holder. To view a copy of this license, visit <http://creativecommons.org/licenses/by/4.0/>.

© The Author(s) 2018

## Discussion

---

Our results indicate that Wnt5a is essential for lysosomal function and is an important component of mTORC1-NPC cholesterol sensing complex. In absence of Wnt5a, lysosomes increase in size and number, and accumulate more cholesterol. These results are in agreement with our previous result in MEF cells LRP1<sup>-/-</sup>. In absence of LRP1, endogenous Wnt5a levels are reduced, thereby increasing cholesterol accumulation (El Asmar *et al.*, 2016).

It has been previously reported that Wnt5a expression increases as the atherosclerosis disease progress (Christman *et al.*, 2008, Woldt *et al.*, 2012). We have also shown in fig.22A that Wnt5a expression in VSMCs increases upon cholesterol accumulation. However, deletion of Wnt5a in VSMCs leads to cholesterol accumulation and atherosclerosis. Thus, this increased expression of Wnt5a might be a compensatory mechanism adopted by the cells to prevent the cholesterol accumulation, and not a risk factor.

Our data are also in agreement with previous reports in LRP1 mutant mice containing a mutated PDGF receptor- $\beta$  kinase domain (Zhou *et al.*, 2009). LRP1 in VSMCs functions cell autonomously in the maintenance of vascular wall integrity and protection from cholesterol-induced atherosclerosis. However, disruption of proatherogenic proliferative pathway, involving PI3K and PDGFR- $\beta$ , prevents lesion development in the aortic arch and the abdominal aorta, where vascular integrity is easily compromised (Zhou *et al.*, 2009). Here, we show that the activation of the PI3K/Akt/mTORC1 pathway in the absence of Wnt5a impairs basic lysosomal functions leading to cholesterol accumulation in LELs. Thus, PI3K integrates both signals from

cellular growth and lysosomal function and is an efficient checkpoint slowing or preventing degenerative disorders of the vascular wall.

It was recently published, mTORC1 inhibits cholesterol trafficking from lysosomes to ER (Castellano *et al.*, 2017) and results in cholesterol accumulation in cells. Our results show that mTORC1 is activated in absence of Wnt5a and cholesterol trafficking is blocked from lysosomes to ER. How mTORC1 is upregulated in absence of Wnt5a could be by activating PI3Kinase/AKT/mTORC1 pathway. Our results show that both PI3Kinase and AKT are activated in absence of Wnt5a. Activation of AKT inhibits TSC1/2 which is the inhibitor of mTORC1, and this results in activation of mTORC1. In addition, to be active TSC1/2 requires activation by AMPK and GSK3. Another reason for activation of mTORC1 could be due to the downregulation of AMPK in the absence of Wnt. Wnt5a activates AMPK signaling. In its absence phospho-AMPK levels are reduced leading to inactivation of TSC1/2 and increased phosphorylation of mTORC1.

Previous observations are consistent with the localization of Wnt signaling in the endosomal compartment. Canonical Wnt signaling Wnt3a causes the relocalization of the Glycogen Synthase Kinase 3 (GSK3) to endosomal compartments (Taelman *et al.*, 2010) allowing Wnt mediated suppression of GSK3 activity (Witze *et al.*, 2008). Following GSK3 inhibition, Wnt3a (or Wnt1) or treatment with GSK3 inhibitors inhibited TSC2 and thus releases GSK3 inhibition on mTORC1 (Inoki *et al.*, 2006). Here, in addition to its localization within Lamp1 positive LELs (Fig. 27B, right panels), we also found that GSK3 inhibition by LiCl increases p-mTORC1 in wild type cells (Fig 33D, lane 3). But surprisingly, GSK3 inhibition by LiCl inhibits p-mTORC1 in human Wnt5a<sup>-/-</sup> VSMCs (Fig 33D, lane 4). This indicates that

Wnt5a behaves differently from other Wnt ligands especially Wnt3a. Through inhibition of Akt and activation of AMPK, Wnt5a down regulates mTORC1. However another Wnt5a dependent unknown pathway or another Wnt ligand (Wnt3a), upon GSK3 inhibition might also participate to mTORC1 regulation.

As it is previously published, NPC1 & 2 are the two cholesterol export proteins in lysosomes (Gong *et al.*, 2016) and NPC1 downregulates mTORC1 to promote cholesterol trafficking from the lysosomes to the ER (Castellano *et al.*, 2017). Our data shows that apart from decreasing mTORC1, Wnt5a also physically interacts with NPC1 and NPC2 proteins and promotes increased cholesterol egress from the lysosomes to ER. Wnt5a also binds to cholesterol due to the presence of five cholesterol binding motifs in its CARC sequence. Thus Wnt5a functions along with mTORC1 and NPC1/2 proteins in sensing and regulating lysosomal cholesterol levels.

## Conclusion

---

In conclusion, the work presented here identifies a previously unrecognized crucial role for Wnt5a in controlling lysosomal function and cholesterol trafficking. Wnt5a is a novel integral component of the lysosomal machinery that decreases mTORC1 activity. As a consequence, the absence of Wnt5a leads to the accumulation of large LELs and of cholesterol and lipofuscin containing vesicles. Accumulation of cholesterol activates the nutrient-dependent mTORC1 axis at the surface of LELs, whereas Wnt5a down regulates this mechanism in a cholesterol dependent manner. Wnt5a interacts in LELs with NPC proteins to communicate lysosomal sterol abundance to the mTORC1 complex. This is required for cholesterol transport across the lysosomal membrane and its trafficking to the ER for subsequent redistribution and export via ABC transporters. This mechanism limits cholesterol accumulation in VSMCs, and protects against atherosclerosis in mice. Our findings have profound implications for atherosclerosis and lysosomal storage diseases, and provide new mechanistic insights into the cholesterol trafficking machinery and the intracellular events mediated by Wnt signaling.

## Future Perspectives

---

Our work identifies that Wnt5a down regulates mTORC1 activity promoting lysosomal trafficking, further studies are needed to analyze how Wnt5a downregulates mTORC1. Our team will try to find out whether Wnt5a decreases mTORC1 by inhibiting Rheb or activating TSC1&2, or it can be by recruiting mTORC1 at lysosomal surface. Moreover, here we have shown that Wnt5a interacts with NPC1 & 2 proteins. We will try to establish the functional significance of this interaction.

As our results show that Wnt5a protects against atherosclerosis development. However, it's difficult to purify and is an unstable protein therefore, it's not possible to inject it in mice. Alternative mechanisms to promote Wnt5a signaling are required to develop new drug therapies.



# References

- Allahverdian, S., Chehroudi, A. C., McManus, B. M., Abraham, T., et alFrancis, G. A. (2014). Contribution of Intimal Smooth Muscle Cells to Cholesterol Accumulation and Macrophage-Like Cells in Human Atherosclerosis. *Circulation*, *129*(15), 1551-1559.
- Angers, S., & Moon, R. T. (2009). Proximal events in Wnt signal transduction. *Nature Reviews Molecular Cell Biology*, *10*, 468.
- Aung, T., Halsey, J., Kromhout, D., Gerstein, H. C., Marchioli, R., Tavazzi, L., Geleijnse, J. M., Rauch, B., Ness, A., Galan, P., Chew, E. Y., Bosch, J., Collins, R., Lewington, S., Armitage, J., et alClarke, R. (2018). Associations of Omega-3 Fatty Acid Supplement Use With Cardiovascular Disease Risks: Meta-analysis of 10 Trials Involving 77917 Individuals. *JAMA Cardiol*, *3*(3), 225-234.
- Bachman, E. S., Dhillon, H., Zhang, C.-Y., Cinti, S., Bianco, A. C., Kobilka, B. K., et alLowell, B. B. (2002).  $\beta$ AR Signaling Required for Diet-Induced Thermogenesis and Obesity Resistance. *Science*, *297*(5582), 843-845.
- Barrans, A., Collet, X., Barbaras, R., Jaspard, B., Manent, J., Vieu, C., Chap, H., et alPerret, B. (1994). Hepatic lipase induces the formation of pre-beta 1 high density lipoprotein (HDL) from triacylglycerol-rich HDL2. A study comparing liver perfusion to in vitro incubation with lipases. *J Biol Chem*, *269*(15), 11572-11577.
- Barter, P. J., Caulfield, M., Eriksson, M., Grundy, S. M., Kastelein, J. J. P., Komajda, M., Lopez-Sendon, J., Mosca, L., Tardif, J.-C., Waters, D. D., Shear, C. L., Revkin, J. H., Buhr, K. A., Fisher, M. R., Tall, A. R., et alBrewer, B. (2007). Effects of Torcetrapib in Patients at High Risk for Coronary Events. *New England Journal of Medicine*, *357*(21), 2109-2122.
- Behari, J., Yeh, T.-H., Krauland, L., Otruba, W., Cieply, B., Hauth, B., Apte, U., Wu, T., Evans, R., et alMonga, S. P. S. (2010). Liver-specific beta-catenin knockout mice exhibit defective bile acid and cholesterol homeostasis and increased susceptibility to diet-induced steatohepatitis. *The American journal of pathology*, *176*(2), 744-753.
- Bennett, C. N., Ross, S. E., Longo, K. A., Bajnok, L., Hemati, N., Johnson, K. W., Harrison, S. D., et alMacDougald, O. A. (2002). Regulation of Wnt signaling during adipogenesis. *J Biol Chem*, *277*(34), 30998-31004.
- Bergheanu, S. C., Bodde, M. C., et alJukema, J. W. (2017). Pathophysiology and treatment of atherosclerosis : Current view and future perspective on lipoprotein modification treatment. *Neth Heart J*, *25*(4), 231-242.
- Bhatt, P. M., Lewis, C. J., House, D. L., Keller, C. M., Kohn, L. D., Silver, M. J., McCall, K. D., Goetz, D. J., et alMalgor, R. (2012). Increased Wnt5a mRNA Expression in Advanced Atherosclerotic Lesions, and Oxidized LDL Treated Human Monocyte-Derived Macrophages. *The open circulation & vascular journal*, *5*, 1-7.
- Bhatt, P. M., & Malgor, R. (2014). Wnt5a: a player in the pathogenesis of atherosclerosis and other inflammatory disorders. *Atherosclerosis*, *237*(1), 155-162.
- Bi, X., & Liao, G. (2010). Cholesterol in Niemann-Pick Type C disease. *Sub-cellular biochemistry*, *51*, 319-335.
- Bligh, E. G., & Dyer, W. J. (1959). A rapid method of total lipid extraction and purification. *Can J Biochem Physiol*, *37*(8), 911-917.
- Blumenthal, A., Ehlers, S., Lauber, J., Buer, J., Lange, C., Goldmann, T., Heine, H., Brandt, E., et alReiling, N. (2006). The Wingless homolog WNT5A and its receptor Frizzled-5 regulate inflammatory responses of human mononuclear cells induced by microbial stimulation. *Blood*, *108*(3), 965-973.
- Boucher, P., Gotthardt, M., Li, W. P., Anderson, R. G., et alHerz, J. (2003). LRP: role in vascular wall integrity and protection from atherosclerosis. *Science*, *300*(5617), 329-332.
- Bravo, R., Parra, V., Gatica, D., Rodriguez, A. E., Torrealba, N., Paredes, F., Wang, Z. V., Zorzano, A., Hill, J. A., Jaimovich, E., Quest, A. F., et alLavandero, S. (2013). Endoplasmic reticulum and the

- unfolded protein response: dynamics and metabolic integration. *Int Rev Cell Mol Biol*, 301, 215-290.
- Brown, M. S., & Goldstein, J. L. (1986). A receptor-mediated pathway for cholesterol homeostasis. *Science*, 232(4746), 34-47.
- Brown, M. S., & Goldstein, J. L. (1996). Heart Attacks: Gone with the Century? *Science*, 272(5262), 629-629.
- Bunn, K. J., Daniel, P., Rösken, H. S., O'Neill, A. C., Cameron-Christie, S. R., Morgan, T., Brunner, H. G., Lai, A., Kunst, H. P. M., Markie, D. M., et al Robertson, S. P. (2015). Mutations in DVL1 cause an osteosclerotic form of Robinow syndrome. *American journal of human genetics*, 96(4), 623-630.
- Camejo, G., Lopez, A., Vegas, H., et al Paoli, H. (1975). The participation of aortic proteins in the formation of complexes between low density lipoproteins and intima-media extracts. *Atherosclerosis*, 21(1), 77-91.
- Casem, M. L. (2016). Chapter 9 - Endocytosis. In M. L. Casem (Ed.), *Case Studies in Cell Biology* (pp. 217-240). Boston: Academic Press.
- Castellano, B. M., Thelen, A. M., Moldavski, O., Feltes, M., van der Welle, R. E., Mydock-McGrane, L., Jiang, X., van Eijkeren, R. J., Davis, O. B., Louie, S. M., Perera, R. M., Covey, D. F., Nomura, D. K., Ory, D. S., et al Zoncu, R. (2017). Lysosomal cholesterol activates mTORC1 via an SLC38A9-Niemann-Pick C1 signaling complex. *Science*, 355(6331), 1306-1311.
- Catapano, A. L., Reiner, Z., De Backer, G., Graham, I., Taskinen, M. R., Wiklund, O., Agewall, S., Alegria, E., Chapman, M. J., Durrington, P., Erdine, S., Halcox, J., Hobbs, R., Kjekshus, J., Perrone Filardi, P., Riccardi, G., Storey, R. F., et al Wood, D. (2011). ESC/EAS Guidelines for the management of dyslipidaemias: the Task Force for the management of dyslipidaemias of the European Society of Cardiology (ESC) and the European Atherosclerosis Society (EAS). *Atherosclerosis*, 217(1), 012.
- Chang, T. Y., Chang, C. C., Ohgami, N., et al Yamauchi, Y. (2006). Cholesterol sensing, trafficking, and esterification. *Annu Rev Cell Dev Biol*, 22, 129-157.
- Chaudhary, R., Garg, J., Shah, N., et al Sumner, A. (2017). PCSK9 inhibitors: A new era of lipid lowering therapy. *World journal of cardiology*, 9(2), 76-91.
- Cheng, C. W., Yeh, J. C., Fan, T. P., Smith, S. K., et al Charnock-Jones, D. S. (2008). Wnt5a-mediated non-canonical Wnt signalling regulates human endothelial cell proliferation and migration. *Biochem Biophys Res Commun*, 365(2), 285-290.
- Christman, M. A., 2nd, Goetz, D. J., Dickerson, E., McCall, K. D., Lewis, C. J., Benencia, F., Silver, M. J., Kohn, L. D., et al Malgor, R. (2008). Wnt5a is expressed in murine and human atherosclerotic lesions. *Am J Physiol Heart Circ Physiol*, 294(6), 2.
- Clevers, H. (2006). Wnt/beta-catenin signaling in development and disease. *Cell*, 127(3), 469-480.
- Curtiss, L. K., & Tobias, P. S. (2009). Emerging role of Toll-like receptors in atherosclerosis. *Journal of lipid research*, 50 Suppl(Suppl), S340-S345.
- Dash, S., Chava, S., Aydin, Y., Chandra, P. K., Ferraris, P., Chen, W., Balart, L. A., Wu, T., et al Garry, R. F. (2016). Hepatitis C Virus Infection Induces Autophagy as a Prosurvival Mechanism to Alleviate Hepatic ER-Stress Response. *Viruses*, 8(5).
- De, A. (2011). Wnt/Ca<sup>2+</sup> signaling pathway: a brief overview. *Acta Biochim Biophys Sin*, 43(10), 745-756.
- Dimmeler, S., Fleming, I., Fisslthaler, B., Hermann, C., Busse, R., et al Zeiher, A. M. (1999). Activation of nitric oxide synthase in endothelial cells by Akt-dependent phosphorylation. *Nature*, 399(6736), 601-605.
- Eid, W., Dauner, K., Courtney, K. C., Gagnon, A., Parks, R. J., Sorisky, A., et al Zha, X. (2017). mTORC1 activates SREBP-2 by suppressing cholesterol trafficking to lysosomes in mammalian cells. *Proceedings of the National Academy of Sciences of the United States of America*, 114(30), 7999-8004.

- El Asmar, Z., Terrand, J., Jenty, M., Host, L., Mlih, M., Zerr, A., Justiniano, H., Matz, R. L., Boudier, C., Scholler, E., Garnier, J.-M., Bertaccini, D., Thiersé, D., Schaeffer, C., Van Dorsselaer, A., Herz, J., Bruban, V., et al Boucher, P. (2016). Convergent Signaling Pathways Controlled by LRP1 (Receptor-related Protein 1) Cytoplasmic and Extracellular Domains Limit Cellular Cholesterol Accumulation. *The Journal of biological chemistry*, *291*(10), 5116-5127.
- Enerbäck, S., Jacobsson, A., Simpson, E. M., Guerra, C., Yamashita, H., Harper, M.-E., et al Kozak, L. P. (1997). Mice lacking mitochondrial uncoupling protein are cold-sensitive but not obese. *Nature*, *387*(6628), 90-94.
- Fang, L.-M., Li, B., Guan, J.-J., Xu, H.-D., Shen, G.-H., Gao, Q.-G., et al Qin, Z.-H. (2017). Transcription factor EB is involved in autophagy-mediated chemoresistance to doxorubicin in human cancer cells. *Acta pharmacologica Sinica*, *38*(9), 1305-1316.
- Fantini, J., Carlus, D., et al Yah, N. (2011). The fusogenic tilted peptide (67-78) of alpha-synuclein is a cholesterol binding domain. *Biochim Biophys Acta*, *10*(51), 5.
- Feng, B., Yao, P. M., Li, Y., Devlin, C. M., Zhang, D., Harding, H. P., Sweeney, M., Rong, J. X., Kuriakose, G., Fisher, E. A., Marks, A. R., Ron, D., et al Tabas, I. (2003). The endoplasmic reticulum is the site of cholesterol-induced cytotoxicity in macrophages. *Nature Cell Biology*, *5*, 781.
- Ference, B. A., Ginsberg, H. N., Graham, I., Ray, K. K., Packard, C. J., Bruckert, E., Hegele, R. A., Krauss, R. M., Raal, F. J., Schunkert, H., Watts, G. F., Borén, J., Fazio, S., Horton, J. D., Masana, L., Nicholls, S. J., Nordestgaard, B. G., van de Sluis, B., Taskinen, M.-R., Tokgözoğlu, L., Landmesser, U., Laufs, U., Wiklund, O., Stock, J. K., Chapman, M. J., et al Catapano, A. L. (2017). Low-density lipoproteins cause atherosclerotic cardiovascular disease. 1. Evidence from genetic, epidemiologic, and clinical studies. A consensus statement from the European Atherosclerosis Society Consensus Panel. *European Heart Journal*, *38*(32), 2459-2472.
- Fisher, E. A., Feig, J. E., Hewing, B., Hazen, S. L., et al Smith, J. D. (2012). High-density lipoprotein function, dysfunction, and reverse cholesterol transport. *Arteriosclerosis, Thrombosis, and Vascular Biology*, *32*(12), 2813-2820.
- Garratt, A. N., Voiculescu, O., Topilko, P., Charnay, P., et al Birchmeier, C. (2000). A dual role of erbB2 in myelination and in expansion of the schwann cell precursor pool. *J Cell Biol*, *148*(5), 1035-1046.
- Glick, D., Barth, S., et al Macleod, K. F. (2010). Autophagy: cellular and molecular mechanisms. *The Journal of pathology*, *221*(1), 3-12.
- Goldstein, J. L., & Brown, M. S. (2015). A century of cholesterol and coronaries: from plaques to genes to statins. *Cell*, *161*(1), 161-172.
- Gong, X., Qian, H., Zhou, X., Wu, J., Wan, T., Cao, P., Huang, W., Zhao, X., Wang, X., Wang, P., Shi, Y., Gao, G. F., Zhou, Q., et al Yan, N. (2016). Structural Insights into the Niemann-Pick C1 (NPC1)-Mediated Cholesterol Transfer and Ebola Infection. *Cell*, *165*(6), 1467-1478.
- Gordon, M. D., & Nusse, R. (2006). Wnt signaling: multiple pathways, multiple receptors, and multiple transcription factors. *J Biol Chem*, *281*(32), 22429-22433.
- Gowans, G. J., & Hardie, D. G. (2014). AMPK: a cellular energy sensor primarily regulated by AMP. *Biochem Soc Trans*, *42*(1), 71-75.
- Griffin, S., Preta, G., et al Sheldon, I. M. (2017). Inhibiting mevalonate pathway enzymes increases stromal cell resilience to a cholesterol-dependent cytotoxin. *Scientific Reports*, *7*(1), 17050.
- Grumolato, L., Liu, G., Mong, P., Mudbhary, R., Biswas, R., Arroyave, R., Vijayakumar, S., Economides, A. N., et al Aaronson, S. A. (2010). Canonical and noncanonical Wnts use a common mechanism to activate completely unrelated coreceptors. *Genes Dev*, *24*(22), 2517-2530.
- Haka, A. S., Grosheva, I., Chiang, E., Buxbaum, A. R., Baird, B. A., Pierini, L. M., et al Maxfield, F. R. (2009). Macrophages create an acidic extracellular hydrolytic compartment to digest aggregated lipoproteins. *Molecular biology of the cell*, *20*(23), 4932-4940.

- Hanukoglu, I. (1992). Steroidogenic enzymes: Structure, function, and role in regulation of steroid hormone biosynthesis. *The Journal of Steroid Biochemistry and Molecular Biology*, 43(8), 779-804.
- Harwood, A. J., Plyte, S. E., Woodgett, J., Strutt, H., et al Kay, R. R. (1995). Glycogen synthase kinase 3 regulates cell fate in Dictyostelium. *Cell*, 80(1), 139-148.
- Hohn, A., & Grune, T. (2013). Lipofuscin: formation, effects and role of macroautophagy. *Redox Biol*, 1, 140-144.
- Holtwick, R., Gotthardt, M., Skryabin, B., Steinmetz, M., Potthast, R., Zetsche, B., Hammer, R. E., Herz, J., et al Kuhn, M. (2002). Smooth muscle-selective deletion of guanylyl cyclase-A prevents the acute but not chronic effects of ANP on blood pressure. *Proc Natl Acad Sci U S A*, 99(10), 7142-7147.
- Hong, W. C., & Amara, S. G. (2010). Membrane cholesterol modulates the outward facing conformation of the dopamine transporter and alters cocaine binding. *The Journal of biological chemistry*, 285(42), 32616-32626.
- Horton, J. D., Goldstein, J. L., et al Brown, M. S. (2002). SREBPs: activators of the complete program of cholesterol and fatty acid synthesis in the liver. *The Journal of clinical investigation*, 109(9), 1125-1131.
- Howell, B. W., & Herz, J. (2001). The LDL receptor gene family: signaling functions during development. *Current Opinion in Neurobiology*, 11(1), 74-81.
- Huang, T. C., Lee, P. T., Wu, M. H., Huang, C. C., Ko, C. Y., Lee, Y. C., Lin, D. Y., Cheng, Y. W., et al Lee, K. H. (2017). Distinct roles and differential expression levels of Wnt5a mRNA isoforms in colorectal cancer cells. *PloS one*, 12(8).
- Infante, R. E., Wang, M. L., Radhakrishnan, A., Kwon, H. J., Brown, M. S., et al Goldstein, J. L. (2008). NPC2 facilitates bidirectional transfer of cholesterol between NPC1 and lipid bilayers, a step in cholesterol egress from lysosomes. *Proc Natl Acad Sci U S A*, 105(40), 15287-15292.
- Inoki, K., Ouyang, H., Zhu, T., Lindvall, C., Wang, Y., Zhang, X., Yang, Q., Bennett, C., Harada, Y., Stankunas, K., Wang, C. Y., He, X., MacDougald, O. A., You, M., Williams, B. O., et al Guan, K. L. (2006). TSC2 integrates Wnt and energy signals via a coordinated phosphorylation by AMPK and GSK3 to regulate cell growth. *Cell*, 126(5), 955-968.
- Ishibashi, S., Brown, M. S., Goldstein, J. L., Gerard, R. D., Hammer, R. E., et al Herz, J. (1993). Hypercholesterolemia in low density lipoprotein receptor knockout mice and its reversal by adenovirus-mediated gene delivery. *J Clin Invest*, 92(2), 883-893.
- Issa, A. R., Sun, J., Petitgas, C., Mesquita, A., Dulac, A., Robin, M., Mollereau, B., Jenny, A., Cherif-Zahar, B., et al Birman, S. (2018). The lysosomal membrane protein LAMP2A promotes autophagic flux and prevents SNCA-induced Parkinson disease-like symptoms in the Drosophila brain. *Autophagy*, 14(11), 1898-1910.
- Janda, C. Y., Waghray, D., Levin, A. M., Thomas, C., et al Garcia, K. C. (2012). Structural basis of Wnt recognition by Frizzled. *Science*, 337(6090), 59-64.
- Jelinek, D., Millward, V., Birdi, A., Trouard, T. P., Heidenreich, R. A., et al Garver, W. S. (2011). Npc1 haploinsufficiency promotes weight gain and metabolic features associated with insulin resistance. *Hum Mol Genet*, 20(2), 312-321.
- Jernberg, T., Henriksson, M., Hasvold, P., Hjelm, H., Thuresson, M., et al Janson, M. (2015). Cardiovascular risk in post-myocardial infarction patients: nationwide real world data demonstrate the importance of a long-term perspective. *European Heart Journal*, 36(19), 1163-1170.
- Jope, R. S. (2003). Lithium and GSK-3: one inhibitor, two inhibitory actions, multiple outcomes. *Trends Pharmacol Sci*, 24(9), 441-443.
- Jope, R. S., Yuskaitis, C. J., et al Beurel, E. (2007). Glycogen synthase kinase-3 (GSK3): inflammation, diseases, and therapeutics. *Neurochemical research*, 32(4-5), 577-595.

- Kaisho, T., & Akira, S. (2006). Toll-like receptor function and signaling. *Journal of Allergy and Clinical Immunology*, *117*(5), 979-987.
- Kasikara, C., Doran, A. C., Cai, B., et al Tabas, I. (2018). The role of non-resolving inflammation in atherosclerosis. *The Journal of clinical investigation*, *128*(7), 2713-2723.
- Kawakami, K., Yamamura, S., Hirata, H., Ueno, K., Saini, S., Majid, S., Tanaka, Y., Kawamoto, K., Enokida, H., Nakagawa, M., et al Dahiya, R. (2011). Secreted frizzled-related protein-5 is epigenetically downregulated and functions as a tumor suppressor in kidney cancer. *International journal of cancer*, *128*(3), 541-550.
- Kim, E., Goraksha-Hicks, P., Li, L., Neufeld, T. P., et al Guan, K.-L. (2008). Regulation of TORC1 by Rag GTPases in nutrient response. *Nature Cell Biology*, *10*(8), 935-945.
- Kim, J., Kim, J., Kim, D. W., Ha, Y., Ihm, M. H., Kim, H., Song, K., et al Lee, I. (2010). Wnt5a induces endothelial inflammation via beta-catenin-independent signaling. *J Immunol*, *185*(2), 1274-1282.
- Kohn, A. D., & Moon, R. T. (2005). Wnt and calcium signaling: beta-catenin-independent pathways. *Cell Calcium*, *38*(3-4), 439-446.
- Komiya, Y., & Habas, R. (2008). Wnt signal transduction pathways. *Organogenesis*, *4*(2), 68-75.
- Kotwal, S., Jun, M., Sullivan, D., Perkovic, V., et al Neal, B. (2012). Omega 3 Fatty acids and cardiovascular outcomes: systematic review and meta-analysis. *Circ Cardiovasc Qual Outcomes*, *5*(6), 808-818.
- Kovsan, J., Bashan, N., Greenberg, A. S., et al Rudich, A. (2010). Potential role of autophagy in modulation of lipid metabolism. *American Journal of Physiology-Endocrinology and Metabolism*, *298*(1), E1-E7.
- Kuhl, M., Geis, K., Sheldahl, L. C., Pukrop, T., Moon, R. T., et al Wedlich, D. (2001). Antagonistic regulation of convergent extension movements in *Xenopus* by Wnt/beta-catenin and Wnt/Ca<sup>2+</sup> signaling. *Mech Dev*, *106*(1-2), 61-76.
- Kwon, H. J., Abi-Mosleh, L., Wang, M. L., Deisenhofer, J., Goldstein, J. L., Brown, M. S., et al Infante, R. E. (2009). Structure of N-terminal domain of NPC1 reveals distinct subdomains for binding and transfer of cholesterol. *Cell*, *137*(7), 1213-1224.
- Lai, K. M., & Pawson, T. (2000). The ShcA phosphotyrosine docking protein sensitizes cardiovascular signaling in the mouse embryo. *Genes Dev*, *14*(9), 1132-1145.
- Laplante, M., & Sabatini, D. M. (2012). mTOR signaling in growth control and disease. *Cell*, *149*(2), 274-293.
- Lemaire-Ewing, S., Lagrost, L., et al Neel, D. (2012). Lipid rafts: a signalling platform linking lipoprotein metabolism to atherogenesis. *Atherosclerosis*, *221*(2), 303-310.
- Levitan, I., Singh, D. K., et al Rosenhouse-Dantsker, A. (2014). Cholesterol binding to ion channels. *Frontiers in physiology*, *5*, 65-65.
- Li, C., Chen, H., Hu, L., Xing, Y., Sasaki, T., Villosis, M. F., Li, J., Nishita, M., Minami, Y., et al Minoo, P. (2008). Ror2 modulates the canonical Wnt signaling in lung epithelial cells through cooperation with Fzd2. *BMC molecular biology*, *9*, 11-11.
- Libby, P., Tabas, I., Fredman, G., et al Fisher, E. A. (2014). Inflammation and its resolution as determinants of acute coronary syndromes. *Circulation Research*, *114*(12), 1867-1879.
- Lin, T. C., Chen, Y. R., Kensicki, E., Li, A. Y., Kong, M., Li, Y., Mohney, R. P., Shen, H. M., Stiles, B., Mizushima, N., Lin, L. I., et al Ann, D. K. (2012). Autophagy: resetting glutamine-dependent metabolism and oxygen consumption. *Autophagy*, *8*(10), 1477-1493.
- Linton MRF, Yancey PG, Davies SS, et al. (2019). The Role of Lipids and Lipoproteins in Atherosclerosis. Endotext. South Dartmouth (MA): MDTText.com, Inc.; 2000-. Available from: <https://www.ncbi.nlm.nih.gov/books/NBK343489/>.
- Logan, C. Y., & Nusse, R. (2004). The Wnt signaling pathway in development and disease. *Annu Rev Cell Dev Biol*, *20*, 781-810.

- Lohse, P., Maas, S., Sewell, A. C., van Diggelen, O. P., et al Seidel, D. (1999). Molecular defects underlying Wolman disease appear to be more heterogeneous than those resulting in cholesteryl ester storage disease. *J Lipid Res*, *40*(2), 221-228.
- Longo, K. A., Wright, W. S., Kang, S., Gerin, I., Chiang, S. H., Lucas, P. C., Opp, M. R., et al MacDougald, O. A. (2004). Wnt10b inhibits development of white and brown adipose tissues. *J Biol Chem*, *279*(34), 35503-35509.
- Lu, F., Liang, Q., Abi-Mosleh, L., Das, A., De Brabander, J. K., Goldstein, J. L., et al Brown, M. S. (2015). Identification of NPC1 as the target of U18666A, an inhibitor of lysosomal cholesterol export and Ebola infection. *eLife*, *4*, e12177.
- Mani, A., Radhakrishnan, J., Wang, H., Mani, A., Mani, M.-A., Nelson-Williams, C., Carew, K. S., Mane, S., Najmabadi, H., Wu, D., et al Lifton, R. P. (2007). LRP6 mutation in a family with early coronary disease and metabolic risk factors. *Science (New York, N.Y.)*, *315*(5816), 1278-1282.
- Manning, B. D., & Cantley, L. C. (2003). United at last: the tuberous sclerosis complex gene products connect the phosphoinositide 3-kinase/Akt pathway to mammalian target of rapamycin (mTOR) signalling. *Biochem Soc Trans*, *31*(Pt 3), 573-578.
- Marinou, K., Christodoulides, C., Antoniadis, C., et al Koutsilieris, M. (2012). Wnt signaling in cardiovascular physiology. *Trends Endocrinol Metab*, *23*(12), 628-636.
- Marques, L. R., Diniz, T. A., Antunes, B. M., Rossi, F. E., Caperuto, E. C., Lira, F. S., et al Gonçalves, D. C. (2018). Reverse Cholesterol Transport: Molecular Mechanisms and the Non-medical Approach to Enhance HDL Cholesterol. *Frontiers in physiology*, *9*, 526-526.
- Maxfield, F. R., & van Meer, G. (2010). Cholesterol, the central lipid of mammalian cells. *Current Opinion in Cell Biology*, *22*(4), 422-429.
- Mega, J. L., Braunwald, E., Wiviott, S. D., Bassand, J.-P., Bhatt, D. L., Bode, C., Burton, P., Cohen, M., Cook-Brunns, N., Fox, K. A. A., Goto, S., Murphy, S. A., Plotnikov, A. N., Schneider, D., Sun, X., Verheugt, F. W. A., et al Gibson, C. M. (2012). Rivaroxaban in Patients with a Recent Acute Coronary Syndrome. *New England Journal of Medicine*, *366*(1), 9-19.
- Menon, S., Dibble, C. C., Talbott, G., Hoxhaj, G., Valvezan, A. J., Takahashi, H., Cantley, L. C., et al Manning, B. D. (2014). Spatial control of the TSC complex integrates insulin and nutrient regulation of mTORC1 at the lysosome. *Cell*, *156*(4), 771-785.
- Mesmin, B., Antony, B., et al Drin, G. (2013). Insights into the mechanisms of sterol transport between organelles. *Cell Mol Life Sci*, *70*(18), 3405-3421.
- Mikels, A., Minami, Y., et al Nusse, R. (2009). Ror2 receptor requires tyrosine kinase activity to mediate Wnt5A signaling. *J Biol Chem*, *284*(44), 30167-30176.
- Mikels, A. J., & Nusse, R. (2006). Purified Wnt5a protein activates or inhibits beta-catenin-TCF signaling depending on receptor context. *PLoS biology*, *4*(4), e115-e115.
- Mill, C., & George, S. J. (2012). Wnt signalling in smooth muscle cells and its role in cardiovascular disorders. *Cardiovasc Res*, *95*(2), 233-240.
- Mill, C., Monk, B. A., Williams, H., Simmonds, S. J., Jeremy, J. Y., Johnson, J. L., et al George, S. J. (2014). Wnt5a-induced Wnt1-inducible secreted protein-1 suppresses vascular smooth muscle cell apoptosis induced by oxidative stress. *Arterioscler Thromb Vasc Biol*, *34*(11), 2449-2456.
- Millard, E. E., Gale, S. E., Dudley, N., Zhang, J., Schaffer, J. E., et al Ory, D. S. (2005). The sterol-sensing domain of the Niemann-Pick C1 (NPC1) protein regulates trafficking of low density lipoprotein cholesterol. *J Biol Chem*, *280*(31), 28581-28590.
- Mizushima, N., Yoshimori, T., et al Levine, B. (2010). Methods in mammalian autophagy research. *Cell*, *140*(3), 313-326.
- Mobius, W., van Donselaar, E., Ohno-Iwashita, Y., Shimada, Y., Heijnen, H. F., Slot, J. W., et al Geuze, H. J. (2003). Recycling compartments and the internal vesicles of multivesicular bodies harbor most of the cholesterol found in the endocytic pathway. *Traffic*, *4*(4), 222-231.

- Moitra, J., Mason, M. M., Olive, M., Krylov, D., Gavrilova, O., Marcus-Samuels, B., Feigenbaum, L., Lee, E., Aoyama, T., Eckhaus, M., Reitman, M. L., et alVinson, C. (1998). Life without white fat: a transgenic mouse. *Genes Dev*, *12*(20), 3168-3181.
- Murphy, A. J., Dragoljevic, D., et alTall, A. R. (2014). Cholesterol efflux pathways regulate myelopoiesis: a potential link to altered macrophage function in atherosclerosis. *Front Immunol*, *5*(490).
- Napoli, C., Martin-Padura, I., de Nigris, F., Giorgio, M., Mansueto, G., Somma, P., Condorelli, M., Sica, G., De Rosa, G., et alPelicci, P. (2003). Deletion of the p66Shc longevity gene reduces systemic and tissue oxidative stress, vascular cell apoptosis, and early atherogenesis in mice fed a high-fat diet. *Proc Natl Acad Sci U S A*, *100*(4), 2112-2116.
- Nascimbeni, A. C., Giordano, F., Dupont, N., Grasso, D., Vaccaro, M. I., Codogno, P., et alMorel, E. (2017). ER-plasma membrane contact sites contribute to autophagosome biogenesis by regulation of local PI3P synthesis. *Embo J*, *36*(14), 2018-2033.
- Nicholls, S. J., Lincoff, A. M., Barter, P. J., Brewer, H. B., Fox, K. A., Gibson, C. M., Grainger, C., Menon, V., Montalescot, G., Rader, D., Tall, A. R., McErlean, E., Riesmeyer, J., Vangerow, B., Ruotolo, G., Weerakkody, G. J., et alNissen, S. E. (2015). Assessment of the clinical effects of cholesteryl ester transfer protein inhibition with evacetrapib in patients at high-risk for vascular outcomes: Rationale and design of the ACCELERATE trial. *Am Heart J*, *170*(6), 1061-1069.
- Orenstein, S. J., & Cuervo, A. M. (2010). Chaperone-mediated autophagy: molecular mechanisms and physiological relevance. *Seminars in cell & developmental biology*, *21*(7), 719-726.
- Orhon, I., & Reggiori, F. (2017). Assays to Monitor Autophagy Progression in Cell Cultures. *Cells*, *6*(3), 20.
- Ouchi, N., Higuchi, A., Ohashi, K., Oshima, Y., Gokce, N., Shibata, R., Akasaki, Y., Shimono, A., et alWalsh, K. (2010). Sfrp5 is an anti-inflammatory adipokine that modulates metabolic dysfunction in obesity. *Science (New York, N. Y.)*, *329*(5990), 454-457.
- Ouimet, M., Franklin, V., Mak, E., Liao, X., Tabas, I., et alMarcel, Y. L. (2011). Autophagy regulates cholesterol efflux from macrophage foam cells via lysosomal acid lipase. *Cell metabolism*, *13*(6), 655-667.
- Owen, J. L., Zhang, Y., Bae, S.-H., Farooqi, M. S., Liang, G., Hammer, R. E., Goldstein, J. L., et alBrown, M. S. (2012). Insulin stimulation of SREBP-1c processing in transgenic rat hepatocytes requires p70 S6-kinase. *Proceedings of the National Academy of Sciences of the United States of America*, *109*(40), 16184-16189.
- Pagani, F., Pariyarath, R., Garcia, R., Stuani, C., Burlina, A. B., Ruotolo, G., Rabusin, M., et alBaralle, F. E. (1998). New lysosomal acid lipase gene mutants explain the phenotype of Wolman disease and cholesteryl ester storage disease. *J Lipid Res*, *39*(7), 1382-1388.
- Paila, Y. D., & Chattopadhyay, A. (2010). Membrane cholesterol in the function and organization of G-protein coupled receptors. *Subcell Biochem*, *51*, 439-466.
- Palmieri, M., Impey, S., Kang, H., di Ronza, A., Pelz, C., Sardiello, M., et alBallabio, A. (2011). Characterization of the CLEAR network reveals an integrated control of cellular clearance pathways. *Hum Mol Genet*, *20*(19), 3852-3866.
- Perera, R. M., & Zoncu, R. (2016). The Lysosome as a Regulatory Hub. *Annual Review of Cell and Developmental Biology*, *32*(1), 223-253.
- Person, A. D., Beiraghi, S., Sieben, C. M., Hermanson, S., Neumann, A. N., Robu, M. E., Schleiffarth, J. R., Billington, C. J., Jr., van Bokhoven, H., Hoogeboom, J. M., Mazzeu, J. F., Petryk, A., Schimmenti, L. A., Brunner, H. G., Ekker, S. C., et alLohr, J. L. (2010). WNT5A mutations in patients with autosomal dominant Robinow syndrome. *Developmental dynamics : an official publication of the American Association of Anatomists*, *239*(1), 327-337.
- Platt, F. M., d'Azzo, A., Davidson, B. L., Neufeld, E. F., et alTiffit, C. J. (2018). Lysosomal storage diseases. *Nature Reviews Disease Primers*, *4*(1), 27.

- Radhakrishnan, A., Goldstein, J. L., McDonald, J. G., et al Brown, M. S. (2008). Switch-like control of SREBP-2 transport triggered by small changes in ER cholesterol: a delicate balance. *Cell metabolism*, 8(6), 512-521.
- Ramsey, S. A., Vengrenyuk, Y., Menon, P., Podolsky, I., Feig, J. E., Aderem, A., Fisher, E. A., et al Gold, E. S. (2014). Epigenome-guided analysis of the transcriptome of plaque macrophages during atherosclerosis regression reveals activation of the Wnt signaling pathway. *PLoS genetics*, 10(12), e1004828-e1004828.
- Robinson, J. G., Farnier, M., Krempf, M., Bergeron, J., Luc, G., Averna, M., Stroes, E. S., Langslet, G., Raal, F. J., El Shahawy, M., Koren, M. J., Lepor, N. E., Lorenzato, C., Pordy, R., Chaudhari, U., et al Kastelein, J. J. P. (2015). Efficacy and Safety of Alirocumab in Reducing Lipids and Cardiovascular Events. *New England Journal of Medicine*, 372(16), 1489-1499.
- Rong, J. X., Shapiro, M., Trogan, E., et al Fisher, E. A. (2003). Transdifferentiation of mouse aortic smooth muscle cells to a macrophage-like state after cholesterol loading. *Proceedings of the National Academy of Sciences of the United States of America*, 100(23), 13531-13536.
- Sabatine, M. S., Giugliano, R. P., Wiviott, S. D., Raal, F. J., Blom, D. J., Robinson, J., Ballantyne, C. M., Somaratne, R., Legg, J., Wasserman, S. M., Scott, R., Koren, M. J., et al Stein, E. A. (2015). Efficacy and Safety of Evolocumab in Reducing Lipids and Cardiovascular Events. *New England Journal of Medicine*, 372(16), 1500-1509.
- Sancak, Y., Bar-Peled, L., Zoncu, R., Markhard, A. L., Nada, S., et al Sabatini, D. M. (2010). Ragulator-Rag complex targets mTORC1 to the lysosomal surface and is necessary for its activation by amino acids. *Cell*, 141(2), 290-303.
- Sancak, Y., Peterson, T. R., Shaul, Y. D., Lindquist, R. A., Thoreen, C. C., Bar-Peled, L., et al Sabatini, D. M. (2008). The Rag GTPases bind raptor and mediate amino acid signaling to mTORC1. *Science (New York, N.Y.)*, 320(5882), 1496-1501.
- Sardiello, M., Palmieri, M., di Ronza, A., Medina, D. L., Valenza, M., Gennarino, V. A., Di Malta, C., Donaudy, F., Embrione, V., Polishchuk, R. S., Banfi, S., Parenti, G., Cattaneo, E., et al Ballabio, A. (2009). A gene network regulating lysosomal biogenesis and function. *Science*, 325(5939), 473-477.
- Schwartz, G. G., Olsson, A. G., Abt, M., Ballantyne, C. M., Barter, P. J., Brumm, J., Chaitman, B. R., Holme, I. M., Kallend, D., Leiter, L. A., Leitersdorf, E., McMurray, J. J. V., Mundl, H., Nicholls, S. J., Shah, P. K., Tardif, J.-C., et al Wright, R. S. (2012). Effects of Dalcetrapib in Patients with a Recent Acute Coronary Syndrome. *New England Journal of Medicine*, 367(22), 2089-2099.
- Scott, C. C., Vossio, S., Vacca, F., Snijder, B., Larios, J., Schaad, O., Guex, N., Kuznetsov, D., Martin, O., Chambon, M., Turcatti, G., Pelkmans, L., et al Gruenberg, J. (2015). Wnt directs the endosomal flux of LDL-derived cholesterol and lipid droplet homeostasis. *EMBO reports*, 16(6), 741-752.
- Sen, M., Lauterbach, K., El-Gabalawy, H., Firestein, G. S., Corr, M., et al Carson, D. A. (2000). Expression and function of wingless and frizzled homologs in rheumatoid arthritis. *Proceedings of the National Academy of Sciences of the United States of America*, 97(6), 2791-2796.
- Shankman, L. S., Gomez, D., Cherepanova, O. A., Salmon, M., Alencar, G. F., Haskins, R. M., Swiatlowska, P., Newman, A. A. C., Greene, E. S., Straub, A. C., Isakson, B., Randolph, G. J., et al Owens, G. K. (2015). KLF4-dependent phenotypic modulation of smooth muscle cells has a key role in atherosclerotic plaque pathogenesis. *Nature medicine*, 21(6), 628-637.
- Siar, C. H., Nagatsuka, H., Han, P. P., Buery, R. R., Tsujigiwa, H., Nakano, K., Ng, K. H., et al Kawakami, T. (2012). Differential expression of canonical and non-canonical Wnt ligands in ameloblastoma. *J Oral Pathol Med*, 41(4), 332-339.
- Skålén, K., Gustafsson, M., Rydberg, E. K., Hultén, L. M., Wiklund, O., Innerarity, T. L., et al Borén, J. (2002). Subendothelial retention of atherogenic lipoproteins in early atherosclerosis. *Nature*, 417(6890), 750-754.

- Song, Y., Kenworthy, A. K., et al Sanders, C. R. (2014). Cholesterol as a co-solvent and a ligand for membrane proteins. *Protein science*, 23(1), 1-22.
- Suckling, K. E., & Stange, E. F. (1985). Role of acyl-CoA: cholesterol acyltransferase in cellular cholesterol metabolism. *J Lipid Res*, 26(6), 647-671.
- Tabas, I. (2004). Apoptosis and plaque destabilization in atherosclerosis: the role of macrophage apoptosis induced by cholesterol. *Cell Death And Differentiation*, 11, S12.
- Tabas, I., Garcia-Cardena, G., et al Owens, G. K. (2015). Recent insights into the cellular biology of atherosclerosis. *J Cell Biol*, 209(1), 13-22.
- Tabas, I., Williams, K. J., et al Borén, J. (2007). Subendothelial Lipoprotein Retention as the Initiating Process in Atherosclerosis. *Circulation*, 116(16), 1832-1844.
- Taelman, V. F., Dobrowolski, R., Plouhinec, J. L., Fuentealba, L. C., Vorwald, P. P., Gumper, I., Sabatini, D. D., et al De Robertis, E. M. (2010). Wnt signaling requires sequestration of glycogen synthase kinase 3 inside multivesicular endosomes. *Cell*, 143(7), 1136-1148.
- Takahashi, J., Orcholski, M., Yuan, K., et al de Jesus Perez, V. (2016). PDGF-dependent  $\beta$ -catenin activation is associated with abnormal pulmonary artery smooth muscle cell proliferation in pulmonary arterial hypertension. *FEBS letters*, 590(1), 101-109.
- Taleb, S. (2016). Inflammation in atherosclerosis *Arch Cardiovasc Dis* (Vol. 109, pp. 708-715).
- Tängemo, C., Weber, D., Theiss, S., Mengel, E., et al Runz, H. (2011). Niemann-Pick Type C disease: characterizing lipid levels in patients with variant lysosomal cholesterol storage. *Journal of lipid research*, 52(4), 813-825.
- Terrand, J., Bruban, V., Zhou, L., Gong, W., El Asmar, Z., May, P., Zurhove, K., Haffner, P., Philippe, C., Woldt, E., Matz, R. L., Gracia, C., Metzger, D., Auwerx, J., Herz, J., et al Boucher, P. (2009). LRP1 controls intracellular cholesterol storage and fatty acid synthesis through modulation of Wnt signaling. *The Journal of biological chemistry*, 284(1), 381-388.
- Terrand, J., Bruban, V., Zhou, L., Gong, W., El Asmar, Z., May, P., Zurhove, K., Haffner, P., Philippe, C., Woldt, E., Matz, R. L., Gracia, C., Metzger, D., Auwerx, J., Herz, J., et al Boucher, P. (2009). LRP1 controls intracellular cholesterol storage and fatty acid synthesis through modulation of Wnt signaling. *J Biol Chem*, 284(1), 381-388.
- Trikha, S., & Jeremic, A. M. (2011). Clustering and internalization of toxic amylin oligomers in pancreatic cells require plasma membrane cholesterol. *The Journal of biological chemistry*, 286(41), 36086-36097.
- Tsaousi, A., Mill, C., et al George, S. J. (2011). The Wnt pathways in vascular disease: lessons from vascular development. *Curr Opin Lipidol*, 22(5), 350-357.
- Tuloup-Minguez, V., Greffard, A., Codogno, P., et al Botti, J. (2011). Regulation of autophagy by extracellular matrix glycoproteins in HeLa cells. *Autophagy*, 7(1), 27-39.
- Ueland, T., Otterdal, K., Lekva, T., Halvorsen, B., Gabrielsen, A., Sandberg, W. J., Paulsson-Berne, G., Pedersen, T. M., Folkersen, L., Gullestad, L., Oie, E., Hansson, G. K., et al Aukrust, P. (2009). Dickkopf-1 enhances inflammatory interaction between platelets and endothelial cells and shows increased expression in atherosclerosis. *Arterioscler Thromb Vasc Biol*, 29(8), 1228-1234.
- Vonbank, A., Saely, C. H., Rein, P., Sturm, D., et al Drexel, H. (2013). Current cholesterol guidelines and clinical reality: a comparison of two cohorts of coronary artery disease patients. *Swiss Med Wkly*, 7(143).
- Wallentin, L., Becker, R. C., Budaj, A., Cannon, C. P., Emanuelsson, H., Held, C., Horrow, J., Husted, S., James, S., Katus, H., Mahaffey, K. W., Scirica, B. M., Skene, A., Steg, P. G., Storey, R. F., et al Harrington, R. A. (2009). Ticagrelor versus Clopidogrel in Patients with Acute Coronary Syndromes. *New England Journal of Medicine*, 361(11), 1045-1057.
- Wang, X., Xiao, Y., Mou, Y., Zhao, Y., Blankesteyn, W. M., et al Hall, J. L. (2002). A role for the  $\beta$ -catenin/T-cell factor signaling cascade in vascular remodeling. *Circ Res*, 90(3), 340-347.

- Wesolowski, R., Abdel-Rasoul, M., Lustberg, M., Paskell, M., Shapiro, C. L., et al Macrae, E. R. (2014). Treatment-related mortality with everolimus in cancer patients. *The oncologist*, *19*(6), 661-668.
- Wilhelm, L. P., Wendling, C., Védie, B., Kobayashi, T., Chenard, M. P., Tomasetto, C., Drin, G., et al Alpy, F. (2017). STARD3 mediates endoplasmic reticulum-to-endosome cholesterol transport at membrane contact sites. *Embo J*, *36*(10), 1412-1433.
- Williams, B., & Insogna, K. (2009). *Where Wnts Went: The Exploding Field of Lrp5 and Lrp6 Signaling in Bone* (Vol. 24).
- Wilt, T. J., Bloomfield, H. E., MacDonald, R., Nelson, D., Rutks, I., Ho, M., Larsen, G., McCall, A., Pineros, S., et al Sales, A. (2004). Effectiveness of Statin Therapy in Adults With Coronary Heart Disease. *Archives of Internal Medicine*, *164*(13), 1427-1436.
- Witze, E. S., Litman, E. S., Argast, G. M., Moon, R. T., et al Ahn, N. G. (2008). Wnt5a control of cell polarity and directional movement by polarized redistribution of adhesion receptors. *Science*, *320*(5874), 365-369.
- Woldt, E., Matz, R. L., Terrand, J., Mlih, M., Gracia, C., Foppolo, S., Martin, S., Bruban, V., Ji, J., Velot, E., Herz, J., et al Boucher, P. (2011). Differential signaling by adaptor molecules LRP1 and ShcA regulates adipogenesis by the insulin-like growth factor-1 receptor. *J Biol Chem*, *286*(19), 16775-16782.
- Woldt, E., Terrand, J., Mlih, M., Matz, R. L., Bruban, V., Coudane, F., Foppolo, S., El Asmar, Z., Chollet, M. E., Ninio, E., Bednarczyk, A., Thiersé, D., Schaeffer, C., Van Dorsselaer, A., Boudier, C., Wahli, W., Chambon, P., Metzger, D., Herz, J., et al Boucher, P. (2012). The nuclear hormone receptor PPAR $\gamma$  counteracts vascular calcification by inhibiting Wnt5a signalling in vascular smooth muscle cells. *Nature Communications*, *3*, 1077.
- Wright, M., Aikawa, M., Szeto, W., et al Papkoff, J. (1999). Identification of a Wnt-responsive signal transduction pathway in primary endothelial cells. *Biochem Biophys Res Commun*, *263*(2), 384-388.
- Wyant, G. A., Abu-Remaileh, M., Wolfson, R. L., Chen, W. W., Freinkman, E., Danai, L. V., Vander Heiden, M. G., et al Sabatini, D. M. (2017). mTORC1 Activator SLC38A9 Is Required to Efflux Essential Amino Acids from Lysosomes and Use Protein as a Nutrient. *Cell*, *171*(3), 642-654.
- Xu, S., Benoff, B., Liou, H. L., Lobel, P., et al Stock, A. M. (2007). Structural basis of sterol binding by NPC2, a lysosomal protein deficient in Niemann-Pick type C2 disease. *J Biol Chem*, *282*(32), 23525-23531.
- Yan, P., Xia, C., Duan, C., Li, S., et al Mei, Z. (2011). Biological characteristics of foam cell formation in smooth muscle cells derived from bone marrow stem cells. *Int J Biol Sci*, *7*(7), 937-946.
- Yang, Q., & Guan, K. L. (2007). Expanding mTOR signaling. *Cell Res*, *17*(8), 666-681.
- Yao, R., Sun, X., Xie, Y., Liu, L., Han, D., Yao, Y., Li, H., Li, Z., et al Xu, K. (2018). Lithium chloride inhibits cell survival, overcomes drug resistance, and triggers apoptosis in multiple myeloma via activation of the Wnt/ $\beta$ -catenin pathway. *American journal of translational research*, *10*(8), 2610-2618.
- Yeagle, P. L., Young, J., et al Rice, D. (1988). Effects of cholesterol on sodium-potassium ATPase ATP hydrolyzing activity in bovine kidney. *Biochemistry*, *27*(17), 6449-6452.
- Yecies, J. L., Zhang, H. H., Menon, S., Liu, S., Yecies, D., Lipovsky, A. I., Gorgun, C., Kwiatkowski, D. J., Hotamisligil, G. S., Lee, C.-H., et al Manning, B. D. (2011). Akt stimulates hepatic SREBP1c and lipogenesis through parallel mTORC1-dependent and independent pathways. *Cell metabolism*, *14*(1), 21-32.
- Zhang, X., Julien-David, D., Miesch, M., Geoffroy, P., Raul, F., Roussi, S., Aoude-Werner, D., et al Marchioni, E. (2005). Identification and quantitative analysis of beta-sitosterol oxides in vegetable oils by capillary gas chromatography-mass spectrometry. *Steroids*, *70*(13), 896-906.

Zhou, L., Takayama, Y., Boucher, P., Tallquist, M. D., et al Herz, J. (2009). LRP1 regulates architecture of the vascular wall by controlling PDGFRbeta-dependent phosphatidylinositol 3-kinase activation. *PLoS one*, 4(9), e6922-e6922.

# Résumé de thèse

# **Role de Wnt5a dans la fonction lysosomale, l'accumulation intra cellulaire du cholestérol, et l'athérosclérose**

## ***Introduction:***

L'accumulation de macrophages et de cellules musculaires lisses vasculaires (CMLV) chargées en ester de cholestérol (CE), également appelées cellules spumeuses, caractérise les lésions athérosclérotiques précoces. Cependant, à mesure que les lésions progressent, le contenu en cholestérol (FC) non estérifié ou «libre» des macrophages et des CMLV augmente progressivement. L'accumulation de grandes quantités de FC conduit à la mort cellulaire et à la nécrose des macrophages et des CMLV se qui constitue un tournant décisif dans l'aggravation de l'athérosclérose. En particulier, la nécrose lésionnelle est un facteur déclenchant de l'érosion et de la rupture de la plaque, ce qui entraîne une thrombose aiguë et une occlusion vasculaire. Dans ce contexte, et étant donné l'importance de cette pathologie, il est primordial de comprendre les mécanismes aboutissant à l'accumulation intracellulaire du cholestérol et d'identifier de nouvelles cibles thérapeutiques.

Le cholestérol exogène qui pénètre dans la cellule est de nature hydrophobe. La cellule absorbe le cholestérol exogène par deux processus, la phagocytose ou l'endocytose par les récepteurs LDL. Les LDLR se séparent des particules de LDL et sont recyclés vers la membrane plasmique, tandis que l'enzyme LIPA (lysosomal acid lipase) des lysosomes agit sur les particules de LDL et induit la déestérification du cholestérol en FC et la libération des triglycérides. Comme le cholestérol libre n'est pas soluble dans l'environnement hydrophile des lysosomes, il nécessite l'action de deux protéines pour son transport hors des lysosomes. Ces protéines sont appelées

NPC1 (Niemann-Pick de type C1) et NPC2 (Niemann-Pick de type C2). NPC1 transporte ensuite le cholestérol des lysosomes vers réticulum endoplasmique (RE). dans le RE, les protéines de liaison aux éléments régulateurs des stérols (SREBP) qui appartiennent à la famille des facteurs de transcription, sont impliquées dans la régulation de la synthèse du cholestérol en association avec deux autres protéines, INSIG1 (protéine du gène 1 induite par l'insuline) et SCAP (protéine d'activation du clivage SREBP). L'export extracellulaire du cholestérol est assuré par deux protéines ABCA1 et ABCG1.

La protéine 1 (LRP1) liée au récepteur des lipoprotéines de basse densité (LDL) appartient aux membres de la famille du gène des récepteurs des LDL (LDLR). C'est un récepteur qui à plus de 40 ligands et qui est largement exprimé dans plusieurs tissus. La suppression du gène LRP1 est létale chez la souris, révélant un rôle critique, mais non défini, dans le développement. Les études de délétion génétique spécifiques dans différents tissus révèlent une contribution importante de LRP1 dans le développement du système vasculaire, du système nerveux central, des macrophages, du foie et des adipocytes. Chez les souris nourries avec un régime alimentaire riche en cholestérol, la suppression de LRP1 dans les macrophages ou dans les CMLV (souris smLRP1-) entraîne le développement de nombreuses lésions d'athérosclérose. Les analyses histologiques révèlent la formation massive de cellules spumeuses et l'accumulation de cristaux de FC en forme d'aiguille dans la paroi artérielle des animaux mutants. Chez l'homme, ces cristaux de cholestérol sont généralement observés dans les régions extracellulaires des lésions athéroscléreuses avancées et dans les macrophages en culture surchargés en cholestérol. De même, les fibroblastes embryonnaires de souris (MEF) dépourvus de LRP1 (LRP1 - / -), lorsqu'ils sont traités avec un cocktail adipogénique, ne forment pas de cellules ressemblant à des adipocytes ni n'accumulent de triglycérides, mais accumulent des

quantités plus importantes de FC et de CE que les MEF de type sauvage. Ainsi, LRP1 protège contre l'accumulation de cholestérol.

Plusieurs études suggèrent un échange fonctionnel entre les membres de la famille du gène LDLR et la voie Wnt dans le processus athérogénique. La perte de fonction des co-récepteurs Wnt LRP5 et LRP6 a été associée à une maladie coronarienne chez l'homme et chez la souris. De plus, lorsque LRP1 est exprimé, le ligand Wnt, Wnt5a est modérément élevé dans les stries adipositaires et dans les lésions athéroscléreuses précoces. L'expression de Wnt5a est également fortement augmentée dans les CMLV lors de la métaplasie cartilagineuse CMLVet dans les zones de calcifications vasculaires. Inversement, l'expression de Wnt5a est diminuée dans les aortes de souris smLRP1-. Dans les MEF, alors que Wnt5a est fortement exprimé en présence de LRP1, il est presque indétectable dans les cellules LRP1 - / -. Nous avons identifié Wnt5a comme un puissant inhibiteur de l'accumulation intracellulaire de FC et de CE. De même, un traitement avec un Wnt5a recombinant ou une re-transfection de MEF LRP1 - / - avec un vecteur d'expression codant pour Wnt5a bloque de manière robuste l'accumulation de cholestérol. Les souris présentant une signalisation Wnt5a accrue dans la paroi vasculaire présentent une formation réduite de cellules spumeuses. Ces données indiquent un rôle potentiel pour la signalisation Wnt, et en particulier Wnt5a dans l'athérosclérose. Cependant, ils ne fournissent pas un mécanisme sous-jacent clair qui pourrait aider à évaluer le potentiel thérapeutique de cette voie. Pour diminuer la teneur en cholestérol cellulaire, Wnt5a peut bloquer la synthèse du cholestérol, favoriser son efflux ou réduire son absorption. Dans cette étude, nous proposons de tester ces hypothèses sur des cSMC et macrophages CMLV. Étant donné que la masse grasse viscérale dans l'abdomen est un puissant facteur de prédiction des maladies cardiovasculaires et que le tissu adipeux et les lésions artérioscléreuses hébergent des groupes communs de gènes

qui affectent l'étendue de l'athérosclérose, nous allons également tester ces hypothèses sur les adipocytes de souris.

### ***Results :***

Nos résultats indiquent que Wnt5a est essentiel pour la fonction lysosomale et est un composant important du complexe de détection du cholestérol mTORC1-NPC. En l'absence de Wnt5a, les lysosomes augmentent en taille et en nombre et accumulent davantage de cholestérol. Ces résultats sont en accord avec nos résultats précédents dans les cellules MEF LRP1 - / -. En l'absence de LRP1, les taux de Wnt5a endogène sont réduits, ce qui augmente l'accumulation de cholestérol (El Asmar *et al.*, 2016). Il a déjà été rapporté que l'expression de Wnt5a augmente à mesure que les atteintes d'athérosclérose progresse (Christman *et al.*, 2008, Woldt *et al.*, 2012). Nous avons également montré (figure 22A) que l'expression de Wnt5a dans les CMLV augmente lors de l'accumulation de cholestérol. Cependant, la suppression de Wnt5a dans les CMLV conduit à une accumulation de cholestérol et à l'athérosclérose. Ainsi, cette expression accrue de Wnt5a pourrait être un mécanisme compensatoire adopté par les cellules pour prévenir l'accumulation de cholestérol, et non un facteur de risque. Nos données sont également en accord avec les rapports précédents sur des souris mutantes LRP1 contenant un domaine muté du récepteur PDGF- $\beta$  kinase (Zhou *et al.*, 2009). LRP1 dans les CMLV fonctionne de manière autonome dans le maintien de l'intégrité de la paroi vasculaire et la protection contre l'athérosclérose induite par le cholestérol. Cependant, la perturbation de la voie de prolifération proathérogène, impliquant PI3K et PDGFR- $\beta$ , empêche le développement de lésions dans la crosse aortique et l'aorte abdominale, zones où l'intégrité vasculaire est facilement compromise (Zhou *et al.*, 2009). Nous avons montré que l'activation de la voie PI3K / Akt / mTORC1 en l'absence de Wnt5a altère les fonctions lysosomales de base

conduisant à une accumulation de cholestérol dans les LEL. Ainsi, PI3K intègre les deux signaux de la croissance cellulaire et la fonction lysosomale et est un point de contrôle efficace ralentissant ou prévenant les troubles dégénératifs de la paroi vasculaire. Il a été publié récemment, que mTORC1 inhibe le trafic de cholestérol des lysosomes aux ER (Castellano *et al.*, 2017) et entraîne une accumulation de cholestérol dans les cellules. Nos résultats montrent que mTORC1 est activé en l'absence de Wnt5a et que le trafic de cholestérol est bloqué des lysosomes aux ER. La régulation positive de mTORC1 en l'absence de Wnt5a pourrait être activée en activant la voie PI3Kinase / AKT / mTORC1. Nos résultats montrent que PI3Kinase et AKT sont activés en l'absence de Wnt5a. L'activation de l'AKT inhibe TSC1 / 2, l'inhibiteur de mTORC1, ce qui entraîne l'activation de mTORC1. De plus, pour être actif, TSC1 / 2 nécessite une activation par AMPK et GSK3. Une autre raison d'activation de mTORC1 pourrait être due à la régulation à la baisse d'AMPK en l'absence de Wnt. Wnt5a active la signalisation AMPK. En son absence, les taux de phospho-AMPK sont réduits, ce qui entraîne l'inactivation de TSC1 / 2 et une phosphorylation accrue de mTORC1. Les observations antérieures concordent avec la localisation de la signalisation Wnt dans le compartiment endosomal. La signalisation canonique Wnt, Wnt3a provoque la relocalisation de la glycogène synthase kinase 3 (GSK3) dans des compartiments endosomaux (Taelman *et al.*, 2010) permettant la suppression de l'activité de la GSK3 induite par Wnt (Witze *et al.*, 2008). L'inhibition de GSK3, Wnt3a (ou Wnt1) entraîne l'inhibition de TSC2 et a donc l'activation de mTORC1 (Inoki *et al.*, 2006). Ici, en plus de sa localisation dans les LEL positives pour Lamp1 (figure 27B, panneaux de droite), nous avons également constaté que l'inhibition de la GSK3 par le LiCl augmentait p-mTORC1 dans les cellules de type sauvage (figure 33D, piste 3). Mais de manière surprenante, l'inhibition de la GSK3 par LiCl inhibe la p-mTORC1 dans les WMCA Wnt5a - / - CMLV (figure 33D, piste 4). Ceci indique que

Wnt5a se comporte différemment des autres ligands Wnt, en particulier Wnt3a. Grâce à l'inhibition d'Akt et à l'activation d'AMPK, Wnt5a diminue l'activation de mTORC1. Cependant, une autre voie inconnue dépendante de Wnt5a ou d'un autre ligand Wnt (Wnt3a) pourrait également participer à la régulation de mTORC1 lors de l'inhibition de GSK3. Comme il a été publié précédemment, NPC1 & 2 sont les deux protéines d'exportation du cholestérol contenu dans les lysosomes (Gong *et al.*, 2016). NPC1 régule mTORC1 afin de promouvoir le trafic de cholestérol des lysosomes au ER (Castellano *et al.*, 2017). Nos données montrent que, mis à part la diminution de la phosphorylation de mTORC1, Wnt5a interagit aussi physiquement avec les protéines NPC1 et NPC2 et favorise une augmentation de la sortie de cholestérol des lysosomes vers le ER. Wnt5a se lie également au cholestérol en raison de la présence de cinq motifs de liaison au cholestérol CARC dans sa séquence peptidique. Ainsi, Wnt5a fonctionne avec les protéines mTORC1 et NPC1 / 2 pour détecter et réguler les niveaux de cholestérol lysosomal.

### ***Conclusion :***

En conclusion, le travail présenté ici identifie un rôle crucial de Wnt5a, inconnu auparavant, sur le contrôle de la fonction lysosomale et du trafic de cholestérol. Wnt5a est un nouveau composant intégral de la machinerie lysosomale qui diminue l'activité de mTORC1. En conséquence, l'absence de Wnt5a entraîne l'accumulation de grandes LIE et de vésicules contenant du cholestérol et de la lipofuscine. L'accumulation de cholestérol active l'axe mTORC1 dépendant des nutriments à la surface des LEL, tandis que Wnt5a régule ce mécanisme de manière dépendante du cholestérol. Wnt5a interagit dans les LEL avec les protéines NPC pour senser l'abondance des stérols lysosomaux et interagir avec le complexe mTORC1. Cela est nécessaire pour le transport du cholestérol à travers la membrane lysosomal et son transfert vers le réticulum endoplasmique pour une redistribution ultérieure et

une exportation via des transporteurs ABC. Ce mécanisme limite l'accumulation de cholestérol dans les CMLV et protège de l'athérosclérose chez la souris. Nos résultats ont de profondes implications dans la compréhension de l'athérosclérose et des maladies à stockage lysosomal, et apportent de nouvelles informations mécanistiques sur le trafic du cholestérol et les événements intracellulaires médiés par la signalisation Wnt.

## Rôle de Wnt5a dans la fonction lysosomale, l'accumulation intracellulaire du cholestérol, et l'athérosclérose

*Nous avons identifié, un ligand de Wnt, Wnt5a, comme faisant partie intégrante du complexe mTORC1, qui régule la fonction lysosomale et favorise le trafic intracellulaire du cholestérol. En diminuant l'activité de mTORC1 et en activant l'axe autophagie-lysosome, Wnt5a adapte les concentrations du cholestérol intracellulaire aux besoins de la cellule. Wnt5a favorise l'export du cholestérol depuis les endosomes/lysosomes (LELs) vers le réticulum endoplasmique (RE), limite l'accumulation intracellulaire du cholestérol, et protège contre l'athérosclérose. D'un point de vue mécanistique, Wnt5a se lie aux membranes riches en cholestérol et interagit spécifiquement avec la protéine membranaire Niemann-Pick C1 (NPC1), la protéine soluble Niemann-Pick C2 (NPC2), deux protéines lysosomales qui régulent l'export du cholestérol à partir des LELs. En conséquence, l'absence de Wnt5a inhibe la fonction lysosomale et l'autophagie, ainsi que la sortie du cholestérol hors des LELs. Ceci résulte en l'accumulation de larges corps d'inclusion intracellulaires, de larges LELs riches en cholestérol, d'une diminution du cholestérol au niveau du RE.*

*Mots clés: Wnt5a, mTORC1, LELs, NPC1&2.*

*We identified the Wnt ligand, Wnt5a, as a member of the nutrient/energy/stress sensor, mTORC1 scaffolding complex, which drives lysosomal function and promotes cholesterol trafficking. By decreasing mTORC1 activity and by activating the autophagy-lysosomal axis, Wnt5a senses changes in dietary cholesterol supply, promotes endosomal/lysosomal (LELs) cholesterol egress to the endoplasmic reticulum (ER), and protects against atherosclerosis. Moreover, Wnt5a binds cholesterol-rich membranes and specifically interacts with two lysosomal proteins Niemann-Pick C1 and Niemann-Pick C2 that regulate cholesterol export from LELs. Consequently, absence of Wnt5a decoupled mTORC1 from variations in LELs cholesterol levels, and this resulted in accumulation of large intracellular inclusion bodies, large LELs and low ER cholesterol.*

*Keywords: Wnt5a, mTORC1, LELs, NPC1&2.*